Myosin Isoforms and Regulation of Tonic and Phasic Contraction in Smooth Muscle

Qian Huang
Marquette University

MYOSIN ISOFORMS AND REGULATION OF TONIC AND PHASIC
CONTRACTION IN SMOOTH MUSCLE

By

Qian Huang, B.S.

A Dissertation submitted to the Faculty of the Graduate School,
Marquette University,
in Partial Fulfillment of the Requirements for
the Degree of Doctor of Philosophy

Milwaukee, Wisconsin

December 2012

ABSTRACT
MYOSIN ISOFORMS AND REGULATION OF TONIC AND PHASIC
CONTRACTION IN SMOOTH MUSCLE

Qian Huang, B.S.

Marquette University, 2012

The contractile properties of smooth muscle (SM) are broadly classified as tonic and phasic. Among the hypothesized underlying regulatory mechanisms for this difference is the different actomyosin ATPase kinetic properties of SM SMA/SMB myosin heavy chain (MHC) isoforms and the preferential expression of SMA and SMB MHC isoforms in tonic and phasic SM respectively. Thus, we hypothesized that SM SMA/B MHC expression determines tonic and phasic contractile patterns in SM.

To test the this hypothesis, the role of SMA and SMB MHC isoforms in tonic and phasic contractions was studied in phasic (longitudinal ileum and stomach circular antrum) and tonic (stomach circular fundus) smooth muscle tissues of SMB knockout mice. Knocking out the SMB MHC gene eliminated SMB MHC protein expression and resulted in up-regulation of the SMA MHC protein without altering the total MHC protein level. Switching from SMB to SMA MHC protein expression decreased the rate of the force transient and increased the sustained tonic force in $SMB^{(-/-)}$ antrum with high potassium (KPSS) or Carbachol (CCh) stimulation. The sustained tonic force in $SMB^{(-/-)}$ ileum was also significantly increased with KPSS stimulation but not with CCh. The increased tonic contraction under depolarized condition was not through changes in second messenger signaling pathways (PKC/CPI-17 or Rho/ROCK signaling pathway) or LC_{20} phosphorylation. Biochemical analyses showed that the expression of contractile regulatory proteins (MLCK, MLCP, PKCδ, and CPI-17) did not change significantly in tissues tested except for PKCα protein expression being significantly decreased in the $SMB^{(-/-)}$ antrum. However, specifically activating PKCα with phorbol dibutyrate (PDBu) was not significantly different in knockout and wild type tissues, with total force being a fraction of the force generation with KPSS or CCh stimulation in $SMB^{(-/-)}$ ileum and antrum. Taken together, these data show inhibiting SMB MHC protein expression results in a compensatory increase in the SMA MHC protein expression and enhanced sustained tonic contraction with a reduced rate of force generation in these phasic tissues. These results are consistent with SMA and SMB MHC regulating tonic and phasic contraction in SM.

ACKNOWLEDGMENTS

Qian Huang, B.S.

It is a pleasure to thank those who made this thesis possible. First of all, I would like to express my deep appreciation to my advisor, Dr. Thomas Eddinger for his guidance and support during my studies at Marquette University. His patience, support and humor helped me overcome difficulties and finish this thesis. I would also like to thank Dr. Robert Fitts, Dr. Stephen Munroe, Dr. James Anderson, and Dr. Robert Balza for their help with specific techniques, general support, and for serving on my dissertation committee. I am also pleased to thank Dr. Muthu Periasamy (Ohio State University), Dr. Gopal Babu (University of Medicine and Dentistry of New Jersey), and Dr. Avril Somlyo (University of Virginia) for providing me with SMB knockout mice and antibodies, without which this project would have been impossible.

I would also like to thank all my friends for their unwavering support and encouragement throughout the years. Finally, I am very grateful to my parents for understanding, love and the constant support that allows me to pursue my dream. This dissertation is also dedicated to them.

TABLE OF CONTENTS

LIST OF TABLES

LIST OF FIGURES

Abbreviations:

Enzymes and proteins

CaM: Calmodulin

CPI-17: PKC-potentiated inhibitory protein for heterotrimeric myosin light chain phosphatase of 17 kDa

ELC: myosin essential light chain

ILK: integrin-linked kinase

LC_{17}: 17kDa essential myosin light chain

LC_{20}: myosin regulatory light chain 20

MARK: microtubule affinity regulating kinse

MLCK: myosin light chain kinase

MYPT1: myosin phosphatase target subunit 1

MLCP: myosin light chain phosphatase

NM MHC: non-muscle myosin heavy chain

PKC: protein Kinase C

RLC: myosin regulatory light chain

ROCK: Rho-associated protein kinase

SM MHC: smooth muscle myosin heavy chain

SMA: smooth muscle myosin A

SMB: smooth muscle myosin B

SM1: smooth muscle myosin 1

SM2: smooth muscle myosin 2

SOCC: store-operated Ca^{2+} channel

VOCC: voltage-operated Ca^{2+} channel

ZIPK: zipper-interacting protein kinase

Buffer and saline

KPSS: high potassium containing physiological saline solution

TAE: Tris-acetate-EDTA buffer

PSS: physiological salt solution

TBST: Tris buffered-saline containing Tween 20

Chemicals

Ach: Acetylcholine

CAPS: N-cyclohexyl-3-aminopropanesulfonic acid

CCh: Carbachol

EDTA: ehtylenediaminetetraacetic acid

MOPS: 3-(N-morpholine) propanesulfonic acid

SDS: sodium dodecyl sulfate

DTT: dithiothreitol

PDBu: phorbol 12,13-dibutyrate

Other

IAS: internal anal sphincter

LES: lower esophageal sphincter

rpm: revolutions per minute

SDS-PAGE: Sodium dodecyl sulfate polyacrylamide gel electrophoresis

SM: smooth muscle

I. Introduction:

Smooth muscle cells are widely distributed throughout the vertebrate body to carry out physiological functions in various organ systems including circulation, digestion, reproduction, respiration, urination, and vision. Their ability to contract and relax is critical to the functioning of these systems, especially the proper regulation and extent of contraction and relaxation. Defects in smooth muscle contractile regulation can lead to clinical diseases, including systematic hypertension, inflammatory bowel diseases, preterm labor, asthma, bladder outlet obstruction, and vision disorders. Thus, understanding regulatory mechanism of smooth muscle contraction is of particular importance.

Overview of myosin

Myosin, a 500kDa protein, is a major component of the contractile apparatus in eukaryotic organisms. It provides motor function for diverse movement related processes such as muscle contraction, cell migration and cytokinesis. In eukaryotic cells, myosins form a super family with at least 18 classes based on phylogenetic analysis of the myosin head domain (Berg et al., 2001; Sellers, 2000). Based on head and tail domain structures, analysis of the human genome results in 12 different classes of myosin encoded by ~40 myosin genes (Berg et al., 2001), of which 15 genes encode the conventional class II myosins (Weiss et al., 1999). The 15 class II human myosin genes encode the skeletal muscle myosin heavy chains (6 genes), smooth muscle myosin heavy chains (1 gene), cardiac muscle myosin heavy chains (2 genes), non-muscle myosin heavy chains (3 genes)

and novel class II myosins (3 genes) (Berg et al., 2001). In addition to different myosin genes, alternative splicing at the transcriptional level increases the diversity of myosin molecule isoforms. Thus, it is not surprising that each cell type expresses more than one myosin heavy chain isoform. In smooth muscle cells at least 4 smooth muscle and 3 non-muscle myosin isoforms are expressed (Morano, 2003).

In smooth muscle, the functional smooth muscle myosin molecule is a hexameric protein consisting of two myosin heavy chains (MHCs) and two pairs of non-identical myosin light chains (MCLs) (Eddinger and Meer, 2007). The MHC with a molecular weight around 200kDa can be divided into two major functional domains by enzymatic degradation: a S1 globular head domain and an α-helical rod domain (Lowey et al., 1969)(see Figure 1). The S1 globular head has ATPase activity and actin binding sites, which are able to transform chemical energy into the mechanical function of contraction. The S1 globular head is connected to the α-helical rod by a protease-sensitive region (S2), and can be subdivided into three proteolytic fragments: a 25kDa fragment, a 50kDa fragment, and a 20kDa fragment (Mornet et al., 1981)(see Figure 2). The 25kDa fragment forms part of the ATP- binding site (near Loop 1) (Rayment et al., 1993; Szilagyi et al., 1979; Walker et al., 1982). The 50kDa fragment is responsible for actin binding. A prominent cleft separates the 50kDa fragment into upper and lower regions and is the actin-binding domain (near Loop 2) (Rayment et al., 1993). The 20kDa fragment includes the MLC

binding sites (Rayment et al., 1993; Szilagyi et al., 1979) (Figure 2B). Functionally, the S1 globular head can also be divided into three functional domains: motor

A
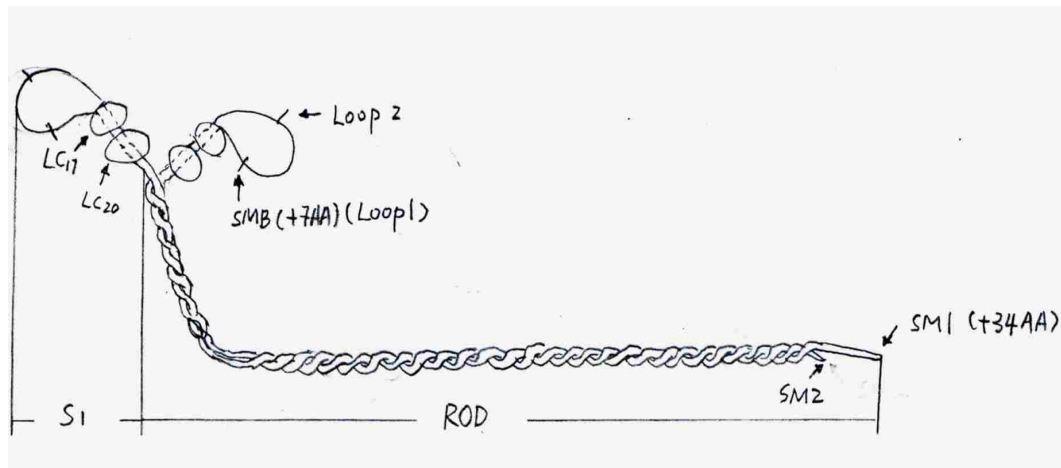
B
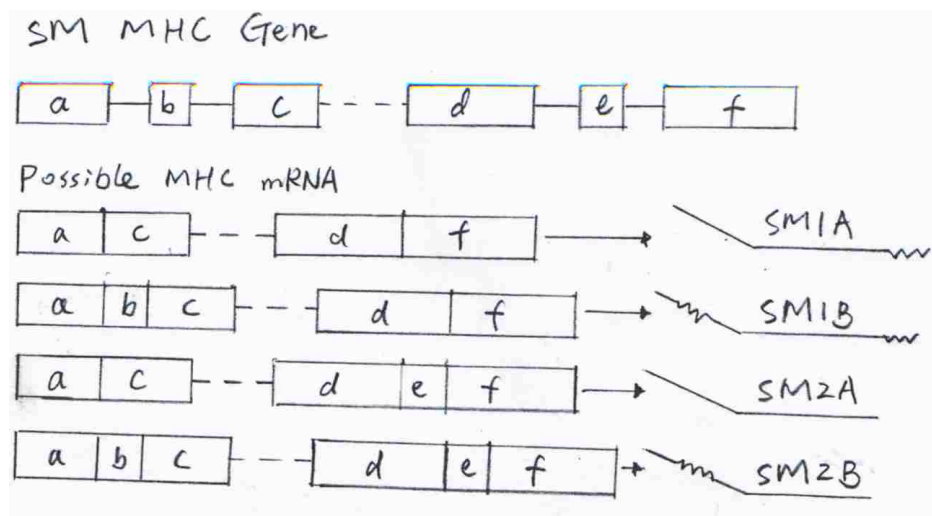
Figure 1. Schematic of smooth muscle myosin molecule and possible smooth muscle MHC pairings modified from Eddinger & Meer. Am J Physiol Cell Physiol 2007.
A. Schematic of smooth muscle myosin. Smooth muscle myosin molecule consists of two SM MHCs and two paired MLCs associated with each MHC. As a result of alternative splicing, four isoforms of MHCs can be found in smooth muscle myosin molecules: SM1, SM2, SMA, and SMB. SM1 and SM2 MHCs (the tail isoforms) differ at MHC tail region, where SM1 is 34aa longer than SM2. SMA and SMB MHCs (the head isoforms) differ at Loop1 of MHC near the ATP binding site, where SMA has an additional 7aa. MLCs (LC_{20} and LC_{17}) bind to the level arm of the S1 head.
B. Four possible SM MHCs resulting from alternative splicing at the transcriptional level.

A
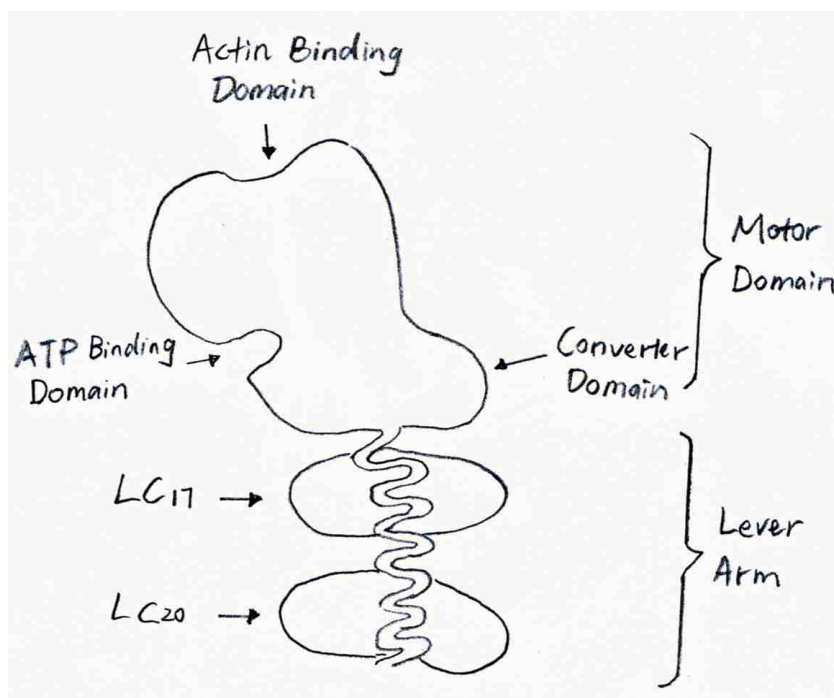
B
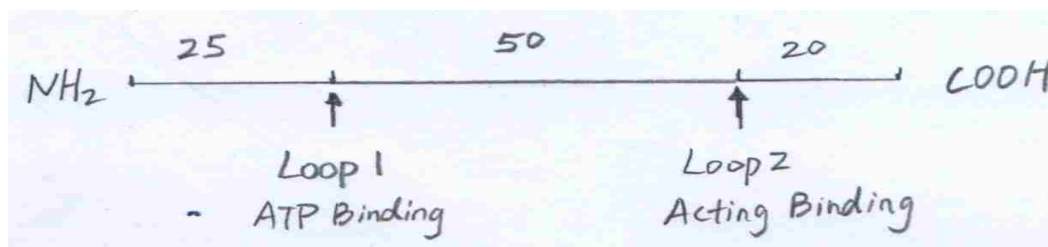
Figure 2. Schematic of the S1 head modified from Eddinger & Meer. Am J Physiol Cell Physiol 2007. A**.** Detailed schematic of the S1 head. The S1 head is composed of three functional domains: motor domain, lever arm, and converter domain. The motor domain includes actin binding domain (near Loop 2) and ATP binding domain (near Loop 1). The lever arm has the MLCs (LC_{17} and LC_{20} binding domains). The converter domain connects the motor domain to the lever arm enabling the relative rotation of lever arm against the motor domain. B. Linear schematic of the S1 head. Three proteolytic fragments: 20kDa, 50kDa, and 25kDa. Loop 1 and Loop 2 are proteolytic cleavage sites and near ATP and actin binding domains respectively. From N-terminus to C-terminus, the 25kDa fragment is located between the motor domain and the lever arm; the 50kDa fragment forms the majority of the motor domain; the 20kDa fragment includes converter domain and lever arm.

domain, lever domain, and converter domain indicated in Figure 2A (Eddinger and

Meer, 2007).

The α-helical rod domain of myosin is a coiled-coil rod structure, which is

composed of 28 periodic 7-amino acid repeats (McLachlan and Karn, 1982; McLachlan

and Karn, 1983). This amino acid distribution (Nagai et al., 1988) has been reported to

contribute to the intramolecular MHC coiled-coil rod structure and intermolecular MHC

association of two α-helical rods by hydrophobic interactions, which facilitates the

polymerization of multiple myosin molecules into filaments (McLachlan and Karn, 1982).

Based on the amino-acid sequence, smooth muscle MLCs are divided into two

subtypes: alkali light chains, also named essential light chains (ELCs), which are 17kDa,

and the regulatory light chains (RLCs) which are 20kDa (Matsuda et al., 1981; Miyanishi

et al., 1985). Based on their molecular weights, ELCs and RLCs are also named LC_{17} and

LC_{20}. Both the light chains belong to the EF-hand protein family, which are able to bind

Ca^{2+} (Grabarek, 2006). The function of the essential light chain is not totally understood

but is reported to be important for the stability of the α-helical lever arm domains of

MHCs (the 20 kDa fragment of the S1 region) (Dominguez et al., 1998; Trybus, 1994). In

smooth muscle and non-muscle myosin isoforms, LC_{20} phosphorylation status regulates

the interactions between actin and myosin via LC_{20} phosphorylation by myosin light

chain kinase (MLCK) (Trybus, 1994) and dephosphorylation by myosin light chain

phosphatase (MLCP) (Somlyo and Somlyo, 2003).

Different smooth muscle (SM) myosin isoforms and their kinetic properties

Smooth muscle myosin belongs to the conventional class II myosin family and is the major contributor to SM contraction. Similarly, like the other members of class II myosin family, SM myosin is a hexamer in structure (Figure 1A). Due to the alternative splicing at the mRNA level different isoforms of SM LCs and SM MHCs are expressed in smooth muscle. Various combinations of these subunit isoforms lead to the different myosin isoforms. So far, there are at least 4 SM MHC isoforms identified. SM1 (204 kDa) and SM2 (200kDa) are two SM MHC isoforms originally identified by SDS polyacrylamide gel (Rovner et al., 1986). The SM1 and SM2 isoforms are identical for most of the amino acid sequences except in the C-terminus, where SM1 is 34 amino-acid longer than SM2. SM2 has a unique 9 amino acids (Figure 1). The size differences between SM1 and SM2 result from a 39-nucleotide insertion with an in frame stop codon in SM2 mRNA (Babij and Periasamy, 1989; Nagai et al., 1989). The other two SM MHC isoforms are SMA and SMB. Unlike SM1 and SM2, the differences between SMA and SMB are located in the S1 head region of SM MHC (Babij et al., 1991; Hamada et al., 1990; Kelley et al., 1993; White et al., 1993). The splice site is located in mRNA encoding the 25kDa and 50kDa fragment junction, which is near the ATP binding site (Rayment et al., 1993). The SMB MHC isoform has an additional 7 amino acids (QGPSFAY for mouse and rat) compared to SMA. Exon 5b in SM MHC mRNA is responsible for encoding this additional 7 amino acids in SMB MHC (Babij and Periasamy, 1989). The 7 amino-acid difference in the S1 head region may be present in either of the SM1 or SM2 isoforms. Thus the four SM MHC isoforms in smooth muscle

cells include SM1A, SM1B, SM2A and SM2B (Figure 1B), which could form 10 kinds

of SM myosin molecules by either homodimeric or heterodimeric MHC combinations.

In addition to the SM MHC isoforms, 3 non-muscle MHC (NM MHC) isoforms, NM

MHC A, B, and C are also expressed in smooth muscle cells (Golomb et al., 2004;

Rochlin et al., 1995). NM MHC isoforms A, B, and C are encoded by 3 separate NM

MHC genes distinct from the SM MHC gene (Eddinger and Meer, 2007; Simons et al.,

1991). The three NM MHC isoforms are similar to the SM MHC in size and sequence

except that they do not have the head (7 amino-acid insertion in SMB MHC) or tail insert

(non coiled tail insertion in SM1). NM MHC C isoform is different from NM MHC A

and B in that NM MHC C has an additional 20 amino acids at the N-terminus and has

more variability in amino acid sequence compared to SM MHC (Golomb et al., 2004).

In addition to the presence of different MHC isoforms, different light chain

isoforms (LC_{17a}, LC_{17b}, LC_{20sm}, and LC_{20nm}) are also expressed in smooth muscle cells.

As a result of alternative splicing, two LC_{17} mRNA are derived from a single gene, which

consists of 7 exons. The difference between the two LC_{17} mRNAs stems from the

absence of a 44-nt insert (exon 6) at the 3'-end (Lenz et al., 1989). LC_{17a} and LC_{17b}

isoforms have different isoelectric points but are the same size (151 amino acids) and

have identical sequence except for 5 of the 9 amino acids at the C terminus, which can be

separated by two- dimensional polyacrylamide gel electrophoresis. The more acidic

isoform is LC_{17a}, and the more basic isoform is LC_{17b} (Hasegawa et al., 1988). There are

also two isoforms of LC_{20}, SM LC_{20} (LC_{20sm}) and NM LC_{20} (LC_{20nm}) in smooth muscle

cells. They are identified by comparing mass spectrometric data from tryptic peptides

with published cDNA sequence and differential expression patterns in smooth muscle

and non muscle tissues and encoded by two different genes which are translated to the

same size proteins (171 amino acids), except for 11 amino acids scattered throughout the

sequences (Kumar et al., 1989; Taubman et al., 1987). LC_{20sm} is more acidic than LC_{20nm}

(Eddinger and Meer, 2007; Gaylinn et al., 1989; Inoue et al., 1989).

SM contractions have been described as slow or fast based on their kinetic

properties. The rate of the actomyosin ATPase, the maximal shortening velocity (V_{max})

and the rate of force development and relaxation are three commonly used parameters to

quantify SM contractile kinetic properties. The cross-bridge contractile mechanism (the

mechanism by which myosin attaches and detaches to the actin) which was originally

proposed by the Huxleys and their collaborators (Hanson and Huxley, 1953; Huxley,

1954; Huxley, 1974; Huxley and Hanson, 1954)for skeletal muscle, is widely accepted to

regulate SM contractile properties. It is also believed to be the case that the cross-bridge

contractile mechanism is the major mechanism underlying the diverse kinetic properties

of SM contraction (Horiuti et al., 1989). Thus, unique contractile properties of myosin

and actin in the SM cells could affect SM contractile properties.

The structural differences among SM myosin isoforms result in their different

contractile properties. Studies have shown that the SMB MHC isoform, which has the

additional 7 amino acids near ATP binding site in the S1 head region, has a two-fold

greater ATPase activity than SMA MHC. Thus it is not surprising that the SMB MHC

isoform moves actin filaments approximately 2.5 folds faster than the SMA MHC

isoform in an *in vitro* motility assay (Kelley et al., 1993; Sweeney et al., 1998). Unloaded

shortening velocity in single rabbit stomach antrum cells expressing predominantly SMB MHC (~100%) is approximately 10 fold greater than single cells expressing predominantly SMA MHC in stomach fundus (~85%) (Eddinger and Meer, 2001). It has also been reported that loss of SMB MHC in mouse bladder decreases smooth muscle shortening velocity (Babu et al., 2001).

The contractile properties of SM1 and SM2 isoforms are less understood. Based on studies using antibodies to distinguish the SM1/2 isoforms, the suggestion was made that the C terminal regions of SM1 and SM2 are essential for filament size and stability and are able to affect ATPase activity (Horowitz and Trybus, 1992; Kuznicki et al., 1985; Pagh and Gerisch, 1986; Rovner et al., 1997; Rovner et al., 2002). Due to the longer non helical tail piece in SM1, the myosin filament formed by SM1 was proposed to be more stable than SM2 (shorter non helical tail piece isoform) (Meer and Eddinger, 1997; Rovner et al., 2002). However SM1 and SM2 isoforms move actin filament at the same rate in the in vivo motility assay (Kelley et al., 1992). In addition, studies from rabbit aortic and carotid single cells and early stages of pregnant rat uterus suggest that the SM1 and SM2 isoforms may not affect shortening velocity of smooth muscle cells (Meer and Eddinger, 1997; Morano et al., 1993).

Though smooth muscle NM MHC is quite similar in size and structure to the SM MHC isoforms, excluding the head and tail inserts appearing in SM MHC, the kinetics of the NM MHC ATPase are slower than SM MHC. Particularly, the NM MHCA and NM MHCB ATPase kinetics are slower than SM MHCs (Kovacs et al., 2003; Wang et al., 2003). This has led some researchers to propose that the NM MHCA and NM MHCB are

involved in the tonic component of smooth muscle contraction(Lofgren et al., 2003; Morano et al., 2000). Because NM MHC expression is very low in most adult SM tissues, this does not seem physiologically relevant (Eddinger and Meer, 2007).

The myosin light chain isoforms may also affect myosin contractile properties. The LC_{17b} isoform has been reported to be positively correlated with increased shortening velocity and ATPase activity (Helper et al., 1988; Malmqvist and Arner, 1991; Morano et al., 1993). Increasing the expression of LC_{17a} in cultured SMCs increases the rate of force development and tension production (Huang et al., 1999). However, the contribution of $LC_{17a/b}$ isoforms to unloading shortening velocity in SM cells and tissues is controversial. Hasegawa et al. reported that the expression of LC_{17b} is negatively correlated to actomyosin ATPase activity using reconstituted aortic myosin (Hasegawa et al., 1988). Similarly, Morano et al. suggested a positive correlation between shortening velocity and LC_{17a} content in smooth muscle of rat uterus (Morano et al., 1993). However, Kelley et al. showed that the content of LC_{17b} has no affect on ATPase activity of purified myosin (mostly SMB) from the turkey gizzard (Kelley et al., 1993). Similarly, Rovner et al. showed that the *in vitro* ATPase activity and motility speed of SMB myosin is not affected by the $LC_{17a/b}$ content (Rovner et al., 1997). Sweeney et al. also failed to find any correlation between LC_{17} isoforms and ATPase activity or in vitro motility sliding velocity of myosin (Sweeney et al., 1998). Work done by Eddinger et al. in isolated smooth muscle cells showed the unloaded shortening velocity of single smooth muscle cells is not correlated with the content of $LC_{17a/b}$ in the cell (Eddinger et al., 2000;

Eddinger and Meer, 2001). Thus the affects of $LC_{17a/b}$ isoform in smooth muscle are inconclusive.

LC_{20} phosphorylation is the primary event in initiation of SM contraction (Adelstein and Conti, 1975). It is reported that phosphorylation of LC_{20} activates actomyosin-ATPase activity by regulating the conformational changes of the S1 head domain, making the myosin more accessible to actin (Baumann et al., 2012; Liu et al., 2003; Nelson et al., 2005; Rovner et al., 2006; Wendt et al., 1999; Wendt et al., 2001). The extent of LC_{20} phosphorylation determines the shortening velocity and tension development (Hai and Murphy, 1989).

Based on the discussion above of published data, the different contractile properties of myosin (including V_{max}, actomyosin ATPase, and the rate of force development and relaxation) are primarily determined by different MHC isoforms. The effect of different LC isoforms (both LC_{17} and LC_{20}) on the contractile properties of myosin is minor and inconsistent and does not appear to be relevant.

Second messenger pathways

As mentioned above, there are reports that the different SM myosin isoforms are expressed uniquely in smooth muscle cells (SMC) and this may affect the contractile function of SMCs and tissues. Uniquely expressed SM MHC isoforms may be part of distinct contractile systems targeted by different secondary messenger signaling pathways most likely acting on regulation of LC_{20} phosphorylation (Figure 3). While LC_{20}

phosphorylation is not always proportional to the force generation in smooth muscle

tissues, it is believed to be a prerequisite for smooth muscle activation of myosin ATPase

activity and generation of force (Butler et al., 1983; Dillon et al., 1981; Persechini and

Hartshorne, 1981). The balance of kinase activities (to phosphorylate LC_{20}) and myosin

light chain phosphatase activities (to dephosphorylate LC_{20}) determines LC_{20}

phosphorylation levels (Kamm and Stull, 1985; Somlyo and Somlyo, 2003).

a. Phosphorylation of LC_{20}

Several kinases are reported to be able to phosphorylate LC_{20} *in vivo* and *in vitro*.

Of these, myosin light chain kinase (MLCK) is the most extensively studied and also

reported to be the primary physiological LC_{20} kinase in smooth muscle tissues. MLCK, a

serine/threonine protein kinase, can be activated by Ca^{2+}/calmodulin (CaM) and

phosphorylates Serine-19 in $LC_{20,}$ which leads to increased ATPase activity and force

production (Gao et al., 2001). Biochemical analysis indicates that MLCK consists of a

catalytic domain, a Ca^{2+}- CaM binding domain, and several actin and myosin binding

domains (Barden et al., 1996; Hong et al., 2011; Kanoh et al., 1993; Sellers and Pato,

1984; Silver et al., 1997; Sobieszek, 1985). Based on the MLCK sequence, MLCK is

proposed to be an elongated and flexible molecule capable of binding to both the actin

and myosin filaments (Kanoh et al., 1993; Silver et al., 1997). In the absence of Ca^{2+}-

CaM, MLCK is catalytically inactive by auto-inhibition. Under excitatory conditions,

elevated cytosolic free Ca^{2+} ($[Ca^{2+}]_i$) binds to CaM. Ca^{2+}-CaM triggers the
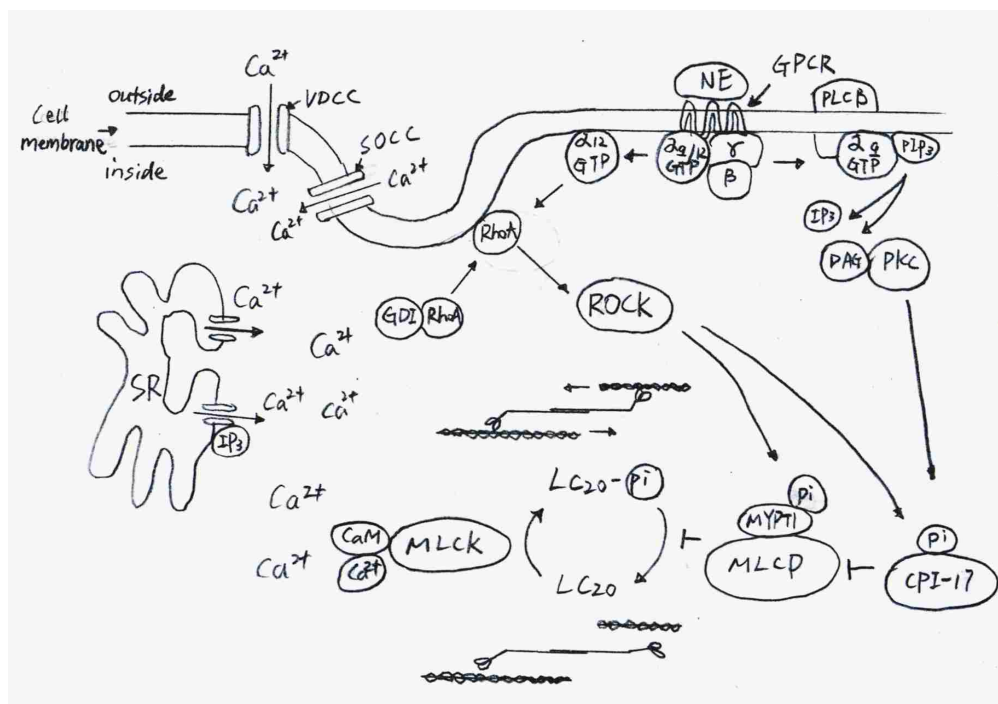
Figure 3. Schematic diagram of cellular signaling pathways regulating smooth muscle contraction (From Ratz et al., Am J Physiol Cell Physiol 2005). Depolarization opens voltage gated Ca^{2+} channels on the smooth muscle cell membrane such as Voltage-Operated Calcium Channel (VOCC), and store-operated Ca^{2+} channel (SOCC) and increases $[Ca^{2+}]_I$ by allowing the influx of extracellular Ca^{2+}. The elevated $[Ca^{2+}]_I$ then binds to CaM and activates MLCK which phosphorylates LC_{20} on myosin. The phosphorylated LC_{20} triggers conformational change of the myosin head to make myosin more accessible to actin filaments, thereby initiating the actomyosin cross-bridge cycling. Furthermore, actin filaments are connected to the cell membrane, extracellular matrix and cytoskeleton by adhesion proteins such as integrin, vinculin et al and dense bodies in the cell. The myosin sliding on actin filaments as a result of actomyosin cross-bridge cycling leads to smooth muscle contraction. G protein coupled receptor (GPCR) agonists such as norepinephrine (NE) can also regulate $[Ca^{2+}]_I$ by activating G proteins. Activated G proteins further activate PLCβ, which hydrolyzes PIP_2 on the cell membrane to inositol 1,4,5-trisphosphate (IP_3). IP_3 binds to IP_3 receptors on the sarcoplasmic reticulum (SR), and release the SR Ca^{2+} to the cytoplasm, which further opens ryanodine receptors (activated by Ca^{2+}) on SR releasing more Ca^{2+}.. MLCK mediated LC_{20} phosphorylation is Ca^{2+} dependent or Ca^{2+} sensitive. On the other hand, in order for LC_{20} to maintain its phosphorylation status, the activity of myosin light chain phosphatase (MLCP) needs to be inhibited. However, neither the activation or inactivation of MLCP requires $[Ca^{2+}]_I$. Therefore, it is Ca^{2+} independent or insensitive. Agonists induced contraction activates Ca^{2+} dependent LC_{20} phosphorylation by increasing $[Ca^{2+}]_I$ (as mentioned above), and inhibits MLCP activity which is Ca^{2+} independent by activating either PKC/CPi-17 signaling pathway or Rho/ROCK signaling pathway.

conformational change of MLCK to relieve its auto-inhibition allowing it to bind to

LC_{20} and ultimately phosphorylate LC_{20}(Barden et al., 1996). The increased $[Ca^{2+}]_i$ is

either from the influx of extracellular Ca^{2+} via depolarizing smooth muscle cells opening

of voltage gated Ca^{2+} channels on the cell membrane, or agonist induced G protein

signaling pathway mediated Ca^{2+} release from the sarcoplasmic reticulum (SR)

(Himpens et al., 1995; Karaki, 2004; Lee et al., 2002; McFadzean and Gibson, 2002).

Thus, LC_{20} phosphorylation depends on MLCK in a Ca^{2+} sensitive manner (Barron et al.,

1979; Hathaway and Adelstein, 1979; Rosenfeld et al., 1998; Trybus et al., 1994)(Figure

3). In addition to MLCK, other kinases such as integrin-linked kinase (ILK), zipper-

interacting protein kinase (ZIPK), Rho-associated kinase (ROCK) have also been

reported to phosphorylate LC_{20} (Amano et al., 1996; Niiro and Ikebe, 2001; Wilson et al.,

2005).

b. Signaling pathways regulating myosin phosphatase

Myosin light chain phosphatase (MLCP) is a trimeric enzyme capable of

dephosphorylating LC_{20}. MLCP consists of a regulatory subunit -myosin phosphatase

target subunit 1 (MYPT1), a catalytic subunit -PP1cδ, and a 20 kDa subunit whose

function is unknown (Hartshorne et al., 1998). The signaling pathways regulating MLCP

activity can be divided into two groups: (1) MLCP inhibiting and (2) MLCP activating.

Inhibition of MLCP activity can increase generation of force in smooth muscle by

allowing an increase in LC_{20} phosphorylation even in the absence of increased basal

kinase phosphorylation of LC_{20}. The LC_{20} phosphorylation level is dependent on the ratio

of kinase (such as MLCK, ILK, ZIPK, ROCK etc.) to MLCP activity. At the same

kinase activity level, the activity of MLCP determines the extent of LC_{20} phosphorylation,

which correlates with the extent of smooth muscle force production at certain levels of

phosphorylation. Thus, in order for smooth muscle to generate force, the MLCP activity

needs to be less than the kinase activity. On the other hand, in order for smooth muscle to

relax, the MLCP activity must be greater than the kinase activity. Neither inhibition nor

activation MLCP activity appears to require participation of Ca^{2+}. Thus, unlike MLCK

activation or inactivation of smooth muscle contraction or relaxation determined by

$[Ca^{2+}]_i$ (Ca^{2+} dependent), force enhancement or inhibition resulting from altered MLCP

activity is reported to be Ca^{2+} insensitive or Ca^{2+} independent (Hori and Karaki, 1998).

Thus, the regulation of LC_{20} phosphorylation and corresponding force generation involve

both Ca^{2+} sensitive (MLCK) and insensitive (MLCP) regulatory pathways (Ratz et al.,

2005)(Figure 3).

Based on MLCP structure, its activity can be regulated via MYPT1 and PP1cδ,

which are the targets of signaling pathways that inhibit MLCP activities. MYPT1 cannot

only activate MLCP by targeting MLCP to LC_{20} but it can also enhance MLCP catalytic

activity by binding to PP1cδ, the catalytic subunit of MLCP (Alessi et al., 1992; Shimizu

et al., 1994). Studies indicate that the small GTPase Rho and its target Rho associated

kinase (ROCK) signaling pathway is able to phosphorylate inhibitory sites on MYPT1

and inactivate MLCP in smooth muscle (Kimura et al., 1996). RhoA is a monomeric

GTPase and can be activated by extracellular G-protein coupled receptor binding in

smooth muscle contraction (Gong et al., 1996). Activated RhoA is reported to translocate

to the cell membrane and activate ROCK tethered there. ROCK is a serine/threonine

kinase protein and is believed to regulate multiple cellular functions including motility,

proliferation, and apoptosis in many cell types (Guilluy et al., 2011; Street and Bryan,

2011). For smooth muscle cells, ROCK is also involved in regulating cell contraction.

When activated, the serine/threonine kinase activity of ROCK is able to phosphorylate

MYPT1 at Threonine-696 and Threonine-853 inactivating MLCP (Feng et al., 1999).

Similarly, MLCP can also be inactivated by inhibiting the activity of its catalytic subunit,

PP1cδ. When activated, potentiated PP1 inhibitory protein of 17 kDa (CPI-17 activated

by PKC not MLCK) acts as a pseudo-substrate of MLCP by binding to PP1cδ and

competing with LC$_{20}$ for phosphorylation (Eto et al., 2004). Thereby, CPI-17 inactivates

MLCP by targeting PP1cδ. Activation of CPI-17 is regulated by phosphorylation of

Threonine-18 on CPI-17. Protein kinase C (PKC) is the major kinase to phosphorylate

CPI-17. PKC is activated by diacylglycerol (DAG), which is produced through agonists

stimulation GTP coupled protein signaling pathways. Thus the inhibitory phosphorylation

of MYPT1 and PP1cδ are significantly mediated by the Rho/ROCK and PKC/CPI-17

pathways respectively. However more and more *in vivo* and *in vitro* evidence suggests

that in the process of smooth muscle contraction there is crosstalk between the

Rho/ROCK and PKC/CPI-17 pathways to fine tune MLCP activity. This enables smooth

muscle tissues to display diverse contractile patterns. The most direct evidence is that

apart from PKC, ROCK is also capable of activating CPI-17 (Koyama et al., 2000).

Likewise, it has also been demonstrated that PKC can mediate activation of ROCK in

porcine coronary artery spasm (Kandabashi et al., 2003). Furthermore, other kinases

(ZIPK, ILK, protein kinase N (PKN)), upstream of MLCP also exhibit inhibitory

phosphorylation of MLCP. The significance of the role they play in controlling smooth

muscle contraction *in vivo* is unknown and still under investigation (Hamaguchi et al.,

2000; MacDonald et al., 2001; Ohama et al., 2003).

Compared to the Rho/ROCK and PKC/CPI-17 MLCP inhibitory pathways, the

signaling pathways that activate or promote MLCP activity are less well understood. The

nitric oxide (NO) pathway is the most studied signaling pathway that relaxes smooth

muscle contraction. The postulated mechanism for NO mediated smooth muscle

relaxation includes inhibiting the Rho/ROCK pathway and counteracting its inhibitory

phosphorylation on MYPT1. NO is able to increase the intracellular level of cGMP which

activates PKG (cGMP-dependent protein kinase). Activated PKG inactivates RhoA by

phosphorylating RhoA at Serine-188. Moreover, activated PKG also phosphorylates

MYPT1 at Serine-695, which activates MLCP and prevents inhibitory phosphorylation at

Threonine-696 on MYPT1 at the same time (Wooldridge et al., 2004). Telokin, an

exclusively expressed smooth muscle protein, is identical to the C terminus of MLCK but

with much smaller size. It has been reported to be involved in promoting MLCP activity

when it is activated by an unknown mechanism (Khromov et al., 2006). Therefore,

MLCP activity appears to be regulated by a network of signaling pathways to modify the

SM contractile response.

c. Other regulatory mechanisms regulating smooth muscle contraction

It is widely accepted that phosphorylation of LC_{20} is not the only mechanism

regulating smooth muscle contraction. The contractile properties of smooth muscles are

broadly classified as tonic and phasic. Upon stimulation, tonic smooth muscle is able

to maintain sustained high force level whereas phasic smooth muscle exhibits a rapid

transient force generation followed by a decrease in force to a low level (Somlyo and

Somlyo, 1968). The differences between tonic and phasic contractile patterns cannot be

explained by the time course of $[Ca^{2+}]_i$ or phosphorylation of LC_{20} upon stimulation. In

both phasic and tonic smooth muscles, the $[Ca^{2+}]_i$ and phosphorylation of LC_{20} increase

rapidly upon stimulation and then decrease to an intermediate steady state (Dillon et al.,

1981; Rembold and Murphy, 1986). The same thing occurs with the maximal shortening

velocity (V_{max}). V_{max} rapidly increases to the maximal value upon stimulation then

decreases to an intermediate level. In phasic smooth muscle, force generation patterns

follow the $[Ca^{2+}]_i$ and phosphorylation levels of LC_{20}. However, in tonic smooth muscle,

after initial force activation, despite decreases in $[Ca^{2+}]_i$ and dephosphorylation of LC_{20} to

submaximal levels, force can be maintained at a sustained high level. This force

maintenance with low $[Ca^{2+}]_i$, LC_{20} phosphorylation and V_{max} is referred to as the "latch

state" (Dillon et al., 1981; Hai and Murphy, 1988; Rembold and Murphy, 1986). The

mechanism underlying the latch state is unknown. Several regulatory mechanisms have

been hypothesized including cytoskeletal remodeling (Gerthoffer and Gunst, 2001; Hu et

al., 2007; Kim et al., 2008; Mehta and Gunst, 1999; Pavalko et al., 1995), second

messenger pathway regulation of MLCK/MLCP activity (Harnett et al., 2005; Jiang and

Morgan, 1987; Poole and Furness, 2007; Rattan et al., 2006; Sohn et al., 2001; Urban et

al., 2003), altered kinetics of phosphorylated vs. dephosphorylated myosin cross-bridges

(Dillon et al., 1981; Hai and Murphy, 1989), and the kinetic properties of actomyosin

ATPase of different myosin isoforms (NM myosin and SM myosin) (Fuglsang et al.,

1993; Khromov et al., 1995; Kovacs et al., 2007; Lofgren et al., 2003; Morano et al., 2000; Rosenfeld et al., 2003; Wang et al., 2003).

An actin related cytoskeletal remodeling mechanism has been suggested to be involved in regulating tonic and phasic contractions as changes in the quantity of actin filament (F-actin) would be proportional to force generation. Thus regulatory proteins and corresponding signaling pathways controlling actin stability and polymerization may play a role in different smooth muscle contractile patterns including tonic and phasic contractions. Haeberle reported that *in vitro* motility of unphosphorylated and phosphorylated myosin purified from chicken gizzard is affected by actin polymerization, which may suggest a role of actin in regulating tonic contraction (Haeberle, 1999). Work from Gunst's group studying tracheal smooth muscle contraction also suggested that actin filament stability and dynamics are critical for tonic contraction (Gerthoffer and Gunst, 2001; Mehta et al., 1998; Mehta and Gunst, 1999). Thus proteins regulating actin polymerization such as cofilin, RhoA, and Arp2/3 complex may also be able to regulate smooth muscle contraction (Zhang et al., 2005; Zhang et al., 2010; Zhao et al., 2008). However, a study from Bednarek et al. indicated that the changes in actin polymerization do not alter tonic and phasic contractions differently, suggesting that the effect of actin filament stability on both the tonic and phasic contractions are the same (Bednarek et al., 2011). Therefore, the inconsistent results from the studies of actin filament stability in smooth muscle contraction indicate that the actin related cytoskeletal-remodeling mechanism might not be sufficient to explain tonic and phasic contractions.

The involvement of differentially recruited secondary messenger signaling

pathways is another mechanism proposed to explain tonic and phasic contractions. As
mentioned above, the key event in secondary messenger signaling pathway mediated
smooth muscle contraction is LC_{20} phosphorylation, the status of which is determined by
MLCK/MLCP activities. It has been suggested that the sustained force is due to the high
level of LC_{20} phosphorylation via inhibiting MLCP activity during tonic contraction in
comparison with phasic contraction. The mechanism underlying is that for both the tonic
and phasic contractions, upon stimulation, $[Ca^{2+}]_I$ increases, which activates MLCK.
Activated MLCK then phosphorylates LC_{20}. At the same time MLCP activity is inhibited
to prevent phosphorylated LC_{20} from being dephosphorylated. The high MLCK activity
vs. low MLCP activity leads to high level of LC_{20} phosphorylation. During this process,
force is initiated and continues to increase until the point when $[Ca^{2+}]_I$ begins to decrease
to a intermediate level. Accordingly, Ca^{2+} dependent MLCK activity also decreases.
During this time MLCP continues to be inhibited in tonic contractions whereas MLCP is
not inhibited or may be activated in phasic contraction. Though decreased MLCK activity
results in less LC_{20} phosphorylation, the inhibited MLCP is unable to dephosphorylate
already phosphorylated LC_{20}, therefore, the LC_{20} phosphorylation level remains high and
results in a high level of sustained force in tonic contraction. For the phasic contraction,
decreased MLCK and activated MCLP activities decrease LC_{20} phosphorylation, which
results in force falling to a low level. This mechanism fails to elucidate the low LC_{20}
phosphorylation and high level of sustained force in tonic contraction. Furthermore,
which secondary signaling pathway regulates tonic contraction is uncertain. Involvement
of PKC/CPI-17signaling pathways mediated tonic contraction is supported by the
following studies: Jiang et al., reported that the PKC/CPI-17 signaling pathway is able to

regulate tonic contraction with phorbol ester stimulation (Jiang and Morgan, 1987).

Work from Sohn et al., suggested that PKCε is responsible for maintenance of tonic tone

induced by PGF2α or a thromboxane analog in lower esophageal sphincter (LES) (Sohn

et al., 2001). Poole et al., reported that PKCδ isoform is able to enhance tonic contraction

in guinea pig ileum (Poole and Furness, 2007). However, it has also been reported that

the Rho/ROCK signaling pathway may be responsible for tonic contraction. Urban et al.,

showed that activation of the Rho/ROCK signaling pathway is involved in the tonic

contraction of femoral and renal arterial smooth muscle (Urban et al., 2003). Others have

also reported that RhoA might be involved in sustained contraction of LES (Harnett et al.,

2005). Rattan et al. demonstrated in single smooth muscle cells that Rho/ROCK plays a

critical role in the rat internal anal sphincter (IAS) tonic contraction (Rattan et al., 2006).

Thus, the inability to explain the relation of a low level of LC_{20} phosphorylation and high

level maintained force in tonic contraction and the inconsistent results obtained in

different smooth muscle tissues leave unresolved the proposal that a mechanism that

differentially recruits secondary messenger pathways is a major factor in determining

tonic and phasic contractions.

The altered kinetics of phosphorylated vs. dephosphorylated myosin cross-bridges

was proposed by Murphy and colleagues to elucidate the mechanism underlying tonic

and phasic contractions (Dillon et al., 1981; Hai and Murphy, 1989). They hypothesized

that cross bridge phosphorylation (phosphorylation of LC_{20}) is required for cross bridge

attachment, but that dephosphorylating of an attached cross bridge reduces its detachment

rate. Both the phosphorylated and dephosphorylated cross bridge are capable of

generating the same amount of force. This can explain high levels of sustained force with intermediate levels of LC_{20} phosphorylation. As mentioned previously, LC_{20} dephosphorylating occurs via MLCP, which is Ca^{2+} independent. Therefore, in this scenario, the low $[Ca^{2+}]_i$ does not affect the ability to maintain force at high level in tonic smooth muscle. However, Murphy and colleagues(Hai and Murphy, 1989) determined that phosphorylated cross bridge is fast cross bridge and dephosphorylated cross bridge is slow cross bridge based on the study from Gorecka et al. (Gorecka et al., 1976), which reported that the ATPase activity of smooth muscle actomyosin is proportional to LC_{20} phosphorylation. But covalent phosphorylation modification of LC_{20} imposes an ATP cost that appears inconsistent with the extraordinary economy of force maintenance (Paul, 1989). A mechanical distinction between phosphorylated and dephosphorylated cross bridges remains unsolved. A better way to test phosphorylated and dephosphorylated cross bridge mechanics needs to be developed.

The expression of different MHC isoforms in smooth muscles and relevance to tonic and phasic contractions.

As mentioned above there are different myosin isoforms with distinct contractile kinetics expressed in smooth muscle. The tonic and phasic contractile patterns may be caused by different myosin isoforms. The contractile properties of the smooth muscle myosin isoforms are determined by its subunits, the MHCs and LCs. There appears to be a preponderance of evidence that the contractile kinetic properties of smooth muscle myosin are LC_{17} isoform independent for both *in vitro* and *in vivo* measurement (Eddinger et al., 2000; Eddinger and Meer, 2001; Kelley et al., 1993; Rovner et al., 1997;

Sweeney et al., 1998). No functional differences for the two LC_{20} isoforms have been definitively identified either. Therefore, the role of smooth muscle myosin isoforms in determining tonic and phasic contractions would need to be primary dependent on the properties of MHC isoforms. There are seven MHC isoforms present in smooth muscle including four SM MHCs (SM1, SM2, SMA, and SMB) and three NM MHCs (NM MHCA, B, and C, however MHCC not expressed in SM to any significant amount). There have been reports supporting the expression of the NM MHCB isoform with tonic contractions. The kinetics of actomyosin ATPase of NM MHCB have been reported to be slower than the other seven MHC isoforms (Wang et al., 2003). In the presence of actin, NM MHCB has high ADP affinity and a low rate of ADP release, which enables NM MHCB to attach to actin for an extended period (Rosenfeld et al., 2003). The actin-myosin- ADP of NM MHCB requires mechanical strain to release ADP. With tonic force maintenance, the long attachment time of NM MHCB to actin could explain the latch cross bridge(Kovacs et al., 2007). Studies from Morano et al. showed that bladder smooth muscle from SM MHC knockout mice generates a slow tonic contraction, whereas the wild type bladder smooth muscle develops a phasic contraction (Morano et al., 2000). A subsequent study from Lofgren et al. supports the role of NM MHCB in the tonic contraction by showing that $[Ca^{2+}]_I$ levels are the same between knockout and wild type bladders and the V_{max} of knockout bladder smooth muscle is more ADP sensitive than wild type bladder (Lofgren et al., 2003). Thus tonic contraction could result from expression of the NM MHCB isoform. However, the expression of NM MHCB is developmentally regulated and tissue specific (Eddinger and Murphy, 1991; Eddinger and Wolf, 1993; Phillips et al., 1995; Tullio et al., 1997). In the adult wild type mouse

bladder where the expression of non-muscle myosin decreases to little or none the tonic contraction continues to be present. In the adult rabbit tissues, the expression of non-muscle myosin is undetectable, however the tonic contractions are still present (Eddinger and Meer, 2007; Giuriato et al., 1992; Han et al., 2006). Thus, the non-muscle myosin isoforms including NM MHCB may not be the major regulator for tonic contractions in adult animals due to their low expression level in these animals.

The tail isoforms of smooth muscle myosin (consisting of SM1 and SM2 SM MHC isoforms) also seem unlikely to be the primary factor in tonic contractions. The SM1-to-SM2 ratio is uncorrelated to distinct contractile kinetics including unloaded shortening velocity and force generation. Studies carried out by Sparrow et al. in skinned rat myometrial muscle indicated SM1 is positively related to shortening velocity. Non-pregnant rat myometrium smooth muscle tissue with higher SM1/SM2 ration has higher V_{max} than non-pregnant rat which has lower SM1/SM2. However when studied with skinned fibers, they obtained a contradictory result that V_{max} of Non pregnant rat uterine smooth muscle fiber is lower than V_{max} of the uterine smooth muscle of pregnant rat (Sparrow et al., 1988). Furthermore, studies using either intact smooth muscle tissues or single smooth muscle cells from variety of smooth muscle organs all fail to find distinct physiological functions of the SM1 and SM2 isoforms (Cai et al., 1995; Kelley et al., 1992; Meer and Eddinger, 1997; Morano, 2003). Results from SM2 knockout mouse bladder and aortic smooth muscles showed enhanced contractility suggesting that SM2 may negatively regulate smooth muscle contraction (Chi et al., 2008). But this conclusion does not take into account possible results from down regulated SM1 and reduced thick

filament with the loss of SM2. In addition, no distinct expression patterns of SM1 and SM2 are reported in tonic or phasic tissues. Rovner and Murphy reported that the SM1 and SM2 are equally expressed in swine carotid and stomach (Rovner et al., 1986). Other studies suggested the SM1:SM2 ratio in different tissues varies within a narrow range from 40:60 to 60:40 (Borrione et al., 1989; Eddinger and Murphy, 1991; Kuro-o et al., 1989; Murakami and Elzinga, 1992; Szymanski et al., 1998). To date, no results have been reported clearly demonstrating that SM1 and SM2 expressions are tonic and phasic tissue related.

In contrast to the SM1 and SM2 isoforms, the expression of SMA and SMB MHC isoforms (the head isoforms) are expressed preferentially in tonic and phasic tissues. It is reported that the mRNA and protein of SMB MHC isoform is predominantly expressed in visceral smooth muscle tissues including colon, ileum, veins such as the vena cava and saphenous, and bladder, which are all phasic tissues (Eddinger, 2009; Han et al., 2006; Rondelli et al., 2007; White et al., 1993). The mRNA and protein of SMA MHC isoform is primarily found in elastic arteries such as aortic, renal and femoral artery, and the uterus, which are tonic tissues(Babij, 1993; Eddinger et al., 2007; Han et al., 2006; Rondelli et al., 2007). Even within a single tissue, the expression of SMB and SMA MHC isoforms are different. In the rabbit stomach tissue, approximately 90% of phasic antrum SM MHC mRNA is the SMB MHC, whereas 90% of tonic fundus SM MHC mRNA is the SMA MHC (Eddinger and Meer, 2001). It appears that SMA /SMB MHC expression is tonic/phasic-tissue specific. Furthermore, the seven amino-acid insertion in the S1 head of SMB MHC makes myosin ATPase activity approximately twofold greater

than SMA MHC, which is consistent with the kinetics of phasic contraction. On the

other hand, the slow ATPase activity of SMA MHC is also consistent with the kinetic of

tonic contraction which has a five times higher MgADP affinity and 3 times lower

second- order rate constant for MgATP than SMB MHC (Dillon et al., 1981; Somlyo et

al., 1998). Thus it is reasonable to postulate the existence of physiological relevance of

SMA and SMB MHC expression to tonic and phasic contractile patterns in corresponding

smooth muscle tissues. In an effort to investigate this hypothesis, several research articles

have been published based on a SMB knockout mouse model. The results of this work

from Periasamy and others showed that SMB knockout bladder and trachea produce

significantly less force than wild type tissues. Similarly, the shortening velocity of SMB

knockout tissues is also slower than wild type controls (Babu et al., 2001; Tuck et al.,

2004). Studies from the same group but using different tissues (aorta and mesenteric

vessels) demonstrated that the SMB knockout tissues are able to produce more force than

wild type tissues. Likewise, the shortening velocity of SMB knockout tissues are

decreased compared to wild type controls (Babu et al., 2004). However, since the

expression of SMB MHC in wild arterial tissues is only trace amounts, the SMB

knockout in these tissues does not result in any significant SMA/B MHC expression shift

between SMB knockout and wild type tissues. They concluded the decreased contractility

in the SMB knockout tissues is due to the increased expression of thin filament regulatory

proteins calponin, microtubule affinity regulating kinase (MARK), and caldesmon (Babu

et al., 2004). Results from Patzak et al. using the same animal model reported that there

is not a correlation between SMB MHC expression and the rate of force generation in

perfused afferent and efferent renal arterioles (Patzak et al., 2005). Hypolite et al.

reported that compared to wild type, the loss of SMB MHC in detrusor smooth muscle increases contraction due to the up-regulation of the PKC mediated signaling pathway (Hypolite et al., 2009).

The results of studies done on the same animal model from different groups in different tissues appear inconsistent. Thus the role of SMA/B MHC isoforms in SM tonic and phasic contractions remains unresolved. The focus of the above reports on the SMB knockout mouse is primarily on the role the SMA/B MHC isoforms play in the peak force generation (phasic component) and shortening velocity of smooth muscle tissues. They did not investigate the relationship between SMA/B MHC isoforms and sustained force maintenance in tonic contraction, which is the primary characteristics distinguishing tonic and phasic contraction. Thus, the question of the contractile patterns (tonic and phasic) and their relationship with SMA/B MHC isoform expression remains to be addressed. The SMB knockout mouse model is a good model to examine this question.

The objective and the significance of the project

Smooth muscle is specialized to generate force and shortening and is responsible for the contraction of hollow organs including the gastrointestinal tract, bladder, uterus and blood vessels. The contraction of smooth muscle needs to be precisely regulated to ensure different spatiotemporally physiological functions including food digestion in the intestine, urine storage in the bladder, and blood pressure maintenance in blood vessels. Since it was postulated more than half a century ago, the Huxley's sliding filament theory

has shed light on the mechanism of muscle contraction (Huxley, 1954; Huxley and

Hanson, 1954). For over three decades, it has also been known that unlike skeletal muscle,

the phosphorylation of LC_{20} on the SM myosin head is a pivotal and unique covalent

modification of smooth muscle myosin that regulates contraction (Sobieszek, 1977).

However, force generation is not always proportional to the level of LC_{20}

phosphorylation. In certain smooth muscle tissues (tonic smooth muscle), force may be

maintained at a high level for minutes to hours, while phosphorylation of LC_{20} is

decreased to near basal level. This state has been referred to as the "latch state". The LC_{20}

phosphorylation mechanism is insufficient to explain this. The mechanism for force

maintenance in tonic contraction compared to phasic contraction is not clear. Based on

the previous discussion, the SMA/B MHC isoforms may be involved in tonic and phasic

contractions. The unique tissue distribution and kinetics of actomyosin ATPase activity

of the SMA and SMB MHC isoforms may contribute to tonic and phasic contractions.

SMA and SMB myosin isoforms may generate their unique contractile patterns in

different tissue types.

The objective of this project is to test the hypothesis that SM SMA and SMB

MHC isoforms are responsible for regulating tonic and phasic contractions respectively

in smooth muscle. To evaluate this hypothesis, three specific aims were carried out (1) To

determine if SMB MHC expression is required for smooth muscle to exhibit phasic

contraction, or phasic charateristics. (2) Investigate if replacing SMB MHC with SMA

MHC isoform is able to cause a tonic contraction or tonic characteristics in a phasic

tissue where SMB MHC is predominantly expressed. (3) Examine in addition to

SMA/SMB MHC isoforms, if the secondary messenger pathways are also involved in regulating tonic and phasic contractions. To do these studies, we utilized a SMB MHC knockout mouse kindly provided by Drs. Babu and Periasamy (Babu et al., 2001).

This project is of significant importance in the following aspects: (1) As discussed previously, six research articles have been published using the SMB knockout mouse model, but the results does not directly address the possible role of the SM SMA/B MHC isoforms on tonic and phasic contraction. This project looked directly at if and how expression of the SMA/B MHC isoforms relates to tonic and phasic contraction in smooth muscle. (2) The latch cross- bridge and latch state has been proposed for long time to explain the sustained force maintenance with low ATPase activity, LC_{20} phosphorylation, and $[Ca^{2+}]_I$ (Dillon et al., 1981; Rembold and Murphy, 1986). However, how the latch state is achieved and why the latch state only appears in some smooth muscle tissue remains unresolved. This project tested whether SMA/B MHC isoform expression can explain the sustained force production (latch state) in SM. (3) The contraction of smooth muscle plays a vital physiological function in various systems including gastrointestinal, cardiovascular, reproductive and respiratory systems. The regulation of smooth muscle contraction is a complicated network composed of various regulatory mechanisms (secondary messenger signaling regulation, cytoskeleton regulation, cross-bridge cycling regulation etc.). Understanding the regulation of tonic and phasic contractile patterns will provide insight to smooth muscle contraction regulatory mechanisms. Additionally, defects of smooth muscle contraction in many of these systems can lead to clinical diseases, including inflammatory bowel diseases,

systematic hypertension, preterm labor, chronic pulmonary obstructive disease, and asthma. It is reported that the expression of SMB MHC is significantly reduced in precapillary hypertensive rats. Thus, the understanding of regulatory mechanisms that control smooth muscle contraction may provide targets for the development of therapeutics to treat these diseases.

II. Materials and methods:

A. Mouse strains:

The B6/129 wild type and SMB$^{(-/-)}$ mice (Babu et al., 2001), 22-25weeks old, were used for all the experiments. All the animals used in this project were approved by the Marquette Institutional Animal Care and Use Committee (IACUC) under protocol number AR-221.

B. Polymerase chain reaction (PCR) genotyping:

SMB $^{(+/-)}$ mice, generously provided by Dr. Periasamy, were crossed to produce wild type and SMB$^{(-/-)}$ offspring. Wild type, SMB $^{(+/-)}$ and SMB $^{(-/-)}$ mice genomic DNAs were extracted from tail clips. 0.5 cm mice tail tips were clipped and digested in a digestion buffer (0.5% Tween 20, 1.0mM EDTA pH 8.0, 50mM Tris base pH 8.0) with 0.8g/L proteinase K overnight at 55°C. Proteinase K was inactivated by heating at 99°C for 5 minutes. Mouse genomic DNA was isolated using 14,000 revolutions per minute (rpm) centrifugation for 5 minutes and used as PCR templates. The PCR reaction system and cycles were as follows: All PCR reactions were conducted in a 50μl, containing 1.0μl 700ng/μl DNA template, 5.0μl 10X platinumTaq polymerase buffer, 1.5μl 1.5mM MgCl$_2$, 1.0μl 10mM dNTP mix, 0.2μl Platinum Taq (Invitrogen, Carlsbad, California) and 2.0μl 100μM primer mix (WT forward: 5'-CAA GGT CCA TCT TTT GCC TAC-3', WT reverse: 5'-GCA ATC CAT CCA GGC TGG AGT-3', KO forward: 5'-GGC ACA ACA GAC AAT CGG CT-3', KO reversed: 5'-ACT TCG CCC AAT AGC AGC CA-3':

Operon, Alameda, CA). The DNA templates were melted at 94°C for 2 minutes and

followed by 44 amplification cycles: 94°C denaturation for 30 seconds, 55°C annealing

for 30 seconds and 72°C extension for 1 minute. The end products were stored at 4°C.

The Ericomp thermoelectric thermocycler (Scientific Plastics, Kansas City, KS) was used

as PCR apparatus. The PCR products generated with WT primers and KO primers are

245bps and 219bps, which correspond to SMB MHC mRNA 5b exon and PGK promoted

neomycin mRNA respectively.

C. Tissue preparations:

Mice were euthanized by Carbon Dioxide (CO_2). Stomach tissues (fundus,

antrum) and ileum were isolated, cleaned of blood, adipose and chyme and kept in

physiological salt solution (PSS: 4.7mM KCl, 140mM NaCl, 1.2mM Na2HPO$_4$, 2.0 mM

3-(N-morpholine) propanesulfonic acid (MOPS), 0.02mM ehtylenediaminetetraacetic

acid (EDTA), 1.2mM MgSO$_4$, 1.6mM CaCl$_2$, 5.6mM glucose, pH 7.4 at 37°C) at 4°C

until processed (no longer than 24 hours).

D. Electrophoretic Analysis:

1. DNA electrophoresis:

3μl Loading dye (2.5 g/L bromophenol blue, 400g/L sucrose)(6x) mixed with

15μl of PCR products were loaded into 1.5% agarose gel pre-stained with 0.2μg/ml

ethidium bromide and run at 100 volts for 30 minutes. Tris-acetate-EDTA buffer (TAE:

40mM Tris base, 20mM acetic acid, 1mM EDTA) was used as the buffer system. The

results of DNA electrophoresis were visualized and images were captured on a U.V.

trans-illuminator (Voytas, 2001).

2. Sodium dodecyl sulfate polyacrylamide gel electrophoresis (SDS-PAGE):

SDS-PAGE gels were made using the methods of Giulian et al (1983). 50mg

Fundus and antrum tissues without mucosa were homogenized in 1ml sample buffer

(0.0625M Tris pH 6.8, 0.1% (v/v) sodium dodecyl sulfate (SDS), 15%(w/v) glycerol.

0.01%(w/v) bromophenol blue, 15mM dithiothreitol (DTT)) using a glass pestle and

boiled at 100°C for 5 minutes followed by centrifugation at 13000 rpm for 10 minutes.

The supernatant was collected as samples for protein analysis. 50mg/ml samples were

loaded onto 8cmx10cmx1mm 15% polyacrylamide gels. Based on the preliminary

protein loading standard curves, the loading volume for analyzing proteins was: β actin,

PKCα, SMB MHC, SMA MHC, total myosin heavy chain (SM+NM), LC_{20},

phosphorylated LC_{20} - 15μl per lane, for MLCK and MYPT1 - 30μl per lane and for

PKCδ, NM myosin, and CPI 17 - 70μl per lane. The SDS-PAGE was run at 20mA/gel at

20°C for 4.5 hours or 5mA/gel overnight using Hoefer SE600. 10 μl PageRuler pre-

stained protein separation ladder (Thermo Scientific, Rockford, IL) with proteins ranging

from 10kDa to 170kDa was loaded into the first lane.

3. Western blot analysis:

After electrophoresis, western blots were run for the analysis of proteins SMA

MHC, SMB MHC, total myosin heavy chain, MLCK, MYPT1, PKCα, and PKCδ.

Gels were equilibrated at room temperature for 1 hour in myosin heavy chain transfer

buffer (25mM Tris HCl, 192mM glycine, 20% methanol, and 0.1% SDS PH 8.3 (Walsh

et al., 2011). Proteins separated by SDS-PAGE then were transferred to nitrocellulose

membrane (0.2μm; Amersham Hybond ECL, GE healthcare, Buckinghamshire, UK) at

200 mA for 4.5 hours at 4°C using Hoefer TE (Hoefer scientific, San Francisco, CA). For

the analysis of proteins β actin, CPI-17, LC_{20}, and phosphorylated LC_{20}, gels were

equilibrated for 30 minutes in myosin light chain transfer buffer (10mM N-cyclohexyl-3-

aminopropanesulfonic acid (CAPS), pH 11 and 10% methanol), and then transferred to

nitrocellulose at 220 mA for 3 hours at 4°C using GENIE blotter (IDEA scientific,

Minneapolis, MN). After blotting, the nitrocellulose membranes were blocked with 5%

non-fat dry milk in Tris buffered-saline containing Tween 20 (TBST: 20mM Tris HCl,

pH 7.5, 137 mM NaCl, 3mM KCl, and 0.05% Tween 20) for 1 hour at room temperature.

The membrane was then incubated with primary antibodies in 1% non-fat dry milk TBST

for 4 hours. Primary antibody information is shown in Table 1. Membranes were washed

in TBST three times for 5 minutes each and then incubated in the secondary antibodies

for 2 hours. Secondary antibody information are summarized in Table 2. The membranes

were washed three times for 5 minutes each in TBST again. Chromomeric substrate-3.3'-

diaminobenzidine (DAB) was used to detect proteins. Nitrocellulose membranes were

incubated in developing solution (0.01% H_2O_2 (v/v), 0.05% DAB (w/v), 0.01M

Imidazole) (Eddinger and Wolf, 1993) for 30 seconds to 2 minutes. The protein bands on

the membranes were scanned by EPSON expression1600 scanner and quantified by

densitometric analysis using the software Image J (http://rsbweb.nih.gov/ij/). To

Primary antibody	Dilution	Catalogue Number	Resources
Polyclonal rabbit anti PKCα	1:500	sc-208	Santa Cruz biotechnology, Santa Cruz, CA
Polyclonal rabbit anti PKCδ	1:200	sc-213	Santa Cruz biotechnology, Santa Cruz, CA
Polyclonal rabbit anti MYPT1	1:500	sc-25618	Santa Cruz biotechnology, Santa Cruz, CA
Polyclonal rabbit anti LC_{20}	1:250	sc-15370	Santa Cruz biotechnology, Santa Cruz, CA
Polyclonal goat anti MLCK	1:500	sc-9452	Santa Cruz biotechnology, Santa Cruz, CA
Polyclonal goat anti CPI-17	1:200	sc-30927	Santa Cruz biotechnology, Santa Cruz, CA
Polyclonal rabbit anti SMA MHC	1:1000	N/A	Eddinger, 2009
Polyclonal rabbit anti SMB MHC	1:1000	N/A	Eddinger, 2009
Polyclonal rabbit anti total myosin chain (SM+NM MHC)	1:2000	BT-562	Biomedical Technologies, Stoughton, MA
Polyclonal rabbit anti non muscle myosin	1:500	BT-561	Biomedical Technologies, Stoughton, MA
Polyclonal rabbit anti phosphorylated LC_{20} at Ser19	1:1000	3381	Minipore, Temecula, CA
Monoclonal mouse anti β actin	1:1000	A1978	Sigma, St. Louis, MO

Table 1. Primary antibody information used in western blot.

Secondary antibody	Dilution	Catalogue Number	Resources
Goat anti rabbit IgG-horseradish peroxidase-conjugated	1: 10,000	111-035-003	Jackson ImmunoResearch Laboratoeries, West Grove, PA
Goat anti mouse IgG-horseradish peroxidase-conjugated	1:10,000	115-035-003	Jackson ImmunoResearch Laboratoeries, West Grove, PA
Donkey anti goat IgG-horseradish peroxidase-conjugated	1:5,000	HAF109	R&D System, Minneapolis, MN

Table 2. Secondary antibody information used in western blot.

minimize variability, tissue samples from a single animal were run in triplicate. Densitometric results of the three runs were averaged, and used as an n=1 for data analysis.

E. Force Measurement:

The mucosa and connective tissues were dissected away from underlying smooth muscle tissues (fundus, antrum, and ileum). The dissection of tissue strips followed the protocol of Driska et al (1981). Circular smooth muscle tissues were cut into strips which were held at each end by tissue clips (PY8 56-5119 Harvard Apparatus, Holliston, MA) mounted on the two hooks to an isometric force transducer (Harvard Apparatus, Holliston, MA) and a stationary post for tension measurements. Force signals obtained from force transducers were processed by an analog to digital converter (PowerLab/8SP, ADInstruments, Sydney, Australia) and analyzed using Chart5 software (ADInstruments, Sydney, Australia) on a personal computer. The strip sizes between the two clips were approximately 3mm in width and 7mm in length. The mounted tissues were bathed in 10 ml glass chambers (Radnoti glass technology, Monrovia, CA) and aerated with 95% O_2/5% CO_2 to maintains the bicarbonate buffering system throughout the experiments at 37°C which was maintained by an immersion circulator (VWR, West Chester, PA). The mounted tissues were equilibrated in PSS for 1 hour at 37°C. By adjusting strip length, a 0.9 g preloaded force was applied for the tissue strip to reach the length for optimal tension development. Tissue strips were contracted using high potassium containing physiological saline solution (KPSS: 109.65mM KCl, 1.2mM Na_2HPO_4, 2.0mM MOPS, 0.02mM EDTA, 1.2mM $MgSO_4$, 5.6mM glucose, 1.6mM $CaCl_2$, 35.1mM NaCl PH 7.4

at 37°C) for three contraction and relaxation cycles. All subsequent experiments

included 1μM phentolamine and 0.1μM propranolol to eliminate the potential

neurotransmitter activities. KPSS responsive force traces were obtained in the presence of

KPSS for at least 15 minutes followed by relaxation via PSS washing three times. For

inhibition of secondary messenger pathways, tissue strips were incubated in PSS with

inhibitors (PKCα inhibitors: 1μM GŐ 6976 or GF 109203X; ROCK inhibitors: 10μM

Y27632 or 0.1μM H1152)(EMD chemicals, Gibbstown, NJ) for 30 minutes, and then

stimulated with KPSS for a minimum of 15 minutes followed by three PSS washes to

completely remove inhibitors. At the end of the experiments, KPSS was applied to test

the tissue viability. For phorbol 12,13-dibutyrate (PDBu; EMD chemicals, Gibbstown, NJ)

induced contractile experiments, tissue strips were bathed in PSS with 1μM PDBu, 1μM

phentolamine and 0.1μM propranolol for 30 minutes followed by three PSS washes to

completely remove residual PDBu. Similarly, at the end of the experiments, KPSS was

applied to test the tissue viability. Stress was calculated according to Herlihy et al.

(Herlihy and Murphy, 1973). Briefly, wet weight was measured for each strip. The force

produced per cross sectional area (stress) was calculated as F/A

$(mN/cm^2)=(m(g)*g)/((wet\ weight\ (g)/(Length(cm)*1.05(g/ml))))\ (g=9.8m/s^2\ )$.

F. Myosin regulatory light chain 20 (LC$_{20}$) phosphorylation   measurements:

A rapid freeze method was used to preserve the phosphorylation status of LC$_{20}$

(Driska et al., 1981). Tissue strips (approximately 3mm x 7mm) were incubated in PSS

with 1μM phentolamine and 0.1μM propranolol for 1 hour, and then activated with KPSS

or CCh. Tissue strips were immediately frozen in dry ice-acetone bath (-78°C) before

stimulation or at 30 second, 1 minute, and 10 minute time points after stimulation. The

frozen tissue strips were stored overnight at -78°C and then allowed to gradually warm to

room temperature in acetone. In this process, acetone replaced the water inside smooth

muscle cells, denatured the endogenous phosphatase, kinase and other enzymatic proteins,

and thereby preserved phosphorylation status of LC_{20} at the time when the tissue strips

were frozen. The dry weights of tissue strips were measured after acetone was thoroughly

evaporated. The wet weights of tissue strips were estimated to be 5 fold greater than the

dry weight (water accounted for 80% of the cell weight) (Hai and Murphy, 1989). Dried

tissue strips were homogenized with sample buffer at 4°C to obtain tissue samples at

10mg/ml dry weight. The homogenates were boiled at 100°C and centrifuged at 13000

rpm for 10 minutes. Supernatant were collected and loaded onto 15% SDS-PAGE at 15μl

per lane (based on protein loading curves showing linearity of signal above and below

this level) for protein separation. The separated proteins were trans blotted to 0.2μl

nitrocellulose membrane, where Ser19 phosphorylated LC_{20} and LC_{20} were detected with

specific antibodies indicated above (western blot analysis section of this dissertation).

The LC_{20} phosphorylation was normalized to β actin and reported as a ratio to total LC_{20}

content for comparison. The arbitrary LC_{20} phosphorylation values (normalized to LC_{20})

from densitometric analysis (ImageJ) are only valid for each western blot run, and thus

cannot be compared to other runs.

G. Quantification of tonic contractile components:

The area under the active force trace (total force minus passive force) was

measured to quantitatively compare the tonic contractile component produced by the tissues. With KPSS or CCh stimulation, force developed very quickly to reach the maximal force levels (peak force), and then gradually decayed to a submaximal level and remained there until stimuli were removed. To standardize the comparison, the force values for a specific agonist were normalized to the peak force values in both the wild type and SMB [(-/-)] tissues. The normalized active force trace from the peak force to 10-minute post peak (force at 10min) was selected and the area under that part of the trace was calculated by summing up all the force values over the time (Integral calculation). Additionally, in our case, 10 minutes after KPSS or CCh stimulation, forces decayed to a steady submaximal level. The ratios of submaximal forces at 10-minute time point to the peak forces (force at 10min/peak force) from the same active force trace were also calculated as an alternative method. The area under the active force trace and the force at 10min/peak force were both analyzed to compare tonic contractions.

H. Analysis of force transient:

Time to peak tension (TPT) (from force initiation to peak force), the area under the active force curve (from force initiation to peak force), and the slope of rapid force transient (steepest slope during initial force generation, dp/dt) were measured to quantitatively compare the initial fast force transient induced by KPSS or CCh. The area under the curve was calculated by summing up all the force values over the time (minutes) (integral calculation).

I. Histological analysis:

Eight-micron thick frozen tissue sections (Leica CM1900) picked up on glass slides were thawed at room temperature and stained with haematoxylin and eosin to examine general morphology(Kiernan, 2008). Wall thickness of ileum, antrum and fundus were measured based on the average of 3 measurements from 4 representative cross sections using a 40X objective for ileum and fundus and 10X objective for antrum (Olympus IX70) and IPLab software (Scanalytics, Fairfax, VA).

J. Statistical data analysis:

For comparison of KPSS stimulated tonic contractile force, protein expression, and LC_{20} phosphorylation levels between wild type and SMB $^{(-/-)}$ tissues, data were examined for significant differences using a two-tailed student's t test with equal variance. Data was deemed significant at P-value of P<0.05. For comparison of tonic contractile force with or without inhibitors in SMB $^{(-/-)}$ tissues, one-way ANOVA was used. Significance was determined as a P value less than 0.05.

III. Results:

Ileum and stomach antrum exhibit phasic smooth muscle contractions, and stomach fundus exhibits tonic smooth muscle contraction (Han et al., 2006, Eddinger et al., 2001, Eddinger 2009, Rondelli et al., 2007, Smolyo et al., 1968, White et al., 1993). Thus, this project used longitudinal ileum and circular antrum as representative phasic smooth muscle tissues and circular fundus as representative tonic smooth muscle tissue to study the role of the SM SMA/B MHC isoforms in phasic and tonic smooth muscle contractions (Longitudinal ileum, circular antrum, and circular fundus will be referred to simply as ileum, antrum, and fundus, respectively).

A. Aim one was to determine if SMB MHC isoform expression is required for smooth muscle to exhibit phasic contraction.

The SM SMB MHC isoform is preferentially expressed in phasic muscle. To understand the role of the SM SMB MHC isoform in phasic contraction, an exon-specific gene targeted SMB knockout approach was used to determine if the SM SMB MHC isoform is necessary for smooth muscle to exhibit phasic contraction.

1. Generation and characterization of SMB knockout (SMB$^{(-/-)}$) mice.

a. SMB$^{(-/-)}$ Mice.

SMB$^{(-/-)}$ mice were kindly provided by Dr. Babu and Dr. Periasamy (Babu et al., 2001). The generation of SMB$^{(-/-)}$ mice has been published (Babu et al. 2001).

b. SMB^(-/-) mice genotype.

To identify wild type (SMB$^{(+/+)}$), heterozygous (SMB$^{(+/-)}$), and knockout (SMB$^{(-/-)}$) mice, genotyping was carried out. Two primer sets specific for the wild type allele (Ex5B/MHC 31 which is SMB specific) and mutant allele (PGK/MHC 31 which is neomycin specific) were used. The DNA electrophoresis results are shown in Figure 4. SMB$^{(+/-)}$ mice have both the SMB Ex5B and neomycin genes. Therefore, the DNA fragments amplified by Ex5B/MHC 31 and PGK/MHC 31 respectively were present in the DNA agarose gel (Figure 4 lane 1 and 2). SMB$^{(+/+)}$ mice do not have the neomycin gene but do have the SM SMB MHC in their genome. Thus only the DNA fragment of Ex5B was amplified (Figure 4 lane 3 and 4). Neomycin replaced Ex5B in SMB$^{(-/-)}$ mice genomes. Thus, only the DNA fragment amplified by PGK/MHC 31 primers was present, with no fragment amplified by Ex5B/MHC 31 primers in SMB$^{(-/-)}$ mice. (Figure 4 lane 5 and 6). The genotyping identified a SMB$^{(+/+)}$ mouse as having the SMB MHC gene but not the neomycin gene, a SMB$^{(+/-)}$ mouse with the inserted neomycin cassette has both the SMB MHC gene and the neomycin cassette, and the SMB$^{(-/-)}$ mouse has the neomycin gene but not SMB MHC gene.

c. SM SMB MHC protein expression in SMB$^{(+/+)}$ and SMB$^{(-/-)}$ mice.

To verify that the insertion of the neomycin cassette took the place of Exon 5B of
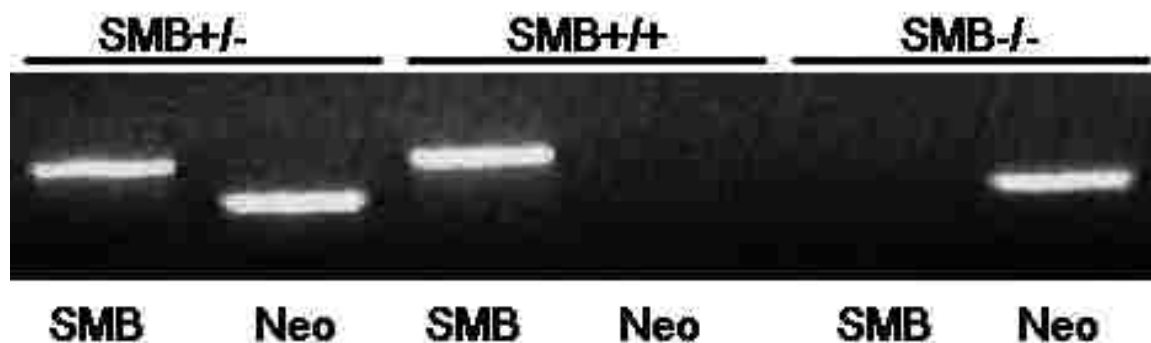
Figure 4. DNA electrophoresis gel results loaded with PCR products from SMB[(+/+)], SMB[(+/-)], and SMB[(-/-)] mice. The fragment of Ex5B (245bps) was amplified in the SMB[(+/+)] mouse. Both the fragments of Ex5B and the PGK neomycin were amplified in the SMB[(+/-)] mouse. The fragment of PGK neomycin (219 bps) was amplified in the SMB[(-/-)]. From left to right: Lane 1-2: Amplified SMB[(+/+)] mouse genome. Lane 3-4: Amplified SMB[(+/+)] mouse genome. Lane 5-6: Amplified SMB[(-/-)] mouse genome (Lane 1,3,5: amplified by Ex5B primers (SMB MHC). Lane 2,4,6: amplified by neomycin primers (Neo)).

SMB MHC and knocked down SMB MHC expression at protein level in SMB$^{(-/-)}$ mice, western blotting was conducted using an anti-SMB serum (Eddinger, 2009). If SM SMB MHC isoform is knocked down in SMB$^{(-/-)}$ mice, the expression of SMB MHC protein will be significantly decreased compared to SMB$^{(+/+)}$.

The proper sample loading volume for SMB MHC quantification on western blot was determined by standard western blot sample-loading curve. Figure 5 shows the representative standard sample-loading curve for β actin (which was used to normalize protein loadings between samples)(Figure 5A) and SMB MHC (Figure 5B). The standard curve typically has a linear portion where the western blot signal is positively correlated with the increasing sampling loading volume. Sample loadings within this range of the curve can be quantified by western blot. Table 3 shows standard sample loading ranges for western blot for various proteins tested in this dissertation. The squared correlation coefficient ranged from 0.94 to 0.99 (R^2=0.94~0.99). To minimize variability, tissue samples from a single animal were run in triplicate. Figure 6 shows western blot example of triplicate loading of phosphorylated LC$_{20}$ of SMB$^{(+/+)}$ and SMB$^{(-/-)}$ fundus.

Quantified western blot analysis results of SMB MHC expression in SMB$^{(+/+)}$ and SMB$^{(-/-)}$ ileum, antrum, and fundus are shown in Table 4. Expression of SMB MHC protein was significantly decreased in SMB$^{(-/-)}$ ileum and antrum compared to SMB$^{(+/+)}$, consistent with the neomycin cassette replacing the Exon 5B and this exon- Additionally, western blot results using SMA MHC specific antibody (Eddinger, 2009) targeting expression of SMA MHC was significantly increased in SMB$^{(-/-)}$ ileum and

SMB$^{(-/-)}$ ileum β actin standard curve

5μl   10μl   5μl   20μl   25μl   30μl   35μl

SMB$^{(-/-)}$ ileum SMB standard curve

50 μl   70μl   90μl   110μl   130μl
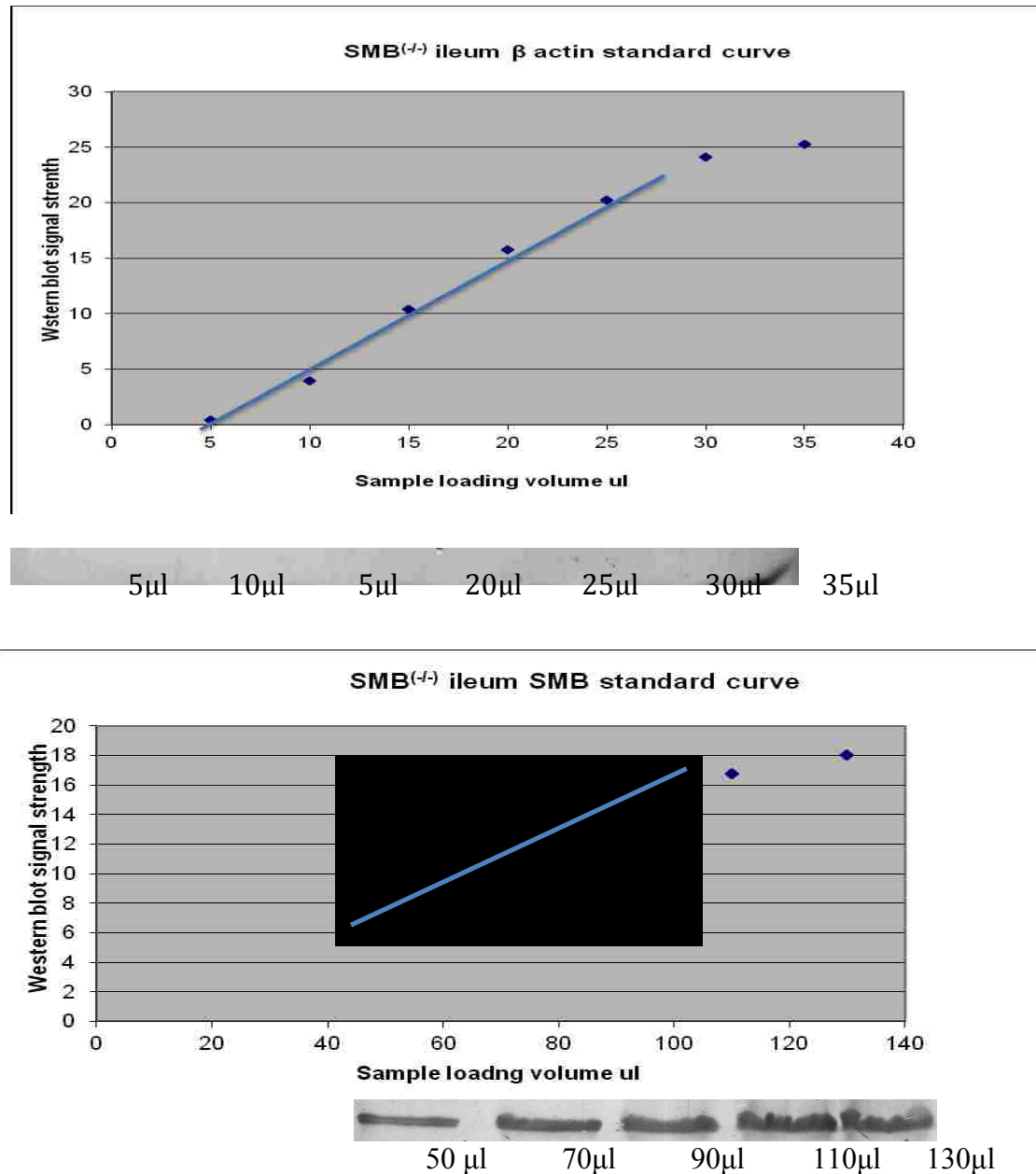
Figure 5. The representative western blot result of standard sample loading curve for SMB$^{(-/-)}$ ileum β actin (loading control) and SMB$^{(-/-)}$ ileum SMB MHC protein. Upper graph: 50mg/ml SMB$^{(-/-)}$ ileum was loaded from 5μl to 35μl with 5μl increment for β actin quantification using β actin specific antibody. From 5μl to 25μl, the loading volume and western blot signal strength shows a linear relationship. (R^2=0.99). Beyond 30μl, the western blot signal strength was saturated. Based on these data, the loading range used for data analysis was between 15μl and 25μl. Lower graph: The standard sample loading curve for SMB MHC protein of SMB$^{(-/-)}$ ileum. The linear range for SMB$^{(-/-)}$ ileum SMB MHC was from 50 μl to 90 μl with R^2=0.97, and loadings for data analysis for SMB MHC was from 50 μl to 90 μl.

Tissue Type	Protein	Loading volume range determined from linear part of standard loading curve (μl).	Loading volume used for western blot analysis (μl).	R^2 value for linear part of standard loading curve
SMB[(+/+)] ileum	SMB MHC	30-70	50	0.98
	SMA MHC	40-80	50	0.96
	Total myosin	30-75	50	0.99
	MLCK	10-50	30	0.96
	MLCP	5-40	30	0.97
	PKCδ	30-40	30	0.96
	PKCα	10-30	15	0.99
	β actin	10-50	15	0.96
	Phosphorylated LC_{20}	10-30	15	0.99
	LC_{20}	10-30	15	0.99
	CPI-17	70-90	70	0.95
SMB[(-/-)] ileum	SMB MHC	50-90	50	0.97
	SMA MHC	30-60	50	0.97
	Total myosin	30-70	50	0.98
	MLCK	10-45	30	0.99
	MLCP	15-55	30	0.98
	PKCδ	30-40	30	0.96
	PKCα	10-50	15	0.98
	β actin	5-25	15	0.99
	Phosphorylated LC_{20}	10-30	15	0.99
	LC_{20}	10-30	15	0.99
	CPI-17	70-95	70	0.96
SMB[(+/+)] antrum	SMB MHC	5-20	15	0.98
	SMA MHC	25-35	30	0.98
	Total myosin	5-35	15	0.95
	MLCK	5-35	30	0.98
	MLCP	5-40	30	0.99
	PKCδ	30-40	30	0.95
	PKCα	5-15	15	0.99
	β actin	10-60	15	0.99
	Phosphorylated LC_{20}	10-30	15	0.99
	LC_{20}	10-30	15	0.99
	CPI-17	70-90	70	0.95
SMB[(-/-)]	SMB MHC	5-25	15	0.94
	SMA MHC	5-35	15	0.99

antrum	Total myosin	15-35	20	0.99
	MLCK	10-30	30	0.99
	MLCP	5-40	30	0.98
	PKCδ	30-40	30	0.99
	PKCα	5-20	15	0.99
	β actin	10-25	15	0.97
	Phosphorylated LC$_{20}$	10-30	15	0.99
	LC$_{20}$	10-30	15	0.98
	CPI-17	70-90	70	0.96
SMB$^{(+/+)}$	SMB MHC	5-25	15	0.99
	SMA MHC	5-35	15	0.98
fundus	Total myosin	5-30	15	0.99
	MLCK	15-30	30	0.98
	MLCP	10-35	30	0.98
	PKCδ	30-40	30	0.96
	PKCα	10-30	15	0.98
	β actin	5-30	15	0.99
	Phosphorylated LC$_{20}$	5-30	15	0.99
	LC$_{20}$	5-35	15	0.98
	CPI-17	65-70	70	0.96
SMB$^{(-/-)}$	SMB MHC	5-25	15	0.95
	SMA MHC	5-35	15	0.97
fundus	Total myosin	5-30	15	0.99
	MLCK	5-30	30	0.99
	MLCP	5-40	30	0.97
	PKCδ	30-40	30	0.95
	PKCα	5-20	15	0.99
	β actin	4-18	15	
	Phosphorylated LC$_{20}$	10-30	15	0.97
	LC$_{20}$	10-30	15	0.97
	CPI-17	65-75	70	0.96

Table 3. Western blot sample loading volumes for various smooth muscle contraction regulatory proteins. The loading volume ranges determined from linear part of standard curves in the table were obtained based on the standard curve specific to each of the corresponding protein. β actin was used as loading control.

$SMB^{(+/+)}$ $SMB^{(-/-)}$ $SMB^{(+/+)}$ $SMB^{(-/-)}$ $SMB^{(+/+)}$ $SMB^{(+/+)}$

Phosphorylated LC_{20}
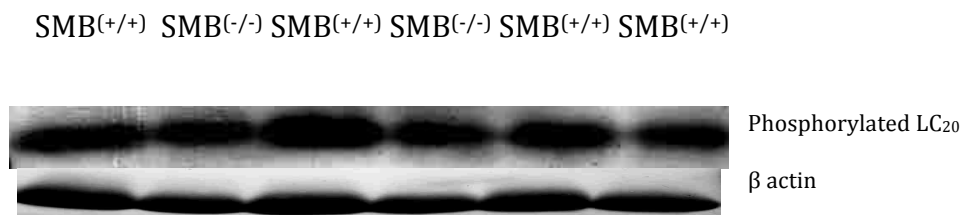
β actin

Figure 6. Western blot example of triplet loading. Western blot result of phosphorylated LC_{20} in $SMB^{(+/+)}$ and $SMB^{(-/-)}$ fundus (top) and the β actin loading control (bottom). 30µl 50mg/ml $SMB^{(+/+)}$ and $SMB^{(-/-)}$ fundus samples from one $SMB^{(+/+)}$ and one $SMB^{(-/-)}$ mouse were loaded in triplicate pairs. The quantified densitometric result from each of the pair were averaged as the n=1 for phosphorylated LC_{20} in $SMB^{(+/+)}$ and $SMB^{(-/-)}$ fundus.

strategy effectively reducing SMB MHC gene expression (Table 4) showed that the antrum compared to SMB$^{(+/+)}$ (Table 4). Because the SMB MHC is expressed at very low/undetectable levels in the SMB$^{(+/+)}$ fundus , the loss of SMB MHC in the SMB$^{(-/-)}$ fundus did not show a significant decrease in SMB MHC or increase in SMA MHC expression compared to SMB$^{(+/+)}$ fundus tissues. Results of western blot using total myosin antibody (SM+NM) ((Cat # BT-562 Biomedical Technologies, Stoughton, MA) indicated that the expressions of total myosin (including both the SMA/B SM MHC and NM MHC) were unaltered in all three tissues (Table 4). The expression of NM MHC was not altered in SMB$^{(-/-)}$ ileum (Table 4). Loss of SMB MHC protein resulted in a compensatory switching from the SMB MHC isoform to the SMA MHC isoform such that neither NM MHC nor total MHC expression was altered.

d. Gross histological organization of SMB$^{(+/+)}$ and SMB$^{(-/-)}$ tissues.

To determine any gross histological alteration in SMB$^{(-/-)}$ animals, ileum, antrum, and fundus tissues were frozen, sectioned and stained with haematoxylin and eosin. Figure 7 shows representative histologic micrographs of haematoxylin and eosin stained cross sections of SMB$^{(+/+)}$ and SMB$^{(-/-)}$ ileum, antrum, and fundus. The width (μm) of the smooth muscle layer of SMB$^{(-/-)}$ tissues was similar to their matched WT tissues (Ileum: 36.9±3.51 (WT), 42.13±7.44 (KO); Antrum: 549.02±42.68 (WT), 524.73±49.23 (KO); Fundus: 82.38±20.75 (WT), 69.89±11.72 (KO); n=3-4). No gross histological differences were observed in these tissues between SMB$^{(-/-)}$ and SMB$^{(+/+)}$ animals.

Tissue type	Protein	SMB$^{(+/+)}$**	SMB$^{(-/-)}$**	P value	Representative western blot results SMB$^{(+/+)}$ SMB$^{(-/-)}$
Ileum	SMB MHC	1.17±0.03	0.03±0.01	4.059E-6*	β actin
	SMA MHC	0.46±0.02	1.64±0.05	2.442E-5*	β actin
	Total myosin	1.12±0.13	1.13±0.15	0.36	β actin
	NM myosin	0.98±0.05	1.19±0.08	0.092	β actin
Antrum	SMB MHC	0.84±0.06	0.13±0.06	0.0001*	β actin
	SMA MHC	0.71±0.15	1.59±0.14	0.012*	β actin
	Total myosin	1.59±0.31	1.66±0.4	0.884	β actin
Fundus	SMB MHC	0.71±0.11	0.81±0.04	0.454	β actin
	SMA MHC	1.00±0.04	1.01±0.04	0.886	β actin
	Total myosin	1.02±0.08	0.99±0.08	0.832	β actin

Table 4. Quantitative western blot results of the expression of SMB and SMA MHC and total myosin in SMB$^{(+/+)}$ and SMB$^{(-/-)}$ ileum (including NM myosin), antrum and fundus with β actin as loading control. The expressions of SMB and SMA MHCs were significantly decreased and increased in SMB$^{(-/-)}$ ileum and antrum respectively compared to SMB$^{(+/+)}$. No significant change of SMB expression was observed in SMB$^{(-/-)}$ fundus. The expressions of total myosin (SM+NM) and NM myosin were not significantly different between SMB$^{(+/+)}$ and SMB$^{(-/-)}$ ileum, antrum, fundus.
Values are mean ± SE. ** Arbitrary densitometric units. * Difference determined by t-test to be significant at P<0.05. n=3 for all groups.

SMB^(+/+)

SMB^(-/-)

| M | CM | LM | **Ileum**

| M | CM | LM | **Fundus**

| M | CM | LM | **Antrum**
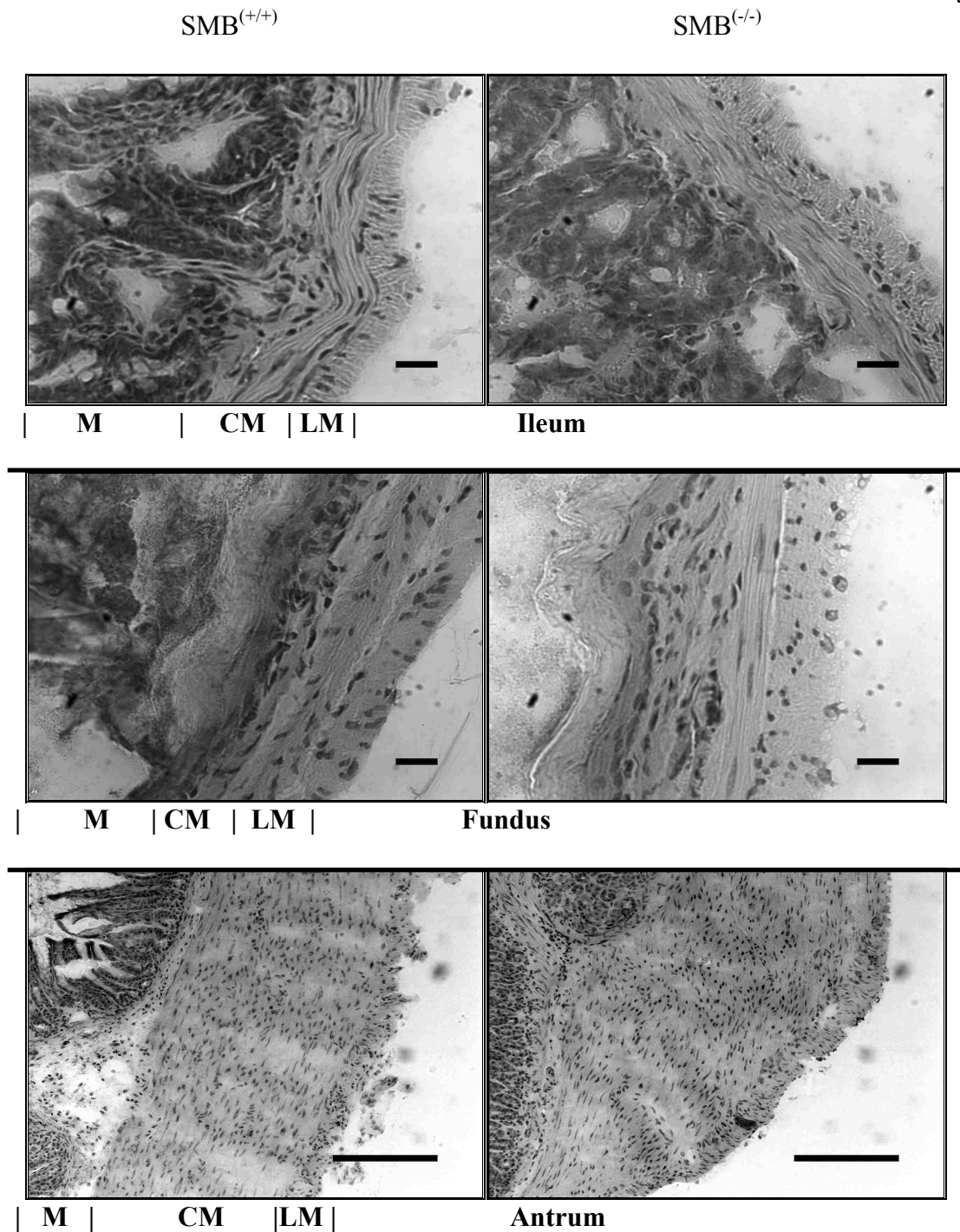
Figure 7. Transverse H&E section through SMB^(+/+) (left) and SMB^(-/-) (right) ileum (upper panels), fundus (middle panels), and antrum (lower panels). There are no obvious gross differences between the SMB^(+/+) and SMB^(-/-) tissues. M: mucosa, muscularis mucosa, and submucosa. CM: circular smooth muscle layer. LM: longitudinal smooth muscle layer. Scale bar equals 20µm (ileum and fundus) or 200µm (antrum).

2. Phasic contractions in SMB$^{(+/+)}$ and SMB$^{(-/-)}$ phasic smooth muscle tissues.

The preferential expression of the SM SMB MHC isoform in phasic tissue, and its greater ATPase activity relative to the SMA MHC isoform suggest that SMB MHC may play an important role in regulating phasic contraction. To determine whether the SMB MHC is involved in phasic contraction, SMB$^{(-/-)}$ phasic tissues (ileum and antrum) were stimulated by depolarization (KPSS) or physiological agonist analog (Carbachol (CCh)). If a phasic contraction requires SMB MHC expression, the phasic contractile pattern of SMB$^{(-/-)}$ ileum and antrum will no longer be maintained. Tonic fundus was used as control.

a. Phasic contraction induced by KPSS in SMB$^{(+/+)}$ and SMB$^{(-/-)}$ ileum and antrum.

KPSS, a physiological saline solution with 109.6mM K$^+$ substituted for Na$^+$, depolarizes muscle to induce contraction. To compare the phasic component of contraction between SMB$^{(+/+)}$ and SMB$^{(-/-)}$ mice, isometric force traces with KPSS stimulation were recorded. The phasic and tonic components of an isometric force trace are shown in Figure 8. The isometric- recorded force trace consists of an initial fast force transition after activation, which is the phasic component of a contraction (enclosed dotted region). After force reaches maximum level, the maintenance of force occurs via the tonic component of the contraction (enclosed solid region). Figure 9 shows representative isometric force traces for SMB$^{(-/-)}$ and SMB$^{(+/+)}$ ileum,
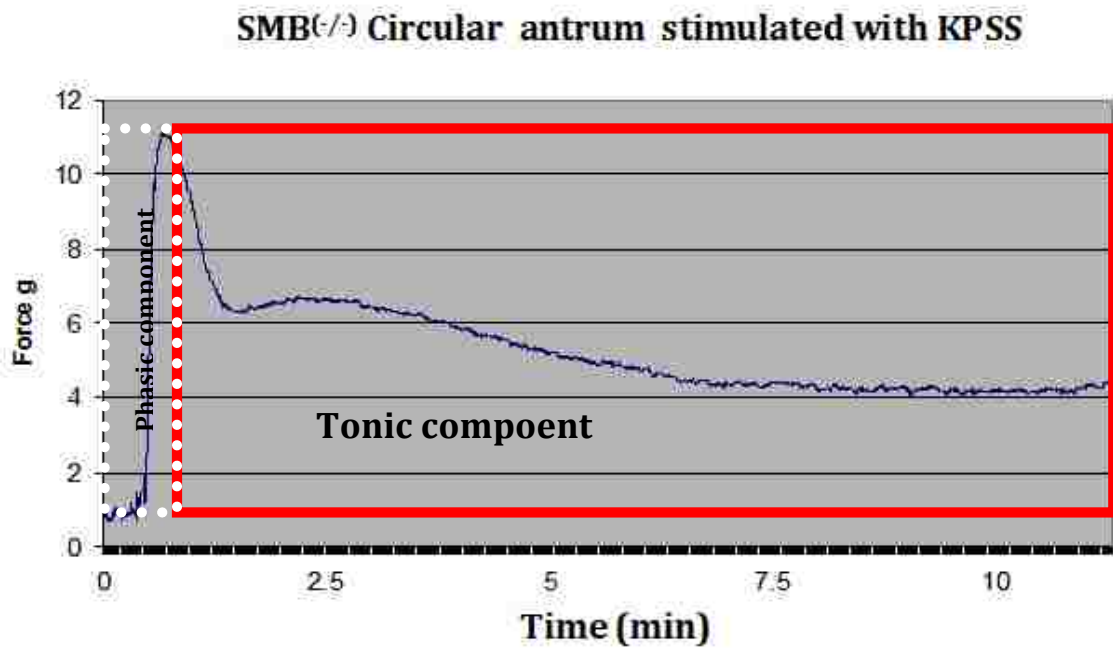
Figure 8. Representative force trace showing the phasic and tonic components of an isometric contraction. The force trace included in dotted region is the phasic component of the contraction. The force trace enclosed with a solid region is the tonic component of the contraction.
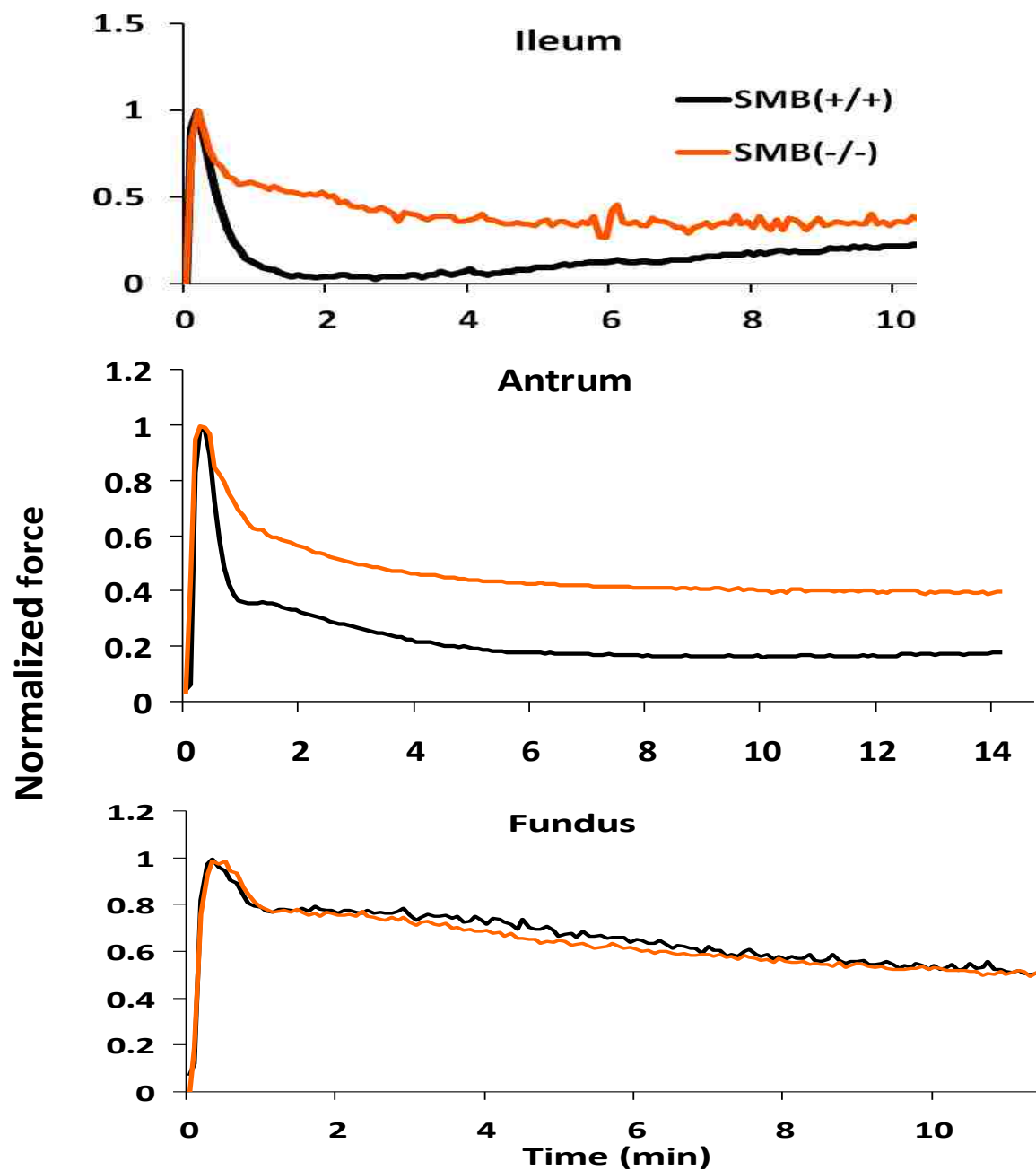
Figure 9. Representative KPSS isometric force traces of SMB[(+/+)] and SMB[(-/-)] ileum, antrum, and fundus. In order to compare the contraction patterns between SMB[(+/+)] and SMB[(-/-)] smooth muscle tissues, active peak forces were normalized to 1. Isometric force traces for SMB[(+/+)] and SMB[(-/-)] ileum (upper panel), SMB[(+/+)] and SMB[(-/-)] antrum (middle panel), and SMB[(+/+)] and SMB[(-/-)] fundus (lower panel). In both the ileum and antrum the tonic force component is significantly increased in the SMB[(-/-)] animals relative to the SMB[(+/+)].

antrum, and fundus induced by KPSS. As shown in Figure 9, a rapid force transition induced with KPSS is still present in SMB$^{(-/-)}$ ileum, antrum and fundus compared to SMB$^{(+/+)}$, suggesting that phasic contraction does not require the SMB MHC. Further analysis of the force transition rate of this phasic contraction revealed that the rate of the force transient for the SMB$^{(-/-)}$ ileum and antrum were significantly slower than the SMB$^{(+/+)}$ tissues. In contrast, there was no difference for the fundus tissue under the same condition. To quantitatively compare the force transition rate for ileum, antrum, and fundus between SMB$^{(+/+)}$ and SMB$^{(-/-)}$, three measurements (the time taken to reach the peak force, slope of the linear part of force transient (Figure 10) and the area under the active force curve from force initiation to peak force (Figure 11)) were carried out for calculating the phasic isometric force induced by KPSS. The area under the active force curve from force initiation to peak force is indicated in Figure 11. Results of three measurements are summarized in Table 5. The time taken from force initiation to peak force and the area under the active force curve from force initiation to peak force were significantly increased, and the slope of the linear force transient was significantly decreased in SMB$^{(-/-)}$ ileum and antrum compared to SMB$^{(+/+)}$. These results suggest that there is a decreased force transient rate in SMB$^{(-/-)}$ verses SMB$^{(+/+)}$ ileum and antrum when activated with KPSS. The fundus control showed no change between the SMB$^{(+/+)}$ and SMB$^{(-/-)}$ tissues.

Thus, in the SMB$^{(-/-)}$ ileum and antrum, stimulated by KPSS, loss of SMB MHC isoform results in a phasic contraction with unaltered maximal tension but a slower force transition rate.
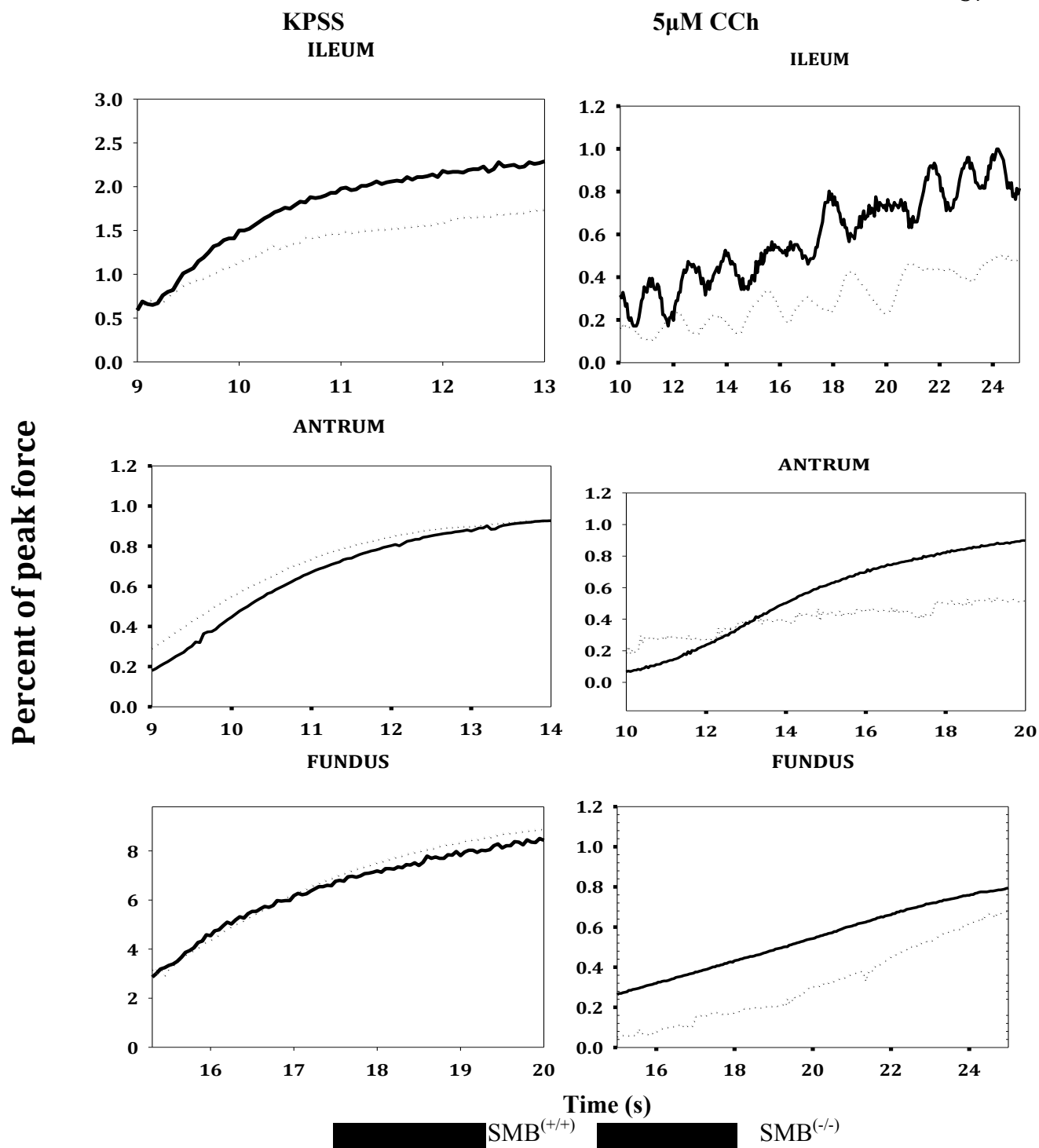
Figure 10. Expanded view of initial isometric force traces activated by KPSS (left) or 5μM CCh (right). Ileum (upper panels), antrum (middle panels), and fundus (lower panels). Force transition rate was significantly slower in SMB[(-/-)] ileum and antrum than SMB[(+/+)], but not for the fundus. X-axis indicates the time (in second) after force initiation
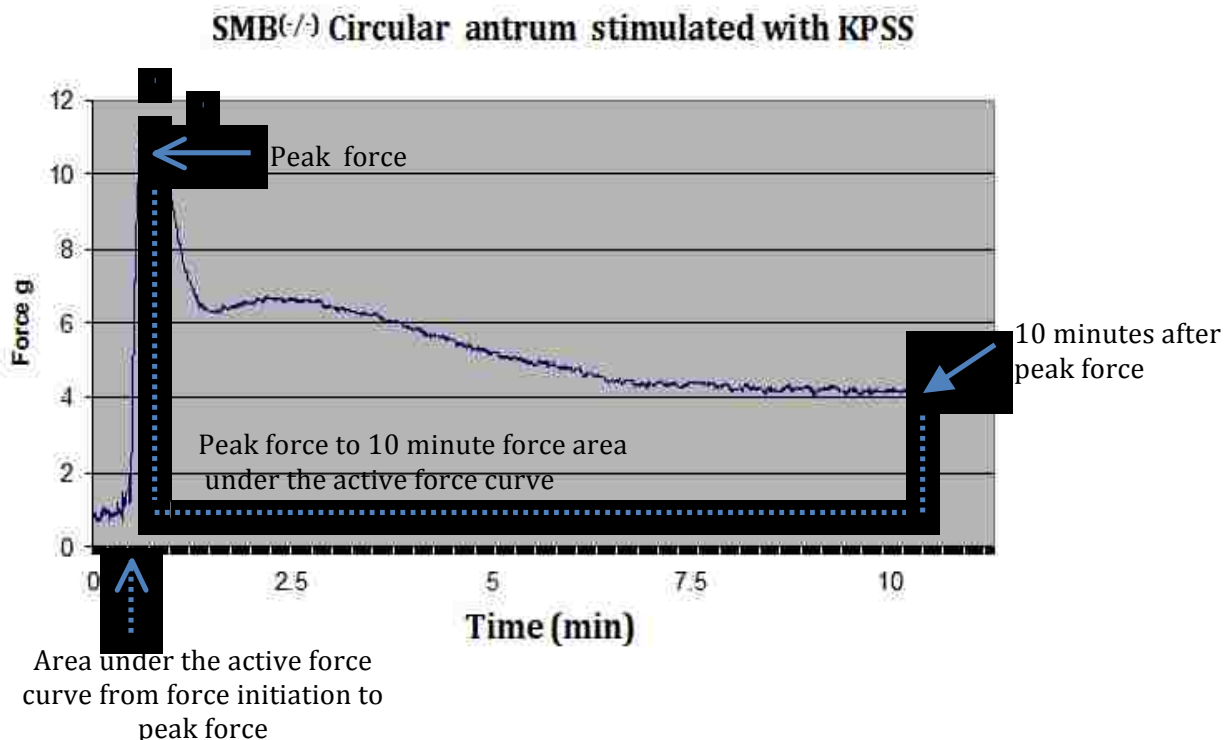
Figure 11. Measurements used to quantitatively compare force transition rate, and tonic contractile component between SMB$^{(+/+)}$ and SMB$^{(-/-)}$. Dotted arrow pointed area was the area under the active force curve from force initiation to peak force, which was used to compare force transient rate. The area under the active force curve (enclose by dotted line) (from peak force (solid arrow) to 10 minutes (solid arrow head) after peak force) and the 10minute force/peak force ratio were used for tonic contractile comparison.

Treatment	Tissue		n	Slope of linear ascending force (g/s)	n	Time to peak tension (min)	n	Area under the curve (Force initiation to peak force)
KPSS	Ileum	SMB^(+/+)	11	0.8±0.14	11	0.19±0.03	11	0.13±0.02
		SMB^(-/-)	12	0.31±0.04	11	0.32±0.04	11	0.21±0.03
	P value			0.002*		0.012*		0.009*
	Antrum	SMB^(+/+)	7	1.16±0.23	12	0.09±0.01	12	0.05±0.01
		SMB^(-/-)	7	0.54±0.1	12	0.24±0.04	12	0.1±0.02
	P value			0.029*		0.001*		0.02*
	Fundus	SMB^(+/+)	12	1.07±0.23	12	0.29±0.02	12	0.2±0.06
		SMB^(-/-)	14	0.66±0.14	13	0.41±0.06	13	0.2±0.02
	P value			0.123		0.091		0.996
CCh	Ileum	SMB^(+/+)	5	0.35±0.13	13	0.44±0.01	13	0.21±0.04
		SMB^(-/-)	8	0.09±0.02	13	0.51±0.01	13	0.43±0.03
	P value			0.029*		0.04*		0.02*
	Antrum	SMB^(+/+)	6	0.61±0.07	12	0.47±0.02	12	0.32±0,02
		SMB^(-/-)	5	0.24±0.06	12	0.74±0.05	12	0.48±0.01
	P value			0.006*		0.01*		0.02*
	Fundus	SMB^(+/+)	6	0.47±0.08	7	0.48±0.07	7	0.42±0.1
		SMB^(-/-)	7	0.35±0.09	7	0.56±0.12	7	0.45±.05
	P value			0.3		0.581		0.732

Table 5. Force transient comparison for SMB^(+/+) and SMB^(-/-) ileum, antrum, and fundus with KPSS or 5μM CCh stimulation. With KPSS stimulation, the force developmental time to reach the peak force and the force initiation to peak force area under the active force curve significantly increased and the slope of linear ascending force is decreased in SMB^(-/-) ileum and antrum, indicating a decreased force developmental rate in these SMB^(-/-) smooth muscle tissue contraction.
Values are mean ± SE. * Difference determined by t-test to be significant at P<0.05.

b. Phasic component of contraction induced by Carbachol (CCh) in SMB$^{(+/+)}$ and SMB$^{(-/-)}$ antrum and ileum.

Acetylcholine (ACh) has been reported to be the major excitatory neurotransmitter released from the enteric nervous system causing gut motility (Bornstein et al., 2004; Furness et al., 1995; Furness, 2012; Murthy, 2006). For our studies, we used an ACh analog (CCh) which is not hydrolysable by the acetylcholine esterase to determine whether the same results with KPSS stimulation will be observed with more physiological stimulati. The maximum stress values are not different between CCh activated SMB$^{(+/+)}$ and SMB$^{(-/-)}$ ileum, antrum and fundus (mN/cm2; ileum: 17.4±2.4 (WT), 22.9±3.6 (KO); antrum: 7.5±2.2 (WT), 13.2±4.3 (KO); fundus: 20.2±3.3 (WT), 20.3±4.0 (KO). n=4~7, P>0.05).

Representative force traces vs. time with 5µM CCh stimulation are shown in Figure 12. The estimates of the rate of phasic contraction were measured in SMB$^{(+/+)}$ and SMB$^{(-/-)}$ ileum, antrum, and fundus. Results are shown in Table 5. Similar to KPSS stimulation, CCh induced contractions in SMB$^{(-/-)}$ ileum and antrum had a phasic component with increased time to peak force and area under the active force curve from force initiation to peak force, and decreased slope of force transient relative to the SMB$^{(+/+)}$ tissues. No difference appeared in fundus tissues tested.

c. LC$_{20}$ phosphorylation in SMB$^{(+/+)}$ and SMB$^{(-/-)}$ tissues.

To determine whether the deceased force transient in SMB$^{(-/-)}$ ileum and antrum was caused by the protein expression switch from "fast" SMB MHC to
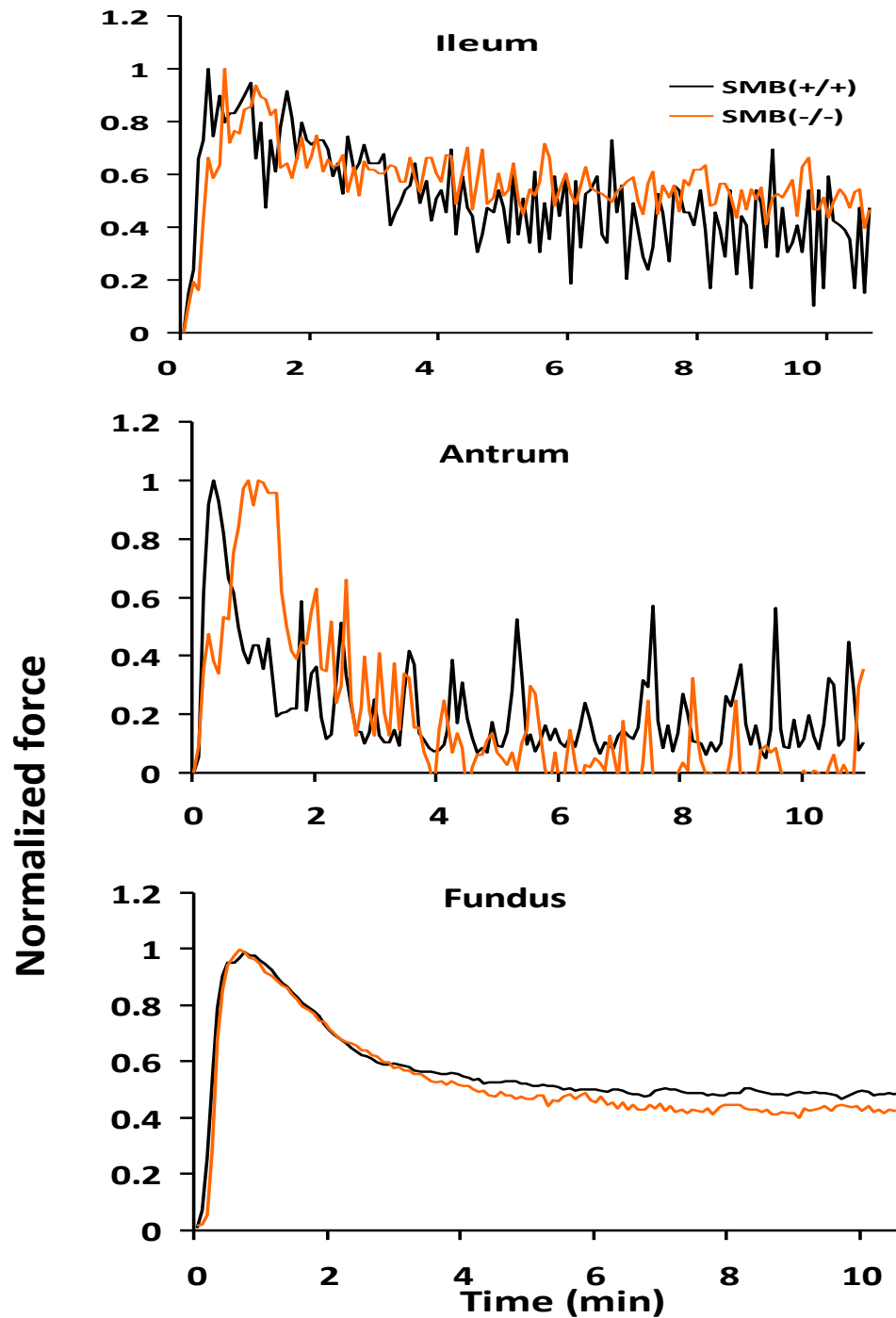
Figure 12. Representative isometric force traces of SMB[(+/+)] and SMB[(-/-)] ileum, antrum, and fundus stimulated by 5μM CCh. In order to compare the contraction patterns between SMB[(+/+)] and SMB[(-/-)] smooth muscle tissues, active peak forces were normalized to 1. "slow" SMA MHC isoform, LC_{20} phosphorylation status at 5 seconds (rapid phasic force

transient) was measured. The phosphorylation status of LC_{20} was not significantly

different between SMB$^{(+/+)}$ and SMB$^{(-/-)}$ in ileum and antrum at 5 second time point (Table 6), which suggested that LC$_{20}$ phosphorylation (5 seconds) is not different during the force transient to the maximal force between SMB$^{(+/+)}$ and SMB$^{(-/-)}$, thus the difference in mechanical response is not due to the differences in LC$_{20}$ phosphorylation levels. Similarly, no significant difference of LC$_{20}$ phosphorylation was observed in SMB$^{(+/+)}$ and SMB$^{(-/-)}$ fundus at this time point (Table 6).

Results of isometric force measurement with either KPSS or CCh in SMB$^{(-/-)}$ ileum and antrum exhibited a phasic component of contraction with increased time to peak and area under the active force curve from force initiation to peak force, and a decreased force transient slope, which suggested a slower force transient rate in these tissues.

B. Aim two was to investigate if the SMA MHC isoform expression alone is able to display a tonic contraction in a phasic tissue where the SMB MHC is originally predominantly expressed.

In the previous section, results indicated that SM SMB MHC was not required for phasic contraction but affected the force transient of the phasic contraction. However, the correlation between predominant expression of SMA MHC isoform in tonic tissues and tonic contraction remains unresolved. To address this, isometric force traces were compared between SMB$^{(+/+)}$and SMB$^{(-/-)}$ ileum, antrum and fundus strips. If SMA MHC isoform is responsible for tonic contraction, loss of SMB MHC protein expression with

Phosphorylation	SMB$^{(+/+)}$	SMB$^{(-/-)}$	P value	Representative
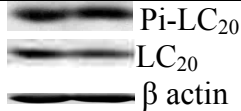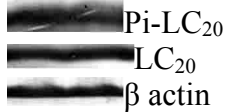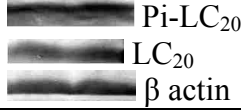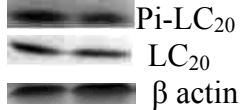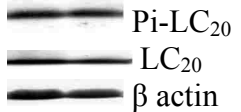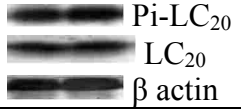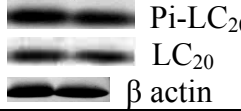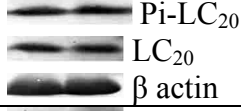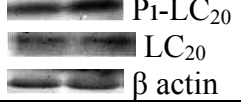
time point				western blot result SMB$^{(+/+)}$ SMB$^{(-/-)}$
Ileum				
LC$_{20}$-Pi at 5 sec **	0.88±0.09	1.08±0.09	0.188	Pi-LC$_{20}$ / LC$_{20}$ / β actin
LC$_{20}$-Pi at 1 min **	0.89±0.2	1.15±0.21	0.425	Pi-LC$_{20}$ / LC$_{20}$ / β actin
LC$_{20}$-Pi at 10 min **	1.15±0.09	1.14±0.09	0.93	Pi-LC$_{20}$ / LC$_{20}$ / β actin
Antrum				
LC$_{20}$-Pi at 5 sec **	0.95±0.14	1.03±0.22	0.786	Pi-LC$_{20}$ / LC$_{20}$ / β actin
LC$_{20}$-Pi at 1 min **	0.89±0.28	1.18±0.15	0.415	Pi-LC$_{20}$ / LC$_{20}$ / β actin
LC$_{20}$-Pi at 10 min**	0.95±0.06	1.02±0.08	0.644	Pi-LC$_{20}$ / LC$_{20}$ / β actin
Fundus				
LC$_{20}$-Pi at 5 sec **	1.04±0.07	0.99±0.06	0.565	Pi-LC$_{20}$ / LC$_{20}$ / β actin
LC$_{20}$-Pi at 1 min **	1.02±0.22	0.93±0.09	0.737	Pi-LC$_{20}$ / LC$_{20}$ / β actin
LC$_{20}$-Pi at 10 min **	1.01±0.1	1.13±0.07	0.363	Pi-LC$_{20}$ / LC$_{20}$ / β actin

Table 6. LC$_{20}$ Phosphorylation status at 5 seconds, 1minute, and 10 minutes time points in KPSS stimulation. There are no significant difference in LC$_{20}$ Phosphorylation status at 5 seconds, 1minute, or10 minutes time points in KPSS stimulation between SMB$^{(+/+)}$ and SMB$^{(-/-)}$ tissues. ** Arbitrary densitometric units. Values are mean of percent phosphorylated LC$_{20}$ (of total SMB$^{(+/+)}$ and SMB$^{(-/-)}$ samples) divided by percent total LC$_{20}$ (of total SMB$^{(+/+)}$ and SMB$^{(-/-)}$ samples) after each was corrected for loading (β actin) ± SE. * Difference determined by t-test to be significant at P<0.05. n=3 for all groups.

an increased SMA MHC protein expression should make SMB$^{(-/-)}$ phasic smooth muscle exhibit a strong tonic contraction.

1. Tonic contractions in SMB$^{(+/+)}$ and SMB$^{(-/-)}$ phasic smooth muscle tissues.

a. Tonic contraction induced by KPSS in SMB$^{(+/+)}$ and SMB$^{(-/-)}$ ileum and antrum.

The isometric force trace with KPSS stimulation examined in the previous section not only had a phasic component but also a tonic component (Figure 9). As shown in Figure 9, after force reached the peak force, it began to decrease. However, forces in SMB$^{(-/-)}$ ileum and antrum did not decrease to the same level as SMB$^{(+/+)}$ tissues, instead they were maintained at a intermediate force level which was higher than the tonic forces in these tissues for SMB$^{(+/+)}$ animals. There were no differences in the tonic forces from SMB$^{(+/+)}$ and SMB$^{(-/-)}$ fundus tissues. To quantitatively compare the tonic component of contraction stimulated with KPSS between SMB$^{(+/+)}$ and SMB$^{(-/-)}$ ileum and antrum, the active peak force from both SMB$^{(+/+)}$ and SMB$^{(-/-)}$ tissues were normalized to 1, and then the area under the active force curve were measured from peak force to 10 minutes after peak force as the indicator of the tonic component (Figure 11). An alternative way to measure the tonic contractile component was the 10 minute force (steady state) (Figure 11). Results from these measurements are summarized in Table 7. The area under the active force curve (peak force to 10 minutes after peak) was significantly larger in SMB$^{(-/-)}$ ileum and antrum compared to SMB$^{(+/+)}$. 10 minute KPSS force was also greater in SMB$^{(-/-)}$ than SMB$^{(+/+)}$ animals. The results from both of the measurements indicated that with KPSS stimulation SMB$^{(-/-)}$ ileum and antrum were more tonic than SMB$^{(+/+)}$.

Tissue		n	Area under the curve**	10 min force**
Ileum	SMB(+/+)	13	4.03±0.36	0.37±0.03
	SMB(-/-)	13	5.47±0.35	0.48±0.04
P value			0.017*	0.044*
Antrum	SMB(+/+)	7	2.73±0.24	0.19±0.02
	SMB(-/-)	7	3.81±0.21	0.27±0.03
P value			0.005*	0.027*
Fundus	SMB(+/+)	11	5.85±0.54	0.47±0.06
	SMB(-/-)	11	5.84±0.47	0.49±0.06
P value			0.991	0.818

Table 7. Quantification of tonic phase activated by KPSS. The tonic component of contraction was quantified by measuring area under force trace from the peak force to 10 minutes after (steady state) and 10 minute force. Increased values for area under force trace or 10 minute force suggested a larger tonic component. KPSS stimulation was more tonic in SMB(-/-) ileum and antrum. In KPSS stimulated fundus, the tonic components between SMB(+/+) and SMB(-/-) were comparable (control). The increased tonic contractions in SMB(-/-)ileum and antrum may be caused by up regulated SMA MHC. **Area under the curve was measured from peak force to 10 minutes after peak force. 10 min force is the 10 minute tonic force normalized to peak force.
Values are mean ± SE. * Significant at P< 0.05.

b. Tonic contraction induced by CCh in SMB$^{(+/+)}$ and SMB$^{(-/-)}$ ileum and antrum

To determine whether switching from SMB MHC expression to SMA MHC expression could also result in increased tonic force via altered agonist stimulation, SMB$^{(+/+)}$ and SMB$^{(-/-)}$ antrum, ileum and fundus strips were activated with 5μM CCh. The tonic component of the isometric force traces of ileum, antrum, and fundus in Figure 12 were quantified and compared between SMB$^{(+/+)}$ and SMB$^{(-/-)}$ using the same measurements mentioned above. The results of the area under the curve and 10 minute force are displayed in Table 8, showing that neither area under the curve (peak force to 10 minutes) nor 10 minute force (steady state) changed significantly between SMB$^{(+/+)}$ and SMB$^{(-/-)}$ except for the ileum. The area under the curve measurement was increased while the 10 minute force measurement was not in the SMB$^{(-/-)}$ ileum (Table 8). The results of the two measurements indicated that with CCh stimulation the tonic component of contraction does not increase in SMB$^{(-/-)}$ antrum. However, the area under the curve measurement showed that the tonic component of contraction in SMB$^{(-/-)}$ ileum increased while 10 minute force measurement indicated no change (Table 8). Unlike KPSS stimulation, CCh activation includes spontaneous contractions of gastrointestinal smooth muscle as shown in Figure 12 (Ehlert et al., 1999; Sinn et al., 2010; Unno et al., 2006), which may confound the area under the curve measurement. To test this, the spontaneous contraction induced by CCh was compared between SMB$^{(+/+)}$ and SMB$^{(-/-)}$ by comparing spike number and average amplitude from the time of peak force to 10 minutes after. No significant difference was observed (Table 9).

Tissue		Area under the curve**	10 min force**
Ileum	SMB$^{(+/+)}$	4.15±0.47	0.58±0.06
	SMB$^{(-/-)}$	5.84±0.18	0.57±0.04
P value		0.007*	0.91
Antrum	SMB$^{(+/+)}$	3.72±1.12	0.21±0.09
	SMB$^{(-/-)}$	2.29±0.31	0.072±0.01
P value		0.179	0.092
Fundus	SMB$^{(+/+)}$	5.49±0.27	0.52±0.03
	SMB$^{(-/-)}$	6.21±0.36	0.53±0.04
P value		0.160	0.844

Table 8. Quantification of tonic phase activated by 5μM CCh. The tonic component of contraction was quantified by measuring area under the curve from peak force to 10 minute and 10 minute force/peak force (steady state). Increased values for those two measurements suggest a larger tonic component. CCh stimulated SMB$^{(-/-)}$ ileum, antrum and fundus were not more tonic than SMB$^{(+/+)}$ by 10 minute force/peak force measurement. However the area under the curve from peak force to 10 minute was significantly larger for SMB$^{(-/-)}$ ileum compared to SMB$^{(+/+)}$, indicating SMB$^{(-/-)}$ ileum was more tonic.
**Area under the curve was measured from peak force to 10 minutes after peak force. 10 min force is the 10 minute tonic force normalized to peak force.
Values are mean ± SE. * Significant at P< 0.05. n=6 for all groups.

5μM CCh	Measurement	SMB$^{(+/+)}$	n	SMB$^{(-/-)}$	n	P value
Ileum	Amplitude (g)	0.29±0.06	5	0.49±0.12	4	0.145
	Spike number	22.4±8.74	5	42.75±9.46	4	0.16
Antrum	Amplitude (g)	0.87±0.21	6	1.35±0.45	6	0.361
	Spike number	15.67±3.16	6	15.57±2.36	6	0.98

Table 9. Comparison of spontaneous contraction induced by 5μM CCh between SMB$^{(+/+)}$ and SMB$^{(-/-)}$ ileum and antrum.
Values are mean ± SE. * Difference determined by t-test to be significant at P<0.05.

2. LC$_{20}$ phosphorylation levels with KPSS contraction.

As mentioned in the introduction, the "latch state" refers to the tonic contraction in which LC$_{20}$ phosphorylation is not proportional with sustained force maintenance. In the "latch state" the LC$_{20}$ phosphorylation level is low but force can be maintained at a high level. The loss of SMB MHC results in compensatory upregulated SMA MHC. It also may result in other alterations in smooth muscle by compensatory mechanisms. Other alterations that contribute to altered smooth muscle contractile pattern may include the change in the sensitivity of LC$_{20}$ phosphorylation to KPSS stimulation, which could be regulated by serial second messenger pathways or by unknown mechanisms. Thus whether the increased tonic contraction induced by KPSS in SMB$^{(-/-)}$ antrum and ileum is caused by elevated LC$_{20}$ phosphorylation level needs to be addressed before we conclude that SMA MHC is responsible for tonic contraction.

The phosphorylation status of LC$_{20}$ in ileum and antrum strips was determined at 1 minute and 10 minutes following KPSS activation. 1 minute was chosen to represent the time in the force trace showing the largest change in force between SMB$^{(+/+)}$ and SMB$^{(-/-)}$ animals. 10 minute in KPSS represents steady state. To verify the validity of phosphorylation measurements, stomach tissues before KPSS stimulation (unstimulated state should have very little or low level of LC$_{20}$phosphorylation) and 30 second in KPSS (peak force when the LC$_{20}$ phosphorylation should be significantly higher than rest state) were analyzed. Western blot results using antibodies specific to quantify phosphorylated LC$_{20}$ showed that the phosphorylation level of LC$_{20}$ was significantly higher following 30 seconds in KPSS than before KPSS stimulation (Table 10). Therefore, this method can be

Protein	Phosphorylation of LC_{20} before KPSS stimulation**	n	Phosphorylation of LC_{20} with 30s KPSS stimulation**	n	P value	Representive western blot result Before KPSS 30s KPSS
Phosphorylated LC_{20}	0.55±0.03	3	1.32±0.26	3	0.04*	β actin
LC_{20}	1.11±0.13	3	1.09±0.05	3	0.9	β actin
Phosphorylated LC_{20}/LC_{20}	0.51±0.04	3	1.21±0.21	3	0.032*	

Table 10. Phosphorylation method positive control. The phosphorylation level of LC20 at 30 seconds in KPSS stimulation was significant higher than before KPSS stimulation, demonstrating that the dry ice acetone method was able to preserve phosphorylation status.
** Arbitrary densitometric units
* Difference determined by t-test to be significant at P<0.05

used to compare the LC_{20} phosphorylation status between $SMB^{(+/+)}$ and $SMB^{(-/-)}$ ileum, antrum and fundus (control) at 1minute and 10minute KPSS. The results of LC_{20} phosphorylation status at 1 minute and 10 minute in KPSS are shown in Table 6. The phosphorylation status of LC_{20} was not significantly different between $SMB^{(+/+)}$and $SMB^{(-/-)}$ ileum and antrum at either the 1 minute or 10 minute KPSS time points suggesting that the increased tonic contraction in $SMB^{(-/-)}$ ileum and antrum is not due to the LC_{20} phosphorylation.

C. Aim three was to examine if the changes in PKC/CPI-17 or Rho/ROCK pathways are involved in changes in tonic and phasic contractions.

The previous section showed that KPSS stimulation resulted in increased tonic contraction in $SMB^{(-/-)}$ ileum and antrum, which was not attributed to the alteration of LC_{20} phosphorylation status. As discussed in the introduction, second messenger pathways PKC/CPI-17 and Rho/ROCK may contribute to the "latch state". Whether the increased tonic contraction is caused by changes in these signaling pathways needs to be investigated.

1. Second messenger pathways in tonic contraction induced by KPSS in $SMB^{(+/+)}$ and $SMB^{(-/-)}$ ileum and antrum.

Two signaling pathways (PKC/CPI-17 and Rho/ROCK) are reported regulate tonic contraction. Inhibitors reported to specifically inhibit these two signaling pathways were used to determine whether changes in the KPSS induced tonic contraction in $SMB^{(-/-)}$ ileum and antrum was caused by these specific second messenger pathways.

a. PKC/CPI-17 signaling pathway in tonic contraction with KPSS stimulation in SMB$^{(+/+)}$ and SMB$^{(-/-)}$ ileum and antrum.

i. PKC inhibitors in tonic contraction in SMB$^{(+/+)}$ and SMB$^{(-/-)}$ ileum and antrum.

To determine if the PKC/CPI-17 signaling pathway is involved in increased tonic contraction in SMB$^{(-/-)}$ ileum and antrum, PKC inhibitors Gõ6976 (inhibiting conventional PKC isoforms) and GF109203X (inhibiting both the conventional and novel isoforms of PKC) were used in KPSS induced isometric force measurement experiments. The peak force (area under the active force curve from peak force to 10 minutes) and 10 minute force (steady state) were measured with or without inhibitors (Gõ6976 1µM, GF109203X 1µM) with KPSS stimulation in SMB$^{(-/-)}$ ileum and antrum. Results are shown in Table 11. Use of the PKC inhibitors Gõ6976 and GF109203X failed to alter the increased tonic component of contraction induced by KPSS in SMB$^{(-/-)}$ ileum and antrum, suggesting that PKC/CPI-17 pathway is not involved in increased tonic contraction in these tissues.

ii.PKC activation with phorbol ester (PDBu)

If KPSS induced increased tonic contraction in SMB$^{(-/-)}$ ileum and antrum is mediated by the PKC/CPI-17 signaling pathway, the one would predict directly activating PKC would have the same result. Phorbol ester (PDBu) is able to mimic the activity of DAG, which is the activator of PKC. Isometric force measurement were analyzed following stimulation with 1µM PDBu in SMB$^{(+/+)}$ and SMB$^{(-/-)}$ ileum and antrum strips. Figure 13 shows representative superimposed force traces for SMB$^{(+/+)}$ and SMB$^{(-/-)}$ ileum

Tissue	Measurements	n	Control	Gő6976	GF109203X
Ileum SMB[(-/-)]	Area under the curve**	13	5.32±0.35	5.55±0.33	5.0573±0.56
	10 min force (g)	8	0.73±0.11	0.59±0.11	0.51±0.12
Antrum SMB[(-/-)]	Area under the curve**	8	3.87±0.21	4.31±0.46	4.59±0.26
	10 min force (g)	8	1.28±0.39	1.73±0.48	1.78±0.38
Tissue	Measurements	n	Control	Y27632	H1152
Ileum SMB[(-/-)]	Area under the curve**	8	5.32±0.35	4.66±0.58	4.66±0.58
	10 min force (g)	5	0.83±0.21	0.69±0.12	0.74±0.15
Antrum SMB[(-/-)]	Area under the curve**	7	3.92±0.21	5.51±0.54	4.99±0.87
	10 min force (g)	5	2.05±0.72	2.24±1.1	2.5±1.1

Table 11. Effects of PKC inhibitors (Gő6976 (1μM), GF109203X (1 μM)) and ROCK inhibitors (Y27632 (10μM), H1152 (0.1μM)). There was no significant difference in KPSS induced tonic component between SMB [(-/-)] ileum, antrum and fundus with inhibitors (either PKC inhibitors or ROCK inhibitors) and control (without any of the inhibitors).
**Area under the curve was measured from peak force to 10 minutes after peak force.
Values are mean ± SE. *Difference determined by ANOVA to be significant at $P<0.05$.
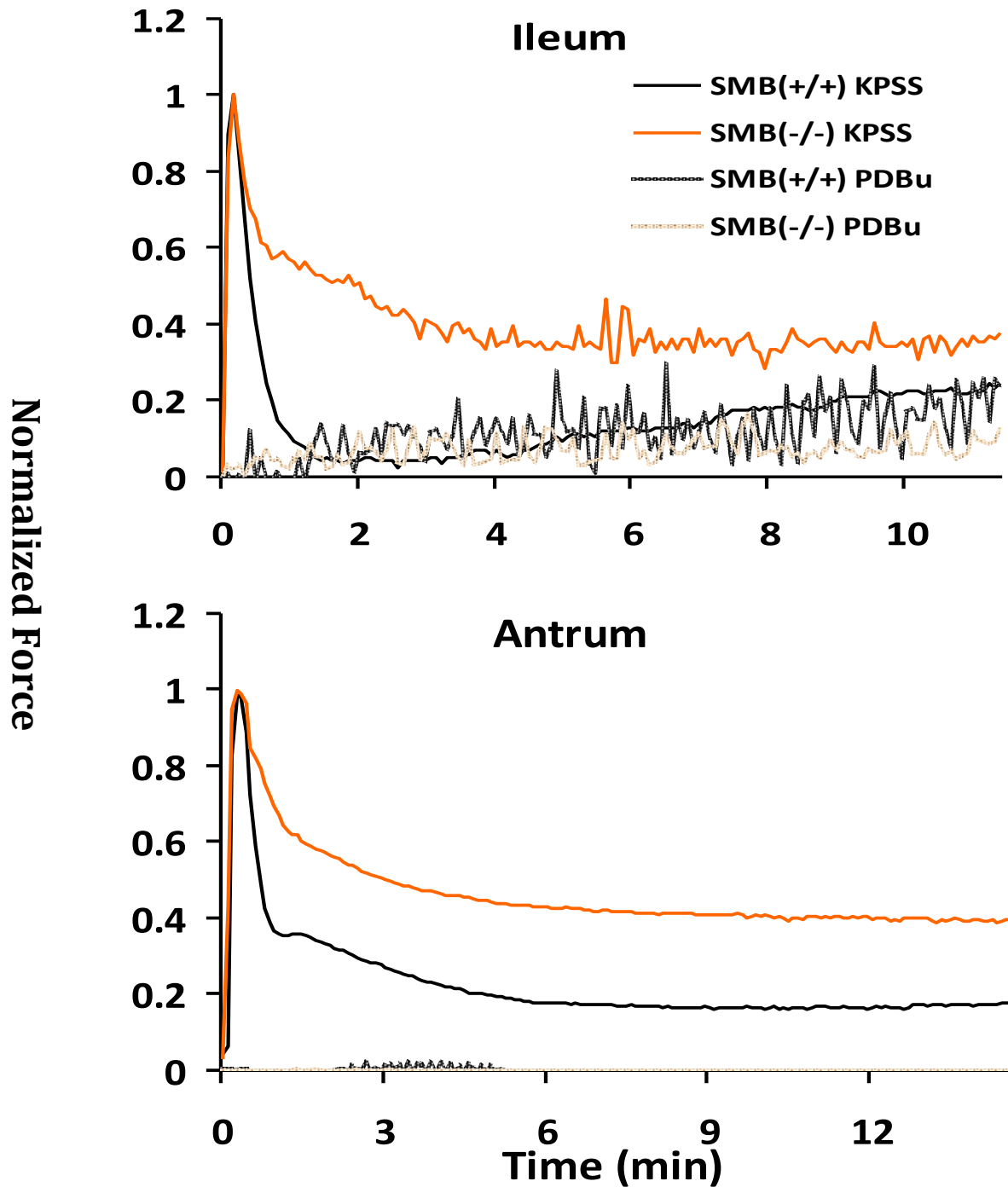
Figure 13. Representative comparison of 1μM PDBu and KPSS isometric force traces of SMB$^{(+/+)}$ and SMB$^{(-/-)}$ ileum and antrum. Force KPSS active peak force is normalized to 1. KPSS tonic force is significantly greater in the KPSS tonic phase of the SMB$^{(-/-)}$ tissues vs. the SMB$^{(+/+)}$. There is no significant difference between the force responses of the SMB$^{(+/+)}$ and SMB$^{(-/-)}$ tissues in response to PDBu

and antrum contractions induced by 1μM PDBu in comparison to the KPSS responses.
The forces induced by PDBu in both the SMB$^{(+/+)}$ and SMB$^{(-/-)}$ tissues were very small
(less than 0.6g compared to ~3 and 6 grams peak force with KPSS for ileum and antrum
respectively) and barely above zero for the antrum. In addition, they were not
significantly different from each other (Table 12). Thus, PKC/CPI-17 signaling pathway
is unlikely involved in increased tonic contraction in KPSS stimulation.

b. Rho/ROCK signaling pathway in KPSS stimulated SMB$^{(+/+)}$ and SMB$^{(-/-)}$ ileum and antrum.

The Rho/ROCK signaling pathway is another second messenger pathway reported to
regulate tonic contraction. To test the involvement of Rho/ROCK signaling pathway in
KPSS induced increased tonic contraction in SMB$^{(-/-)}$ ileum and antrum, ROCK inhibitors
H1152 and Y27632 were used to eliminate tonic contraction in these tissues. Similar to
the pharmacological experiments with PKC inhibitors, the isometric force measurement
was carried out in KPSS stimulation with or without ROCK inhibitors (H1152 0.1μM,
Y27632 10μM). Results are shown in Table 11. The tonic component of contraction
induced by KPSS in tissues with H1152 or Y27632 was not decreased compared to
tissues without inhibitors. ROCK inhibitors were unable to decrease the increased tonic
contraction in SMB$^{(-/-)}$ ileum and antrum, indicating that Rho/ROCK may not play a role
in KPSS induced increased tonic contraction in these tissues.

Inhibitors for PKC and ROCK failed to eliminate the tonic contraction in SMB$^{(-/-)}$
ileum and antrum. Force generated by specifically activating PKC with PDBu was too

Tissue		n	Area under the curve**	30 min force**
Ileum	SMB$^{(+/+)}$	6	15.01±2.83	0.28±0.09
	SMB$^{(-/-)}$	8	15.79±1.49	0.49±0.07
P value			0.799	0.074
Antrum	SMB$^{(+/+)}$	4	5.63±1.76	0.14±0.02
	SMB$^{(-/-)}$	5	7.7±5.99	0.16±0.1
P value			0.774	0.817

Table 12. Quantification of tonic phase activated by 1μM PDBu.
**Area under the curve was measured from peak force to 30 minutes. 30 min force is the 30 minute tonic force normalized to peak force.
Values are mean ± SE. * Significant at P< 0.05.

small to account for the increased tonic component of contraction in the SMB$^{(-/-)}$ ileum and antrum. Thus, the increased tonic contraction of SMB$^{(-/-)}$ ileum and antrum induced by KPSS was not regulated by either the PKC/CPI-17 or Rho/ROCK signaling pathway.

2. Other contractile regulatory proteins in SMB$^{(+/+)}$ and SMB$^{(-/-)}$ ileum and antrum

The SMB$^{(-/-)}$ mouse model that we are working with appears anatomically and physically normal. In order for the mouse to survive, the loss of SMB MHC isoform may result in up or down regulation of certain proteins in SM (including the up regulation of SMA MHC isoform). In the SMB$^{(-/-)}$ animal, the expression of proteins involved in smooth muscle contractile regulation needs to be examined. Western blotting was carried out to quantitatively compare the expression of various contractile regulatory proteins including MLCK, MLCP, PKCδ, PKCα and CPI-17 in SMB$^{(-/-)}$ and SMB$^{(+/+)}$ ileum, antrum and fundus, that could also be altered as a result of compensatory changes in the SMB$^{(-/-)}$ mice. Results (Table 13) show that for all of the SM tissues studied, the levels of the above mentioned proteins except PKCα were not significantly altered between the SMB$^{(-/-)}$ and SMB$^{(+/+)}$ animals (Table 13). PKCα protein expression was significantly reduced in the antrum, but not in the ileum or fundus of SMB$^{(-/-)}$ mice.
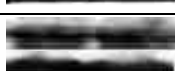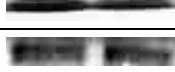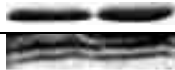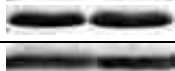
Tissue type	Protein	SMB$^{(+/+)}$ **	SMB$^{(-/-)}$ **	P value	Representative western blot result SMB$^{(+/+)}$ SMB$^{(-/-)}$
Ileum	MLCK	0.9±0.1	1.04±0.13	0.449	β actin
	MLCP	1.13±0.06	1.12±0.13	0.974	β actin
	PKCδ	1.09±0.26	1.09±0.31	0.997	β actin
	PKCα	0.99±0.03	1.04±0.02	0.24	β actin
	CPI-17	0.89±0.2	1.15±0.21	0.425	β actin
Antrum	MLCK	1.08±0.16	1.14±0.12	0.779	β actin
	MLCP	1.06±0.07	0.95±0.07	0.286	β actin
	PKCδ	1.27±0.13	1.11±0.22	0.564	β actin
	PKCα	1.08±0.02	0.93±0.02	0.005*	β actin
	CPI-17	1.01±0.04	0.98±0.04	0.575	β actin
Fundus	MLCK	1.02±0.09	0.99±0.09	0.779	β actin
	MLCP	1.13±0.29	0.85±0.06	0.401	β actin
	PKCδ	0.99±0.03	1.01±0.12	0.878	β actin
	PKCα	1.03±0.06	0.98±0.06	0.585	β actin
	CPI-17	1.00±0.03	1.03±0.08	0.788	β actin

Table 13. Quantitative western blot results of the expression of various contraction regulatory proteins in SMB$^{(+/+)}$ and SMB$^{(-/-)}$ ileum, antrum and fundus with β actin as loading control. The expression of PKCα was decreased in SMB$^{(-/-)}$ antrum compared to SMB$^{(+/+)}$.
Values are mean ± SE. ** Arbitrary densitometric units. * Difference determined by t-test to be significant at P<0.05. n=3 for all groups.

IV. Discussion:

The mechanism underlying the sustained tonic force of smooth muscle contraction remains unknown. The kinetics of actomyosin ATPase activity of SMA MHC is slower than the SMB MHC isoform (Kelley et al., 1993; Sweeney et al., 1998). In addition, SMA and SMB MHC protein expression is preferential to tonic and phasic tissues, respectively (Babij, 1993; Eddinger and Meer, 2001; Eddinger et al., 2007; Eddinger, 2009; Han et al., 2006; Rondelli et al., 2007; White et al., 1993). And the SMA/B MHC isoforms are predominantly or exclusively expressed in adult animal smooth muscle tissues(Eddinger and Murphy, 1991; Eddinger and Wolf, 1993; Giuriato et al., 1992). Thus, we hypothesized that the SMA and SMB MHC isoforms are responsible for regulating tonic and phasic contractions respectively in smooth muscle. To test this hypothesis, we used SMB MHC knockout mouse (Babu et al., 2001) phasic (ileum and antrum) and tonic tissues (fundus) to investigate whether loss of SMB MHC protein would lead to an increased sustained tonic force and a deceased rate of force generation in SM tissues.

The SMB$^{(-/-)}$ mice appear physically and anatomically normal. Histological analysis of SMB$^{(-/-)}$ ileum, antrum and fundus smooth muscle layers reveals no gross differences relative to wild type mice (Figure 7), which is consistent with previous reports (Babu et al., 2001) suggesting that the loss of the SMB MHC isoform does not cause muscle pathology or affect animal survival. This could be due to the compensatory upregulation of the SMA MHC isoform, which appears to compensate in maintaining the

smooth muscle structure and function in SMB$^{(-/-)}$ mice.

Phasic smooth muscle tissues such as ileum and stomach antrum express predominantly the SMB MHC isoform. The loss of the SMB MHC isoform in these tissues is compensated for by the upregulation of the SMA MHC isoform. Fundus, which primarily expresses the SMA MHC isoform (Eddinger and Meer, 2001), did not show upregulation of SMA MHC protein in the SMB$^{(-/-)}$ mice. Our data (Table 4) also show that the total SM myosin (SM+NM) content is not altered in all of the three tissues, suggesting that loss of SMB MHC is compensated for by the up regulated SMA MHC isoform. Besides the SM MHC isoform, non-muscle (NM) MHC may also affect the total MHC content. Furthermore, NM myosin has been reported to regulate tonic contraction (Lofgren et al., 2003; Morano et al., 2000). Therefore, comparison of the expression of NM MHC in SMB$^{(+/+)}$ and SMB$^{(-/-)}$ needed to be examined. Measurement of NM MHC protein expression in the ileum shows no significant difference between the SMB$^{(-/-)}$ and wild type control (Table 4). Consistently, Babu et al. (Babu et al., 2001) also reported that the expression of NM MHC is unchanged in SMB$^{(+/+)}$ and SMB$^{(-/-)}$ mouse bladder. Furthermore, multiple studies (Borrione et al., 1989; Eddinger and Murphy, 1991; Eddinger and Wolf, 1993; Frid et al., 1993; Giuriato et al., 1992; Loukianov et al., 1997) have reported that the expression of NM MHC is developmentally regulated and not abundantly expressed in adult animal tissues. Taken together, these data show that the SM MHC isoform in SMB$^{(-/-)}$ ileum and antrum switches from SMB to SMA MHC, without a significant change in NM MHC expression.

The low and unaltered NM MHC expression in SMB[(-/-)] animals is thus unlikely to participate in any changes of smooth muscle contractile patterns in SMB[(-/-)] tissues.

If the SMA MHC is responsible for tonic contraction, it is expected that the sustained tonic force would increase in SMB[(-/-)] phasic tissues where the SMB MHC isoform switches to the SMA MHC isoform. Our data show that with KPSS stimulation, switching from SMB to SMA MHC significantly increases the sustained tonic force in SMB[(-/-)] ileum and antrum tissues (Figure 9, Table 7). Tonic fundus tissue, where there is only limited expression of the SMB MHC isoform in SMB [(+/+)] animals, does not show a significant change in tonic contraction as there is not a significant change in SMB MHC protein expression. These data provide support for the hypothesis that the SMA MHC isoform is a major determinant of tonic contraction.

Second messenger pathway regulation of LC_{20} phosphorylation has been proposed to play an important role in tonic contraction. There have been numerous studies reporting the involvement of PKC/CPI-17 and Rho/ROCK second messenger pathways in regulating tonic contraction via control of LC_{20} phosphorylation (Ratz et al., 2005; Somlyo and Somlyo, 2003). Jiang et al. (Jiang and Morgan, 1987) reported that the PKC/CPI-17 signaling pathway is able to regulate tonic contraction via phorbol ester stimulation. Work from Sohn et al. (Sohn et al., 2001) suggested that PKCε is responsible for maintenance of tonic tone induced by PGF2α or a thromboxane analog in lower esophageal sphincter (LES), and Poole et al. (Poole and Furness, 2007) reported that the PKCδ isoform is able to enhance tonic contraction in guinea pig ileum. Additionally, the Rho/ROCK signaling pathway has also been reported to be responsible for tonic

contraction (Harnett et al., 2005; Rattan et al., 2006; Urban et al., 2003). We tested this hypothesis by using PKC or ROCK inhibitors to block the PKC/CPI-17 or Rho/ROCK signaling pathways respectively. Results show both PKC inhibtors (Gδ6976 - PKC_{α}, and $PKC_{\beta1}$ inhibitor, GF109203X - $PKC_{\alpha,-\beta1,-\beta2,\gamma,\varepsilon,\delta}$ inhibitor) and ROCK inhibitors (Y27632, H1152) fail to eliminate the increased sustained tonic force in these tissues (Table 11), suggesting that the PKC/CPI-17 and Rho/ROCK signaling pathways are not responsible for the increased tonic contraction in the $SMB^{(-/-)}$ animals. Consistent with this, when directly activating PKC with PDBu, tonic force generated by PDBu stimulation is not different between $SMB^{(-/-)}$ and $SMB^{(+/+)}$ tissues (Table 12). In addition, only minimal force is produced in both $SMB^{(+/+)}$ and $SMB^{(-/-)}$ tissues with PDBu activation, which is insignificant compared to the increased KPSS tonic force in $SMB^{(-/-)}$ ileum and antrum. Thus, changes in the PKC/CPI-17 and Rho/ROCK signaling pathways are unlikely to be the cause of the increased tonic contraction observed in $SMB^{(-/-)}$ ileum and antrum (Table 7).

There are many other regulatory pathways that may also affect LC_{20} phosphorylation that we did not measure. To test for this possible effect, we examined the LC_{20} phosphorylation status of $SMB^{(-/-)}$ and $SMB^{(+/+)}$ ileum, antrum and fundus at 1 minute (the most prominent point of enhanced tonic contraction in $SMB^{(-/-)}$ ileum and antrum) and 10 minute (steady state tonic force) time points. The phosphorylation status of LC_{20} is not different between $SMB^{(+/+)}$ and $SMB^{(-/-)}$ tissues following KPSS activation, indicating that the increased tonic contraction in $SMB^{(-/-)}$ ileum and antrum is not a result of different levels of LC_{20} phosphorylation (Table 6). This suggests that changes in

second messenger pathway mechanisms to alter LC_{20} phosphorylation are not responsible for the tonic contraction enhancement with KPSS activation in $SMB^{(-/-)}$ ileum and antrum.

Other mechanisms hypothesized to explain tonic contraction include calponin or caldesmon dependent actin-to- myosin cross-links (Sutherland and Walsh, 1989; Szymanski and Tao, 1997) and cytoskeletal remodeling (Gerthoffer and Gunst, 2001; Hu et al., 2007; Kim et al., 2008; Mehta and Gunst, 1999; Pavalko et al., 1995). It has been reported that the thin filament regulatory protein calponin expression is increased and caldesmon expression is decreased in the $SMB^{(-/-)}$ aorta (Babu et al., 2004). This occurs without a SMB to SMA MHC expression switching and results in decreased maximal force, suggesting that these thin filament regulatory proteins may play a role in regulating smooth muscle contraction (Babu et al., 2004). In addition, the result from a follow-up study in mesenteric vessels, knocking out h1-calponin in $SMB^{(-/-)}$ mice showed loss of calponin is able to restore the decreased maximal force level to wild type values. However, this result may also be caused by significantly decreased α-actin expression and increased caldesmon in these SMB MHC and h1-calponin double knockout mesenteric vessels (Babu et al., 2006). With limited data relative to possible changes in α-actin, calponin and caldesmon in the $SMB^{(-/-)}$ mice, their possible function in tonic force maintenance, and lack of quantitation of these proteins in this study, it remains unclear if the enhanced tonic force of $SMB^{(-/-)}$ animals can also be affected by cytoskeletal remodeling (α actin related) or altered calponin or caldesmon dependent actin –to –myosin cross links.

Tonic force was also measured using agonist activation. CCh, an acetylcholine analog, is a M3 receptor agonist and the major activator of gastrointestinal smooth muscle contraction (Furness, 2012; Kitazawa et al., 2007; Murthy, 2006). Our results indicate no increase in the tonic contractile component of the tissues examined with the exception of the area under the curve measurement for the ileum (Figure 12, Table 8). Why this may be remains unclear. It could be that the M3 receptor becomes inactivated (G-protein turns off) or calcium channels turn off ($[Ca^{2+}]_i$ decreases). Regulation of these systems may also contribute to whether a tissue physiologically produces tonic contractions. It has been reported that CCh activation results in spontaneous contraction of gastrointestinal smooth muscle (Sinn et al., 2010; Unno et al., 2006), and our force trace data shows spontaneous contractions caused by CCh (Figure 12). The presence of spontaneous contractions superimposed on a tonic contraction may interfere with tonic force maintenance even though the frequency and average amplitude of the spontaneous contractions between SMB[(+/+)] and SMB[(-/-)] ileum and antrum were not found to be significantly different (Table 9). In addition, the unaltered spontaneous contractions in SMB[(-/-)] ileum and antrum suggests that SMB MHC may not be required in order for phasic tissues to produce the fast and transient contractions that occur during rhythmic contraction. The "slow" myosin isoform, SMA MHC, may be capable to support these rapid contractions.

As reported, the loss of SMB MHC isoform in the SMB[(-/-)] tissues also results in down regulation of PKCα in antrum and up regulation of SMA MHC in antrum and ileum. While this could also happen for other proteins, we did not find this to be the case for any of the other proteins we measured (MLCK, MLCP, PKCδ, and CPI-17) (Table

13). PKCα down regulation in SMB$^{(-/-)}$ antrum is inconsistent with the study from

Hypolite et al. (Hypolite et al., 2009) reporting PKCα protein expression is upregulated in

detrusor smooth muscle. The difference may be tissue specific regulation of PKCα in

SMB$^{(-/-)}$ mice. The minimal total force generated, and lack of change in this force induced

by PDBu between SMB$^{(+/+)}$ and SMB$^{(-/-)}$ suggest the change in KPSS tonic force is not

due to the down regulation of PKCα in the antrum (Table 12).

It has been reported that maximum stress is decreased in the SMB$^{(-/-)}$ bladder but

increased in mesenteric vessels under depolarized conditions (Babu et al., 2001; Babu et

al., 2004). In addition, Hypolite et al. (Hypolite et al., 2009) reported that the maximum

stress of SMB$^{(-/-)}$ bladder detrusor smooth muscle is significantly increased over SMB$^{(+/+)}$

tissue. Studies from Karagiannis et al. (Karagiannis et al., 2003) using permeabilized

bladder tissues showed that the maximum stress is not altered in SMB$^{(-/-)}$ bladder, and

Patzak et al. (Patzak et al., 2005) also failed to find any difference of maximal stress

induced by KCl between SMB$^{(+/+)}$ and SMB$^{(-/-)}$ afferent arterioles. Tuck et al. (Tuck et al.,

2004) also reported no significant difference in SMB$^{(-/-)}$ airway peak resistance in

response to methacholine. We also tried to determine if there is any correlation between

SMA/SMB MHC isoform expression and maximal force generation in the phasic ileum

and antrum and tonic fundus. Our data show that replacing the SMB MHC with the SMA

MHC isoform in ileum, antrum, and fundus does not significantly alter the maximum

stress these tissues generate when activated either by KCl or CCh (see results),

suggesting that the different kinetic properties of SMA/B MHC isoforms do not affect

smooth muscle maximum force production. It remains unclear why the results of these

studies are not consistent regarding the relationship of SMA/SMB MHC isoform

expression and maximum stress generation. A possible explanation for these

seemingly contradictory results may be a result of different experimental methods used.

Babu and Karagiannis (Babu et al., 2004; Karagiannis et al., 2004) used skinned bladder

tissue (which layer of bladder smooth muscle was tested is not clear), and Hypolite and

colleagues (Hypolite et al., 2009) used intact longitudinal layer of detrusor smooth

muscle of bladder. Although skinned tissue is good for manipulating the $[Ca^{2+}]_I$, small

contractile regulatory proteins such as CaM may diffuse out from skinned tissue. In the

work by Babu et al., (2004), exogenous CaM was added to the SMB$^{(+/+)}$ and SMB$^{(-/-)}$

tissues to compensate for CaM loss. Whether the exogenous CaM is able to redistribute

to the correct cellular location and function as the endogenous CaM is unclear.

Furthermore, they did not take into consideration the expression of CaM may be altered

in intact SMB$^{(-/-)}$ tissue compared to SMB$^{(+/+)}$. Thus, studies in intact tissue are more

physiological. Reported differences between studies on small arteries using SMB$^{(-/-)}$

mice also suggest differences of maximal arteriole stress(Babu et al., 2001; Babu et al.,

2004; Tuck et al., 2004). Differences here could be due to different arterioles studied

(Buba et al., 2004: mesenteric vessel, Tuck et al., 2004: renal afferent and efferent

arterioles). In addition, Tuck et al., 2004 did not directly measure force generation from

these renal arterioles but established a relationship between lumen diameter and pressure

applied. They assumed that an index of lumen diameter reflected the force generation in

these arterioles. However, while there may be a correlation between lumen diameter and

wall stress, other factors including the intracellular elastic component and extracellular

matrix also contribute to wall stress, in a non linear fashion, especially at extreme

conditions. Thus, the alteration of lumen diameter is indicative of but not the same as the

force generation status of smooth muscle. Babu et al., 2004 did directly measure the

isometric force of mesenteric vessel in SMB$^{(+/+)}$ and SMB$^{(-/-)}$.

To estimate whether SMA/SMB MHC isoforms affect V_{max} in phasic and tonic

gastrointestinal tissues, we used three measurements to compare the isometric force

transient (as an estimate of V_{max}) with either KPSS or CCh stimulation in SMB$^{(+/+)}$ and

SMB$^{(+/+)}$ ileum antrum, and fundus. Our results show that the force transient is

significantly slower in SMB$^{(-/-)}$ ileum and antrum (Table 5). This is consistent with the

results from other studies reporting a decreased V_{max} using this SMB$^{(-/-)}$ mouse model

(Babu et al., 2001; Babu et al., 2004; Babu et al., 2006; Hypolite et al., 2009; Karagiannis

et al., 2003; Karagiannis et al., 2004; Tuck et al., 2004), and results that the SMB MHC

isoform has a two-fold greater ATPase activity and moves actin filament 2.5 folds faster

than SMA MHC in an *in vitro* motility assay (Kelley et al., 1993; Sweeney et al., 1998).

Because the rate of the force transient is also correlated with LC$_{20}$ phosphorylation, we

also measured this. LC$_{20}$ phosphorylation induced by KPSS at 5 seconds following tissue

activation is not different between the SMB$^{(+/+)}$ and SMB$^{(-/-)}$ tissues suggesting the slower

force transient in SMB$^{(-/-)}$ ileum and antrum is not caused by lower LC$_{20}$ phosphorylation

(Table 6). The decreased force transient is correlated with and perhaps caused by the

slower kinetic properties of SMA MHC, and not a difference in LC$_{20}$ phosphorylation.

The isometric force transient of fundus does not change, which is consistent with no

detectable SMB to SMA MHC protein expression switching in this tissue. The slow vs.

fast actomyosin ATPase activity of SMA/SMB MHC isoform may be important for SMA

MHC to maintain force in tonic tissues. Slow kinetics of actomyosin ATPase could result

in high ADP affinity and a low rate of ADP release in the presence of actin, which

enables SMA MHC to remain attached to actin longer. The actin-myosin- ADP state of SMA MHC has been reported to require mechanical strain to release ADP (Kovacs et al., 2007). With tonic force maintenance, the long attachment time of SMA MHC to actin may explain the hypothesized latch cross bridge.

Our study based on SMB$^{(-/-)}$ mice shows SMB MHC expression is turned off and SMA MHC isoform expression is increased in SMB$^{(-/-)}$ phasic ileum and antrum tissues. The reduced rate of force generation in the ileum and antrum is likely a result of the increased expression of the SMA MHC protein that cannot generate phasic force as quickly as the SMB MHC isoform. The increased SMA MHC expression enhances the sustained tonic contraction observed in these phasic tissues, suggesting SMA MHC isoform is a major determinant of tonic contraction. Further work is required to uncover the mechanism by which SMA MHC isoform reduces the rate of tension development and decreases V_{max} and unequivocally determine whether other thin filament regulatory proteins and cytoskeletal remodeling mechanisms also contribute to increased tonic contraction observed in SMB$^{(-/-)}$ phasic tissues.

V. Summary:

The major goal of this project was to test the hypothesis that the tissue specific distribution and kinetic properties of SMA and SMB MHC play a role in tonic vs. phasic contraction. A SMB$^{(-/-)}$ mouse model was used in this study with these mice appearing physically, anatomically and histologically normal. The lack of grossly observable pathological conditions may be attributable to up regulation of the SMA MHC isoform which compensates for the loss of SMB MHC isoform in these animals. Mechanical changes observed in the SMB$^{(-/-)}$ animals include: (1) In the absence of SMB MHC, the maximal stress induced either by KPSS or CCh stimulation was not altered in phasic tissues (ileum and antrum). As expected, the isometric force transient rate was decreased in these tissues, in which compensatory upregulation of the "slow" SMA replaced the "fast" SMB MHC isoform. These results suggest that the SMA MHC isoform is able to generate the same amount of force but with a slower dp/dt than the SMB MHC; (2) The loss of SMB MHC and up regulated SMA MHC isoform expression resulted in elevated tonic force maintenance with KPSS activation in SMB$^{(-/-)}$ ileum and antrum suggesting a role in tonic contraction regulation. As a negative control, tonic fundus did not show any different in contractions between SMB$^{(+/+)}$ and SMB$^{(-/-)}$ tissues. Furthermore, the increased tonic force maintenance in these tissues was not the result of the changes in LC$_{20}$ phosphorylation or the extensively studied second messenger pathways PKC/CPI17 or Rho/ROCK; (3) The spontaneous contractions (phasic contractions) induced by CCh in SMB$^{(-/-)}$ ileum and antrum were not affected either in its frequency or amplitude.

These results suggest that (a) SMB MHC is not required for a phasic contraction but the rate of tension generation is reduced in the absence of SMB MHC. SMA MHC is able to generate the same amount of maximum force as SMB MHC during phasic contraction. The slower force developmental rate in tissue expression only SMA MHC does not affect normal physiological function of these tissues. (b) SMA MHC is responsible for tonic contraction when ileum and antrum are fully activated by KPSS. This study also showed that up regulated SMA MHC failed to cause increased tonic force maintenance in SMB$^{(-/-)}$ ileum and antrum when stimulated with the physiological agonist CCh. While the reason for this is not completely clear, it is possible that unloading stress at the cross bridge during a tonic contraction (via the superimposed spontaneous contractions) allows cross bridge to dissociate and therefore reduces tonic force maintenance or it could be that the receptors become inactivated, that G proteins turn off, or that calcium channels turned off, which could mask the effect of increased SMA MHC expression. Thus it may be that the SMA MHC is required for enhanced tonic force, but this only occurs when the proper regulatory pathways are also invoked to bring about this maintained force generation. (c) Spontaneous contractions are critical for gastrointestinal peristalsis and food digestion. Unaltered spontaneous contractions insure the normal physiological function of gastrointestinal system in SMB$^{(-/-)}$ animal.

As mentioned above, the fact that SMB$^{(-/-)}$ animals appear normal suggested that SMB MHC function can be replaced by SMA MHC under nonstressed conditions. It is unclear if SMB$^{(-/-)}$ mice would show dysfunction under stressed conditions such as reduced caloric intakes , hypoxia, extreme exertion, or with certain diseases. This study

provides clues to address this question. Changes in the myosin isoforms in hypertrophy related diseases have been reported in skeletal(D'Antona et al., 2006; Stone et al., 1996), cardiac(Pandya et al., 2006; Pandya et al., 2008; Sucharov et al., 2004), and smooth muscle(Austin et al., 2004; DiSanto et al., 2003; Lofgren et al., 2002; Wetzel et al., 1998). Partial bladder outlet obstruction (PBOO) induced hypertrophy in mice and rabbits results in a shift from SMB MHC to SMA MHC (DiSanto et al., 2003). The expression of SMB MHC in precapillary arterioles of left ventricle of the spontaneous hypertensive rats is also significantly decreased (Wetzel et al., 1998). Down regulated SMB MHC was also observed in the mega colon in Hirschsprang's disease and partial obstructive ileum (Lofgren et al., 2002; Siegman et al., 1997). Results from our study demonstrating a slower force transient rate of SMA MHC correlated with lower ATPase activity (Kelley et al., 1993; Sweeney et al., 1998) seem to not affect the normal physiological function of SMB $^{(-/-)}$ smooth muscle tissues, indicating that SMA MHC may substitute for SMB MHC in a more energy efficient manner. Thus we speculate that under unfavorable conditions, smooth muscle may switch its myosin heavy chain composition from SMB MHC to the more economical SMA MHC to conserve energy. This could explain the observations that hypertrophied detrusor smooth muscle (DSM), ileum smooth muscle and mega colon in Hirschsprang's disease or cardiac vessels of hypertensive rats have decreased SMB MHC expression.

Our study suggested that SMA MHC is able to maintain force at a higher level than SMB MHC, which propose possible explanation for a common phenomenon in smooth muscle hypertrophy that SMB MHC isoform changes towards to SMA MHC.

(Sjuve et al., 1998) In hypertrophic organs, the tension generated from smooth muscle wall must be increased to maintain a given intraluminal pressure. The change in contractile properties from SMB to SMA MHC isoform might be beneficial in such conditions where the tension needs to be maintained for longer period of time

Besides disease pathology, further test for whether SMA MHC is able to completely replace SMB MHC and maintain normal physiological function in smooth muscle tissues, could focus on effects of stress conditions (coloric restriction, hypoxia, pH etc.) on smooth muscle contractile characteristics as well as the overall performance of SMB$^{(-/-)}$ mice on vomiting, constipation, diarrhea, etc.

This study provided information about the distribution and kinetic properties of SMA and SMB MHC isoforms in regulating tonic and phasic contractile patterns in smooth muscle tissues. It also provided insight to correlate SMA/B MHC isoforms with disease pathology such as hypertrophy. The results that SMA MHC is able to replace SMB MHC in maintaining maximum force generation while increasing efficiency makes SMA MHC a more favorable MHC isoform under stressed conditions, which is very interesting and worth investigating.

VI. Bibliography

Adelstein, R.S., and Conti, M.A. (1975). Phosphorylation of platelet myosin increases actin-activated myosin ATPase activity. Nature *256,* 597-598.

Alessi, D., MacDougall, L.K., Sola, M.M., Ikebe, M., and Cohen, P. (1992). The control of protein phosphatase-1 by targetting subunits. The major myosin phosphatase in avian smooth muscle is a novel form of protein phosphatase-1. Eur. J. Biochem. *210,* 1023-1035.

Amano, M., Ito, M., Kimura, K., Fukata, Y., Chihara, K., Nakano, T., Matsuura, Y., and Kaibuchi, K. (1996). Phosphorylation and activation of myosin by Rho-associated kinase (Rho-kinase). J. Biol. Chem. *271,* 20246-20249.

Austin, J.C., Chacko, S.K., DiSanto, M., Canning, D.A., and Zderic, S.A. (2004). A male murine model of partial bladder outlet obstruction reveals changes in detrusor morphology, contractility and Myosin isoform expression. J. Urol. *172,* 1524-1528.

Babij, P. (1993). Tissue-specific and developmentally regulated alternative splicing of a visceral isoform of smooth muscle myosin heavy chain. Nucleic Acids Res. *21,* 1467-1471.

Babij, P., Kelly, C., and Periasamy, M. (1991). Characterization of a mammalian smooth muscle myosin heavy-chain gene: complete nucleotide and protein coding sequence and analysis of the 5' end of the gene. Proc. Natl. Acad. Sci. U. S. A. *88,* 10676-10680.

Babij, P., and Periasamy, M. (1989). Myosin heavy chain isoform diversity in smooth muscle is produced by differential RNA processing. J. Mol. Biol. *210,* 673-679.

Babu, G.J., Celia, G., Rhee, A.Y., Yamamura, H., Takahashi, K., Brozovich, F.V., Osol, G., and Periasamy, M. (2006). Effects of h1-calponin ablation on the contractile properties of bladder versus vascular smooth muscle in mice lacking SM-B myosin. J. Physiol. *577,* 1033-1042.

Babu, G.J., Loukianov, E., Loukianova, T., Pyne, G.J., Huke, S., Osol, G., Low, R.B., Paul, R.J., and Periasamy, M. (2001). Loss of SM-B myosin affects muscle shortening velocity and maximal force development. Nat. Cell Biol. *3,* 1025-1029.

Babu, G.J., Pyne, G.J., Zhou, Y., Okwuchukuasanya, C., Brayden, J.E., Osol, G., Paul, R.J., Low, R.B., and Periasamy, M. (2004). Isoform switching from SM-B to SM-A myosin results in decreased contractility and altered expression of thin filament regulatory proteins. Am. J. Physiol. Cell. Physiol. *287,* C723-9.

Barden, J.A., Sehgal, P., and Kemp, B.E. (1996). Structure of the pseudosubstrate recognition site of chicken smooth muscle myosin light chain kinase. Biochim. Biophys. Acta *1292,* 106-112.

Barron, J.T., Barany, M., and Barany, K. (1979). Phosphorylation of the 20,000-dalton light chain of myosin of intact arterial smooth muscle in rest and in contraction. J. Biol. Chem. *254,* 4954-4956.

Baumann, B.A., Taylor, D.W., Huang, Z., Tama, F., Fagnant, P.M., Trybus, K.M., and Taylor, K.A. (2012). Phosphorylated smooth muscle heavy meromyosin shows an open conformation linked to activation. J. Mol. Biol. *415,* 274-287.

Bednarek, M.L., Speich, J.E., Miner, A.S., and Ratz, P.H. (2011). Active tension adaptation at a shortened arterial muscle length: inhibition by cytochalasin-D. Am. J. Physiol. Heart Circ. Physiol. *300,* H1166-73.

Berg, J.S., Powell, B.C., and Cheney, R.E. (2001). A millennial myosin census. Mol. Biol. Cell *12,* 780-794.

Bornstein, J.C., Costa, M., and Grider, J.R. (2004). Enteric motor and interneuronal circuits controlling motility. Neurogastroenterol. Motil. *16 Suppl 1,* 34-38.

Borrione, A.C., Zanellato, A.M., Scannapieco, G., Pauletto, P., and Sartore, S. (1989). Myosin heavy-chain isoforms in adult and developing rabbit vascular smooth muscle. Eur. J. Biochem. *183,* 413-417.

Butler, T.M., Siegman, M.J., Mooers, S.U., and Barsotti, R.J. (1983). Myosin light chain phosphorylation does not modulate cross-bridge cycling rate in mouse skeletal muscle. Science *220,* 1167-1169.

Cai, S., Ferguson, D.G., Martin, A.F., and Paul, R.J. (1995). Smooth muscle contractility is modulated by myosin tail-S2-LMM hinge region interaction. Am. J. Physiol. *269,* C1126-32.

Chi, M., Zhou, Y., Vedamoorthyrao, S., Babu, G.J., and Periasamy, M. (2008). Ablation of smooth muscle myosin heavy chain SM2 increases smooth muscle contraction and results in postnatal death in mice. Proc. Natl. Acad. Sci. U. S. A. *105,* 18614-18618.

D'Antona, G., Lanfranconi, F., Pellegrino, M.A., Brocca, L., Adami, R., Rossi, R., Moro, G., Miotti, D., Canepari, M., and Bottinelli, R. (2006). Skeletal muscle hypertrophy and structure and function of skeletal muscle fibres in male body builders. J. Physiol. *570,* 611-627.

Dillon, P.F., Aksoy, M.O., Driska, S.P., and Murphy, R.A. (1981). Myosin phosphorylation and the cross-bridge cycle in arterial smooth muscle. Science *211,* 495-497.

DiSanto, M.E., Stein, R., Chang, S., Hypolite, J.A., Zheng, Y., Zderic, S., Wein, A.J., and Chacko, S. (2003). Alteration in expression of myosin isoforms in detrusor smooth muscle following bladder outlet obstruction. Am. J. Physiol. Cell. Physiol. *285,* C1397-410.

Dominguez, R., Freyzon, Y., Trybus, K.M., and Cohen, C. (1998). Crystal structure of a vertebrate smooth muscle myosin motor domain and its complex with the essential light chain: visualization of the pre-power stroke state. Cell *94,* 559-571.

Driska, S.P., Aksoy, M.O., and Murphy, R.A. (1981). Myosin light chain phosphorylation associated with contraction in arterial smooth muscle. Am. J. Physiol. *240,* C222-33.

Eddinger, T.J. (2009). Unique contractile and structural protein expression in dog ileal inner circular smooth muscle. J. Smooth Muscle Res. *45,* 217-230.

Eddinger, T.J., Korwek, A.A., Meer, D.P., and Sherwood, J.J. (2000). Expression of smooth muscle myosin light chain 17 and unloaded shortening in single smooth muscle cells. Am. J. Physiol. Cell. Physiol. *278,* C1133-42.

Eddinger, T.J., and Meer, D.P. (2007). Myosin II isoforms in smooth muscle: heterogeneity and function. Am. J. Physiol. Cell. Physiol. *293,* C493-508.

Eddinger, T.J., and Meer, D.P. (2001). Single rabbit stomach smooth muscle cell myosin heavy chain SMB expression and shortening velocity. Am. J. Physiol. Cell. Physiol. *280,* C309-16.

Eddinger, T.J., Meer, D.P., Miner, A.S., Meehl, J., Rovner, A.S., and Ratz, P.H. (2007). Potent inhibition of arterial smooth muscle tonic contractions by the selective myosin II inhibitor, blebbistatin. J. Pharmacol. Exp. Ther. *320,* 865-870.

Eddinger, T.J., and Murphy, R.A. (1991). Developmental changes in actin and myosin heavy chain isoform expression in smooth muscle. Arch. Biochem. Biophys. *284,* 232-237.

Eddinger, T.J., and Wolf, J.A. (1993). Expression of four myosin heavy chain isoforms with development in mouse uterus. Cell Motil. Cytoskeleton *25,* 358-368.

Ehlert, F.J., Sawyer, G.W., and Esqueda, E.E. (1999). Contractile role of M2 and M3 muscarinic receptors in gastrointestinal smooth muscle. Life Sci. *64,* 387-394.

Eto, M., Kitazawa, T., and Brautigan, D.L. (2004). Phosphoprotein inhibitor CPI-17 specificity depends on allosteric regulation of protein phosphatase-1 by regulatory subunits. Proc. Natl. Acad. Sci. U. S. A. *101,* 8888-8893.

Feng, J., Ito, M., Ichikawa, K., Isaka, N., Nishikawa, M., Hartshorne, D.J., and Nakano, T. (1999). Inhibitory phosphorylation site for Rho-associated kinase on smooth muscle myosin phosphatase. J. Biol. Chem. *274,* 37385-37390.

Frid, M.G., Printesva, O.Y., Chiavegato, A., Faggin, E., Scatena, M., Koteliansky, V.E., Pauletto, P., Glukhova, M.A., and Sartore, S. (1993). Myosin heavy-chain isoform composition and distribution in developing and adult human aortic smooth muscle. J. Vasc. Res. *30,* 279-292.

Fuglsang, A., Khromov, A., Torok, K., Somlyo, A.V., and Somlyo, A.P. (1993). Flash photolysis studies of relaxation and cross-bridge detachment: higher sensitivity of tonic than phasic smooth muscle to MgADP. J. Muscle Res. Cell. Motil. *14,* 666-677.

Furness, J.B. (2012). The enteric nervous system and neurogastroenterology. Nat. Rev. Gastroenterol. Hepatol. *9,* 286-294.

Furness, J.B., Young, H.M., Pompolo, S., Bornstein, J.C., Kunze, W.A., and McConalogue, K. (1995). Plurichemical transmission and chemical coding of neurons in the digestive tract. Gastroenterology *108,* 554-563.

Gao, Y., Ye, L.H., Kishi, H., Okagaki, T., Samizo, K., Nakamura, A., and Kohama, K. (2001). Myosin light chain kinase as a multifunctional regulatory protein of smooth muscle contraction. IUBMB Life *51,* 337-344.

Gaylinn, B.D., Eddinger, T.J., Martino, P.A., Monical, P.L., Hunt, D.F., and Murphy, R.A. (1989). Expression of nonmuscle myosin heavy and light chains in smooth muscle. Am. J. Physiol. *257,* C997-1004.

Gerthoffer, W.T., and Gunst, S.J. (2001). Invited review: focal adhesion and small heat shock proteins in the regulation of actin remodeling and contractility in smooth muscle. J. Appl. Physiol. *91,* 963-972.

Giuriato, L., Scatena, M., Chiavegato, A., Tonello, M., Scannapieco, G., Pauletto, P., and Sartore, S. (1992). Non-muscle myosin isoforms and cell heterogeneity in developing rabbit vascular smooth muscle. J. Cell. Sci. *101 (Pt 1),* 233-246.

Golomb, E., Ma, X., Jana, S.S., Preston, Y.A., Kawamoto, S., Shoham, N.G., Goldin, E., Conti, M.A., Sellers, J.R., and Adelstein, R.S. (2004). Identification and characterization of nonmuscle myosin II-C, a new member of the myosin II family. J. Biol. Chem. *279,* 2800-2808.

Gong, M.C., Iizuka, K., Nixon, G., Browne, J.P., Hall, A., Eccleston, J.F., Sugai, M., Kobayashi, S., Somlyo, A.V., and Somlyo, A.P. (1996). Role of guanine nucleotide-binding proteins--ras-family or trimeric proteins or both--in Ca2+ sensitization of smooth muscle. Proc. Natl. Acad. Sci. U. S. A. *93,* 1340-1345.

Gorecka, A., Aksoy, M.O., and Hartshorne, D.J. (1976). The effect of phosphorylation of gizzard myosin on actin activation. Biochem. Biophys. Res. Commun. *71,* 325-331.

Grabarek, Z. (2006). Structural basis for diversity of the EF-hand calcium-binding proteins. J. Mol. Biol. *359,* 509-525.

Guilluy, C., Garcia-Mata, R., and Burridge, K. (2011). Rho protein crosstalk: another social network? Trends Cell Biol. *21,* 718-726.

Haeberle, J.R. (1999). Thin-filament linked regulation of smooth muscle myosin. J. Muscle Res. Cell. Motil. *20,* 363-370.

Hai, C.M., and Murphy, R.A. (1989). Cross-bridge dephosphorylation and relaxation of vascular smooth muscle. Am. J. Physiol. *256,* C282-7.

Hai, C.M., and Murphy, R.A. (1988). Cross-bridge phosphorylation and regulation of latch state in smooth muscle. Am. J. Physiol. *254,* C99-106.

Hamada, Y., Yanagisawa, M., Katsuragawa, Y., Coleman, J.R., Nagata, S., Matsuda, G., and Masaki, T. (1990). Distinct vascular and intestinal smooth muscle myosin heavy chain mRNAs are encoded by a single-copy gene in the chicken. Biochem. Biophys. Res. Commun. *170,* 53-58.

Hamaguchi, T., Ito, M., Feng, J., Seko, T., Koyama, M., Machida, H., Takase, K., Amano, M., Kaibuchi, K., Hartshorne, D.J., and Nakano, T. (2000). Phosphorylation of CPI-17, an inhibitor of myosin phosphatase, by protein kinase N. Biochem. Biophys. Res. Commun. *274,* 825-830.

Han, S., Speich, J.E., Eddinger, T.J., Berg, K.M., Miner, A.S., Call, C., and Ratz, P.H. (2006). Evidence for absence of latch-bridge formation in muscular saphenous arteries. Am. J. Physiol. Heart Circ. Physiol. *291,* H138-46.

Hanson, J., and Huxley, H.E. (1953). Structural basis of the cross-striations in muscle. Nature *172,* 530-532.

Harnett, K.M., Cao, W., and Biancani, P. (2005). Signal-transduction pathways that regulate smooth muscle function I. Signal transduction in phasic (esophageal) and tonic (gastroesophageal sphincter) smooth muscles. Am. J. Physiol. Gastrointest. Liver Physiol. *288,* G407-16.

98

Hartshorne, D.J., Ito, M., and Erdodi, F. (1998). Myosin light chain phosphatase:
subunit composition, interactions and regulation. J. Muscle Res. Cell. Motil. *19,* 325-341.

Hasegawa, Y., Ueno, H., Horie, K., and Morita, F. (1988). Two isoforms of 17-kDa
essential light chain of aorta media smooth muscle myosin. J. Biochem. *103,* 15-18.

Hathaway, D.R., and Adelstein, R.S. (1979). Human platelet myosin light chain kinase
requires the calcium-binding protein calmodulin for activity. Proc. Natl. Acad. Sci.
U. S. A. *76,* 1653-1657.

Helper, D.J., Lash, J.A., and Hathaway, D.R. (1988). Distribution of isoelectric variants
of the 17,000-dalton myosin light chain in mammalian smooth muscle. J. Biol. Chem.
263, 15748-15753.

Herlihy, J.T., and Murphy, R.A. (1973). Length-tension relationship of smooth muscle of
the hog carotid artery. Circ. Res. *33,* 275-283.

Himpens, B., Missiaen, L., and Casteels, R. (1995). Ca2+ homeostasis in vascular smooth
muscle. J. Vasc. Res. *32,* 207-219.

Hong, F., Haldeman, B.D., Jackson, D., Carter, M., Baker, J.E., and Cremo, C.R. (2011).
Biochemistry of smooth muscle myosin light chain kinase. Arch. Biochem. Biophys.
510, 135-146.

Hori, M., and Karaki, H. (1998). Regulatory mechanisms of calcium sensitization of
contractile elements in smooth muscle. Life Sci. *62,* 1629-1633.

Horiuti, K., Somlyo, A.V., Goldman, Y.E., and Somlyo, A.P. (1989). Kinetics of
contraction initiated by flash photolysis of caged adenosine triphosphate in tonic and
phasic smooth muscles. J. Gen. Physiol. *94,* 769-781.

Horowitz, A., and Trybus, K.M. (1992). Inhibition of smooth muscle myosin's activity
and assembly by an anti-rod monoclonal antibody. J. Biol. Chem. *267,* 26091-26096.

Hu, K., Ji, L., Applegate, K.T., Danuser, G., and Waterman-Storer, C.M. (2007).
Differential transmission of actin motion within focal adhesions. Science *315,* 111-115.

Huang, Q.Q., Fisher, S.A., and Brozovich, F.V. (1999). Forced expression of essential
myosin light chain isoforms demonstrates their role in smooth muscle force
production. J. Biol. Chem. *274,* 35095-35098.

Huxley, A.F. (1974). Muscular contraction. J. Physiol. *243,* 1-43.

Huxley, A.F. (1954). Structural changes in muscle during contraction; interference microscopy of living muscle fibres. Nature *173,* 971-973.

Huxley, H., and Hanson, J. (1954). Changes in the cross-striations of muscle during contraction and stretch and their structural interpretation. Nature *173,* 973-976.

Hypolite, J.A., Chang, S., LaBelle, E., Babu, G.J., Periasamy, M., Wein, A.J., and Chacko, S. (2009). Deletion of SM-B, the high ATPase isoform of myosin, upregulates the PKC-mediated signal transduction pathway in murine urinary bladder smooth muscle. Am. J. Physiol. Renal Physiol. *296,* F658-65.

Inoue, A., Yanagisawa, M., Takano-Ohmuro, H., and Masaki, T. (1989). Two isoforms of smooth muscle myosin regulatory light chain in chicken gizzard. Eur. J. Biochem. *183,* 645-651.

Jiang, M.J., and Morgan, K.G. (1987). Intracellular calcium levels in phorbol ester-induced contractions of vascular muscle. Am. J. Physiol. *253,* H1365-71.

Kamm, K.E., and Stull, J.T. (1985). The function of myosin and myosin light chain kinase phosphorylation in smooth muscle. Annu. Rev. Pharmacol. Toxicol. *25,* 593-620.

Kandabashi, T., Shimokawa, H., Miyata, K., Kunihiro, I., Eto, Y., Morishige, K., Matsumoto, Y., Obara, K., Nakayama, K., Takahashi, S., and Takeshita, A. (2003). Evidence for protein kinase C-mediated activation of Rho-kinase in a porcine model of coronary artery spasm. Arterioscler. Thromb. Vasc. Biol. *23,* 2209-2214.

Kanoh, S., Ito, M., Niwa, E., Kawano, Y., and Hartshorne, D.J. (1993). Actin-binding peptide from smooth muscle myosin light chain kinase. Biochemistry *32,* 8902-8907.

Karagiannis, P., Babu, G.J., Periasamy, M., and Brozovich, F.V. (2004). Myosin heavy chain isoform expression regulates shortening velocity in smooth muscle: studies using an SMB KO mouse line. J. Muscle Res. Cell. Motil. *25,* 149-158.

Karagiannis, P., Babu, G.J., Periasamy, M., and Brozovich, F.V. (2003). The smooth muscle myosin seven amino acid heavy chain insert's kinetic role in the crossbridge cycle for mouse bladder. J. Physiol. *547,* 463-473.

Karaki, H. (2004). Historical techniques: cytosolic Ca2+ and contraction in smooth muscle. Trends Pharmacol. Sci. *25,* 388-393.

Kelley, C.A., Sellers, J.R., Goldsmith, P.K., and Adelstein, R.S. (1992). Smooth muscle myosin is composed of homodimeric heavy chains. J. Biol. Chem. *267,* 2127-2130.

Kelley, C.A., Takahashi, M., Yu, J.H., and Adelstein, R.S. (1993). An insert of seven amino acids confers functional differences between smooth muscle myosins from the intestines and vasculature. J. Biol. Chem. *268,* 12848-12854.

Khromov, A., Somlyo, A.V., Trentham, D.R., Zimmermann, B., and Somlyo, A.P. (1995). The role of MgADP in force maintenance by dephosphorylated cross-bridges in smooth muscle: a flash photolysis study. Biophys. J. *69,* 2611-2622.

Khromov, A.S., Wang, H., Choudhury, N., McDuffie, M., Herring, B.P., Nakamoto, R., Owens, G.K., Somlyo, A.P., and Somlyo, A.V. (2006). Smooth muscle of telokin-deficient mice exhibits increased sensitivity to Ca2+ and decreased cGMP-induced relaxation. Proc. Natl. Acad. Sci. U. S. A. *103,* 2440-2445.

Kiernan, J.A. (2008). Histological and histochemical methods: theory and practice (Bloxham: Scion).

Kim, H.R., Gallant, C., Leavis, P.C., Gunst, S.J., and Morgan, K.G. (2008). Cytoskeletal remodeling in differentiated vascular smooth muscle is actin isoform dependent and stimulus dependent. Am. J. Physiol. Cell. Physiol. *295,* C768-78.

Kimura, K., Ito, M., Amano, M., Chihara, K., Fukata, Y., Nakafuku, M., Yamamori, B., Feng, J., Nakano, T., Okawa, K., Iwamatsu, A., and Kaibuchi, K. (1996). Regulation of myosin phosphatase by Rho and Rho-associated kinase (Rho-kinase). Science *273,* 245-248.

Kitazawa, T., Hashiba, K., Cao, J., Unno, T., Komori, S., Yamada, M., Wess, J., and Taneike, T. (2007). Functional roles of muscarinic M2 and M3 receptors in mouse stomach motility: studies with muscarinic receptor knockout mice. Eur. J. Pharmacol. *554,* 212-222.

Kovacs, M., Thirumurugan, K., Knight, P.J., and Sellers, J.R. (2007). Load-dependent mechanism of nonmuscle myosin 2. Proc. Natl. Acad. Sci. U. S. A. *104,* 9994-9999.

Kovacs, M., Wang, F., Hu, A., Zhang, Y., and Sellers, J.R. (2003). Functional divergence of human cytoplasmic myosin II: kinetic characterization of the non-muscle IIA isoform. J. Biol. Chem. *278,* 38132-38140.

Koyama, M., Ito, M., Feng, J., Seko, T., Shiraki, K., Takase, K., Hartshorne, D.J., and Nakano, T. (2000). Phosphorylation of CPI-17, an inhibitory phosphoprotein of smooth muscle myosin phosphatase, by Rho-kinase. FEBS Lett. *475,* 197-200.

Kumar, C.C., Mohan, S.R., Zavodny, P.J., Narula, S.K., and Leibowitz, P.J. (1989). Characterization and differential expression of human vascular smooth muscle myosin light chain 2 isoform in nonmuscle cells. Biochemistry *28,* 4027-4035.

Kuro-o, M., Nagai, R., Tsuchimochi, H., Katoh, H., Yazaki, Y., Ohkubo, A., and Takaku, F. (1989). Developmentally regulated expression of vascular smooth muscle myosin heavy chain isoforms. J. Biol. Chem. *264,* 18272-18275.

Kuznicki, J., Cote, G.P., Bowers, B., and Korn, E.D. (1985). Filament formation and actin-activated ATPase activity are abolished by proteolytic removal of a small peptide from the tip of the tail of the heavy chain of Acanthamoeba myosin II. J. Biol. Chem. *260,* 1967-1972.

Lee, C.H., Poburko, D., Kuo, K.H., Seow, C.Y., and van Breemen, C. (2002). Ca(2+) oscillations, gradients, and homeostasis in vascular smooth muscle. Am. J. Physiol. Heart Circ. Physiol. *282,* H1571-83.

Lenz, S., Lohse, P., Seidel, U., and Arnold, H.H. (1989). The alkali light chains of human smooth and nonmuscle myosins are encoded by a single gene. Tissue-specific expression by alternative splicing pathways. J. Biol. Chem. *264,* 9009-9015.

Liu, J., Wendt, T., Taylor, D., and Taylor, K. (2003). Refined model of the 10S conformation of smooth muscle myosin by cryo-electron microscopy 3D image reconstruction. J. Mol. Biol. *329,* 963-972.

Lofgren, M., Ekblad, E., Morano, I., and Arner, A. (2003). Nonmuscle Myosin motor of smooth muscle. J. Gen. Physiol. *121,* 301-310.

Lofgren, M., Fagher, K., Wede, O.K., and Arner, A. (2002). Decreased shortening velocity and altered myosin isoforms in guinea-pig hypertrophic intestinal smooth muscle. J. Physiol. *544,* 707-714.

Loukianov, E., Loukianova, T., and Periasamy, M. (1997). Myosin heavy chain isoforms in smooth muscle. Comp. Biochem. Physiol. B. Biochem. Mol. Biol. *117,* 13-18.

Lowey, S., Slayter, H.S., Weeds, A.G., and Baker, H. (1969). Substructure of the myosin molecule. I. Subfragments of myosin by enzymic degradation. J. Mol. Biol. *42,* 1-29.

MacDonald, J.A., Eto, M., Borman, M.A., Brautigan, D.L., and Haystead, T.A. (2001). Dual Ser and Thr phosphorylation of CPI-17, an inhibitor of myosin phosphatase, by MYPT-associated kinase. FEBS Lett. *493,* 91-94.

Malmqvist, U., and Arner, A. (1991). Correlation between isoform composition of the 17 kDa myosin light chain and maximal shortening velocity in smooth muscle. Pflugers Arch. *418,* 523-530.

Matsuda, G., Maita, T., Kato, Y., Chen, J.I., and Umegane, T. (1981). Amino acid sequences of the cardiac L-2A, L-2B and gizzard 17 000-Mr light chains of chicken muscle myosin. FEBS Lett. *135,* 232-236.

McFadzean, I., and Gibson, A. (2002). The developing relationship between receptor-operated and store-operated calcium channels in smooth muscle. Br. J. Pharmacol. *135,* 1-13.

McLachlan, A.D., and Karn, J. (1983). Periodic features in the amino acid sequence of nematode myosin rod. J. Mol. Biol. *164,* 605-626.

McLachlan, A.D., and Karn, J. (1982). Periodic charge distributions in the myosin rod amino acid sequence match cross-bridge spacings in muscle. Nature *299,* 226-231.

Meer, D.P., and Eddinger, T.J. (1997). Expression of smooth muscle myosin heavy chains and unloaded shortening in single smooth muscle cells. Am. J. Physiol. *273,* C1259-66.

Mehta, D., and Gunst, S.J. (1999). Actin polymerization stimulated by contractile activation regulates force development in canine tracheal smooth muscle. J. Physiol. *519 Pt 3,* 829-840.

Mehta, D., Wang, Z., Wu, M.F., and Gunst, S.J. (1998). Relationship between paxillin and myosin phosphorylation during muscarinic stimulation of smooth muscle. Am. J. Physiol. *274,* C741-7.

Miyanishi, T., Maita, T., Morita, F., Kondo, S., and Matsuda, G. (1985). Amino acid sequences of the two kinds of regulatory light chains of adductor smooth muscle myosin from Patinopecten yessoensis. J. Biochem. *97,* 541-551.

Morano, I. (2003). Tuning smooth muscle contraction by molecular motors. J. Mol. Med. (Berl) *81,* 481-487.

Morano, I., Chai, G.X., Baltas, L.G., Lamounier-Zepter, V., Lutsch, G., Kott, M., Haase, H., and Bader, M. (2000). Smooth-muscle contraction without smooth-muscle myosin. Nat. Cell Biol. *2,* 371-375.

Morano, I., Erb, G., and Sogl, B. (1993). Expression of myosin heavy and light chains changes during pregnancy in the rat uterus. Pflugers Arch. *423,* 434-441.

Mornet, D., Bertrand, R.U., Pantel, P., Audemard, E., and Kassab, R. (1981). Proteolytic approach to structure and function of actin recognition site in myosin heads. Biochemistry *20,* 2110-2120.

Murakami, N., and Elzinga, M. (1992). Immunohistochemical studies on the distribution of cellular myosin II isoforms in brain and aorta. Cell Motil. Cytoskeleton *22,* 281-295.

Murthy, K.S. (2006). Signaling for contraction and relaxation in smooth muscle of the gut. Annu. Rev. Physiol. *68,* 345-374.

Nagai, R., Kuro-o, M., Babij, P., and Periasamy, M. (1989). Identification of two types of smooth muscle myosin heavy chain isoforms by cDNA cloning and immunoblot analysis. J. Biol. Chem. *264,* 9734-9737.

Nagai, R., Larson, D.M., and Periasamy, M. (1988). Characterization of a mammalian smooth muscle myosin heavy chain cDNA clone and its expression in various smooth muscle types. Proc. Natl. Acad. Sci. U. S. A. *85,* 1047-1051.

Nelson, W.D., Blakely, S.E., Nesmelov, Y.E., and Thomas, D.D. (2005). Site-directed spin labeling reveals a conformational switch in the phosphorylation domain of smooth muscle myosin. Proc. Natl. Acad. Sci. U. S. A. *102,* 4000-4005.

Niiro, N., and Ikebe, M. (2001). Zipper-interacting protein kinase induces Ca(2+)-free smooth muscle contraction via myosin light chain phosphorylation. J. Biol. Chem. *276,* 29567-29574.

Ohama, T., Hori, M., Sato, K., Ozaki, H., and Karaki, H. (2003). Chronic treatment with interleukin-1beta attenuates contractions by decreasing the activities of CPI-17 and MYPT-1 in intestinal smooth muscle. J. Biol. Chem. *278,* 48794-48804.

Pagh, K., and Gerisch, G. (1986). Monoclonal antibodies binding to the tail of Dictyostelium discoideum myosin: their effects on antiparallel and parallel assembly and actin-activated ATPase activity. J. Cell Biol. *103,* 1527-1538.

Pandya, K., Cowhig, J., Brackhan, J., Kim, H.S., Hagaman, J., Rojas, M., Carter, C.W.,Jr, Mao, L., Rockman, H.A., Maeda, N., and Smithies, O. (2008). Discordant on/off switching of gene expression in myocytes during cardiac hypertrophy in vivo. Proc. Natl. Acad. Sci. U. S. A. *105,* 13063-13068.

Pandya, K., Kim, H.S., and Smithies, O. (2006). Fibrosis, not cell size, delineates beta-myosin heavy chain reexpression during cardiac hypertrophy and normal aging in vivo. Proc. Natl. Acad. Sci. U. S. A. *103,* 16864-16869.

Patzak, A., Petzhold, D., Wronski, T., Martinka, P., Babu, G.J., Periasamy, M., Haase, H., and Morano, I. (2005). Constriction velocities of renal afferent and efferent arterioles of mice are not related to SMB expression. Kidney Int. *68,* 2726-2734.

Paul, R.J. (1989). Smooth muscle energetics. Annu. Rev. Physiol. *51,* 331-349.

Pavalko, F.M., Adam, L.P., Wu, M.F., Walker, T.L., and Gunst, S.J. (1995). Phosphorylation of dense-plaque proteins talin and paxillin during tracheal smooth muscle contraction. Am. J. Physiol. *268,* C563-71.

Persechini, A., and Hartshorne, D.J. (1981). Phosphorylation of smooth muscle myosin: evidence for cooperativity between the myosin heads. Science *213,* 1383-1385.

Phillips, C.L., Yamakawa, K., and Adelstein, R.S. (1995). Cloning of the cDNA encoding human nonmuscle myosin heavy chain-B and analysis of human tissues with isoform-specific antibodies. J. Muscle Res. Cell. Motil. *16,* 379-389.

Poole, D.P., and Furness, J.B. (2007). PKC delta-isoform translocation and enhancement of tonic contractions of gastrointestinal smooth muscle. Am. J. Physiol. Gastrointest. Liver Physiol. *292,* G887-98.

Rattan, S., De Godoy, M.A., and Patel, C.A. (2006). Rho kinase as a novel molecular therapeutic target for hypertensive internal anal sphincter. Gastroenterology *131,* 108-116.

Ratz, P.H., Berg, K.M., Urban, N.H., and Miner, A.S. (2005). Regulation of smooth muscle calcium sensitivity: KCl as a calcium-sensitizing stimulus. Am. J. Physiol. Cell. Physiol. *288,* C769-83.

Rayment, I., Rypniewski, W.R., Schmidt-Base, K., Smith, R., Tomchick, D.R., Benning, M.M., Winkelmann, D.A., Wesenberg, G., and Holden, H.M. (1993). Three-dimensional structure of myosin subfragment-1: a molecular motor. Science *261,* 50-58.

Rembold, C.M., and Murphy, R.A. (1986). Myoplasmic calcium, myosin phosphorylation, and regulation of the crossbridge cycle in swine arterial smooth muscle. Circ. Res. *58,* 803-815.

Rochlin, M.W., Itoh, K., Adelstein, R.S., and Bridgman, P.C. (1995). Localization of myosin II A and B isoforms in cultured neurons. J. Cell. Sci. *108 (Pt 12),* 3661-3670.

Rondelli, C.M., Szasz, I.T., Kayal, A., Thakali, K., Watson, R.E., Rovner, A.S., Eddinger, T.J., Fink, G.D., and Watts, S.W. (2007). Preferential myosin heavy chain isoform B Expression may contribute to the faster velocity of contraction in veins versus arteries. J. Vasc. Res. *44,* 264-272.

Rosenfeld, S.S., Xing, J., Chen, L.Q., and Sweeney, H.L. (2003). Myosin IIb is unconventionally conventional. J. Biol. Chem. *278,* 27449-27455.

Rosenfeld, S.S., Xing, J., Cheung, H.C., Brown, F., Kar, S., and Sweeney, H.L. (1998). Structural and kinetic studies of phosphorylation-dependent regulation in smooth muscle myosin. J. Biol. Chem. *273,* 28682-28690.

Rovner, A.S., Fagnant, P.M., Lowey, S., and Trybus, K.M. (2002). The carboxyl-terminal isoforms of smooth muscle myosin heavy chain determine thick filament assembly properties. J. Cell Biol. *156,* 113-123.

Rovner, A.S., Fagnant, P.M., and Trybus, K.M. (2006). Phosphorylation of a single head of smooth muscle myosin activates the whole molecule. Biochemistry *45,* 5280-5289.

Rovner, A.S., Freyzon, Y., and Trybus, K.M. (1997). An insert in the motor domain determines the functional properties of expressed smooth muscle myosin isoforms. J. Muscle Res. Cell. Motil. *18,* 103-110.

Rovner, A.S., Thompson, M.M., and Murphy, R.A. (1986). Two different heavy chains are found in smooth muscle myosin. Am. J. Physiol. *250,* C861-70.

Sellers, J.R. (2000). Myosins: a diverse superfamily. Biochim. Biophys. Acta *1496,* 3-22.

Sellers, J.R., and Pato, M.D. (1984). The binding of smooth muscle myosin light chain kinase and phosphatases to actin and myosin. J. Biol. Chem. *259,* 7740-7746.

Shimizu, H., Ito, M., Miyahara, M., Ichikawa, K., Okubo, S., Konishi, T., Naka, M., Tanaka, T., Hirano, K., and Hartshorne, D.J. (1994). Characterization of the myosin-binding subunit of smooth muscle myosin phosphatase. J. Biol. Chem. *269,* 30407-30411.

Siegman, M.J., Butler, T.M., Mooers, S.U., Trinkle-Mulcahy, L., Narayan, S., Adam, L., Chacko, S., Haase, H., and Morano, I. (1997). Hypertrophy of colonic smooth muscle: contractile proteins, shortening velocity, and regulation. Am. J. Physiol. *272,* G1571-80.

Silver, D.L., Vorotnikov, A.V., Watterson, D.M., Shirinsky, V.P., and Sellers, J.R. (1997). Sites of interaction between kinase-related protein and smooth muscle myosin. J. Biol. Chem. *272,* 25353-25359.

Simons, M., Wang, M., McBride, O.W., Kawamoto, S., Yamakawa, K., Gdula, D., Adelstein, R.S., and Weir, L. (1991). Human nonmuscle myosin heavy chains are encoded by two genes located on different chromosomes. Circ. Res. *69,* 530-539.

Sinn, D.H., Min, B.H., Ko, E.J., Lee, J.Y., Kim, J.J., Rhee, J.C., Kim, S., Ward, S.M., and Rhee, P.L. (2010). Regional differences of the effects of acetylcholine in the human gastric circular muscle. Am. J. Physiol. Gastrointest. Liver Physiol. *299,* G1198-203.

Sjuve, R., Arner, A., Li, Z., Mies, B., Paulin, D., Schmittner, M., and Small, J.V. (1998). Mechanical alterations in smooth muscle from mice lacking desmin. J. Muscle Res. Cell. Motil. *19,* 415-429.

Sobieszek, A. (1985). Phosphorylation reaction of vertebrate smooth muscle myosin: an enzyme kinetic analysis. Biochemistry *24,* 1266-1274.

Sobieszek, A. (1977). Ca-linked phosphorylation of a light chain of vertebrate smooth-muscle myosin. Eur. J. Biochem. *73,* 477-483.

Sohn, U.D., Cao, W., Tang, D.C., Stull, J.T., Haeberle, J.R., Wang, C.L., Harnett, K.M., Behar, J., and Biancani, P. (2001). Myosin light chain kinase- and PKC-dependent contraction of LES and esophageal smooth muscle. Am. J. Physiol. Gastrointest. Liver Physiol. *281,* G467-78.

Somlyo, A.P., and Somlyo, A.V. (2003). Ca2+ sensitivity of smooth muscle and nonmuscle myosin II: modulated by G proteins, kinases, and myosin phosphatase. Physiol. Rev. *83,* 1325-1358.

Somlyo, A.P., and Somlyo, A.V. (1968). Vascular smooth muscle. I. Normal structure, pathology, biochemistry, and biophysics. Pharmacol. Rev. *20,* 197-272.

Somlyo, A.V., Matthew, J.D., Wu, X., Khromov, A.S., and Somlyo, A.P. (1998). Regulation of the cross-bridge cycle: the effects of MgADP, LC17 isoforms and telokin. Acta Physiol. Scand. *164,* 381-388.

Sparrow, M.P., Mohammad, M.A., Arner, A., Hellstrand, P., and Ruegg, J.C. (1988). Myosin composition and functional properties of smooth muscle from the uterus of pregnant and non-pregnant rats. Pflugers Arch. *412,* 624-633.

Stone, J., Brannon, T., Haddad, F., Qin, A., and Baldwin, K.M. (1996). Adaptive responses of hypertrophying skeletal muscle to endurance training. J. Appl. Physiol. *81,* 665-672.

Street, C.A., and Bryan, B.A. (2011). Rho kinase proteins--pleiotropic modulators of cell survival and apoptosis. Anticancer Res. *31,* 3645-3657.

Sucharov, C.C., Helmke, S.M., Langer, S.J., Perryman, M.B., Bristow, M., and Leinwand, L. (2004). The Ku protein complex interacts with YY1, is up-regulated in human heart failure, and represses alpha myosin heavy-chain gene expression. Mol. Cell. Biol. *24,* 8705-8715.

Sutherland, C., and Walsh, M.P. (1989). Phosphorylation of caldesmon prevents its interaction with smooth muscle myosin. J. Biol. Chem. *264,* 578-583.

Sweeney, H.L., Rosenfeld, S.S., Brown, F., Faust, L., Smith, J., Xing, J., Stein, L.A., and Sellers, J.R. (1998). Kinetic tuning of myosin via a flexible loop adjacent to the nucleotide binding pocket. J. Biol. Chem. *273,* 6262-6270.

Szilagyi, L., Balint, M., Sreter, F.A., and Gergely, J. (1979). Photoaffinity labelling with an ATP analog of the N-terminal peptide of myosin. Biochem. Biophys. Res. Commun. *87,* 936-945.

Szymanski, P.T., Chacko, T.K., Rovner, A.S., and Goyal, R.K. (1998). Differences in contractile protein content and isoforms in phasic and tonic smooth muscles. Am. J. Physiol. *275,* C684-92.

Szymanski, P.T., and Tao, T. (1997). Localization of protein regions involved in the interaction between calponin and myosin. J. Biol. Chem. *272,* 11142-11146.

Taubman, M.B., Grant, J.W., and Nadal-Ginard, B. (1987). Cloning and characterization of mammalian myosin regulatory light chain (RLC) cDNA: the RLC gene is expressed in smooth, sarcomeric, and nonmuscle tissues. J. Cell Biol. *104,* 1505-1513.

Trybus, K.M. (1994). Role of myosin light chains. J. Muscle Res. Cell. Motil. *15,* 587-594.

Trybus, K.M., Waller, G.S., and Chatman, T.A. (1994). Coupling of ATPase activity and motility in smooth muscle myosin is mediated by the regulatory light chain. J. Cell Biol. *124,* 963-969.

Tuck, S.A., Maghni, K., Poirier, A., Babu, G.J., Periasamy, M., Bates, J.H., Leguillette, R., and Lauzon, A.M. (2004). Time course of airway mechanics of the (+)insert myosin isoform knockout mouse. Am. J. Respir. Cell Mol. Biol. *30,* 326-332.

Tullio, A.N., Accili, D., Ferrans, V.J., Yu, Z.X., Takeda, K., Grinberg, A., Westphal, H., Preston, Y.A., and Adelstein, R.S. (1997). Nonmuscle myosin II-B is required for normal development of the mouse heart. Proc. Natl. Acad. Sci. U. S. A. *94,* 12407-12412.

Unno, T., Matsuyama, H., Izumi, Y., Yamada, M., Wess, J., and Komori, S. (2006). Roles of M2 and M3 muscarinic receptors in cholinergic nerve-induced contractions in mouse ileum studied with receptor knockout mice. Br. J. Pharmacol. *149,* 1022-1030.

Urban, N.H., Berg, K.M., and Ratz, P.H. (2003). K+ depolarization induces RhoA kinase translocation to caveolae and Ca2+ sensitization of arterial muscle. Am. J. Physiol. Cell. Physiol. *285,* C1377-85.

Walker, J.E., Saraste, M., Runswick, M.J., and Gay, N.J. (1982). Distantly related sequences in the alpha- and beta-subunits of ATP synthase, myosin, kinases and other ATP-requiring enzymes and a common nucleotide binding fold. EMBO J. *1,* 945-951.

Walsh, M.P., Thornbury, K., Cole, W.C., Sergeant, G., Hollywood, M., and McHale, N. (2011). Rho-associated kinase plays a role in rabbit urethral smooth muscle contraction, but not via enhanced myosin light chain phosphorylation. Am. J. Physiol. Renal Physiol. *300,* F73-85.

Wang, F., Kovacs, M., Hu, A., Limouze, J., Harvey, E.V., and Sellers, J.R. (2003). Kinetic mechanism of non-muscle myosin IIB: functional adaptations for tension generation and maintenance. J. Biol. Chem. *278,* 27439-27448.

Weiss, A., McDonough, D., Wertman, B., Acakpo-Satchivi, L., Montgomery, K., Kucherlapati, R., Leinwand, L., and Krauter, K. (1999). Organization of human and mouse skeletal myosin heavy chain gene clusters is highly conserved. Proc. Natl. Acad. Sci. U. S. A. *96,* 2958-2963.

Wendt, T., Taylor, D., Messier, T., Trybus, K.M., and Taylor, K.A. (1999). Visualization of head-head interactions in the inhibited state of smooth muscle myosin. J. Cell Biol. *147,* 1385-1390.

Wendt, T., Taylor, D., Trybus, K.M., and Taylor, K. (2001). Three-dimensional image reconstruction of dephosphorylated smooth muscle heavy meromyosin reveals asymmetry in the interaction between myosin heads and placement of subfragment 2. Proc. Natl. Acad. Sci. U. S. A. *98,* 4361-4366.

Wetzel, U., Lutsch, G., Haase, H., Ganten, U., and Morano, I. (1998). Expression of smooth muscle myosin heavy chain B in cardiac vessels of normotensive and hypertensive rats. Circ. Res. *83,* 204-209.

White, S., Martin, A.F., and Periasamy, M. (1993). Identification of a novel smooth muscle myosin heavy chain cDNA: isoform diversity in the S1 head region. Am. J. Physiol. *264,* C1252-8.

Wilson, D.P., Sutherland, C., Borman, M.A., Deng, J.T., Macdonald, J.A., and Walsh, M.P. (2005). Integrin-linked kinase is responsible for Ca2+-independent myosin diphosphorylation and contraction of vascular smooth muscle. Biochem. J. *392,* 641-648.

Wooldridge, A.A., MacDonald, J.A., Erdodi, F., Ma, C., Borman, M.A., Hartshorne, D.J., and Haystead, T.A. (2004). Smooth muscle phosphatase is regulated in vivo by exclusion of phosphorylation of threonine 696 of MYPT1 by phosphorylation of Serine 695 in response to cyclic nucleotides. J. Biol. Chem. *279,* 34496-34504.

Zhang, W., Du, L., and Gunst, S.J. (2010). The effects of the small GTPase RhoA on the muscarinic contraction of airway smooth muscle result from its role in regulating actin polymerization. Am. J. Physiol. Cell. Physiol. *299,* C298-306.

Zhang, W., Wu, Y., Du, L., Tang, D.D., and Gunst, S.J. (2005). Activation of the Arp2/3 complex by N-WASp is required for actin polymerization and contraction in smooth muscle. Am. J. Physiol. Cell. Physiol. *288,* C1145-60.

Zhao, R., Du, L., Huang, Y., Wu, Y., and Gunst, S.J. (2008). Actin depolymerization factor/cofilin activation regulates actin polymerization and tension development in canine tracheal smooth muscle. J. Biol. Chem. *283,* 36522-36531.